KBS TEKNISK RAPPORT

54
:03

Groundwater movements around a repository

Regional groundwater flow analyses
Part 1 Intial conditions
Part 2 Long term residual conditions

Anthony Burgess

Hagconsult AB oktober 1977

KÄRN - BRÄNSLE - SÄKERHET

POSTADRESS: Kärnbränslesäkerhet, Fack. 102 40 Stockholm. Telefon 08-67 95 40

GROUNDWATER MOVEMENTS AROUND A REPOSITORY

REGIONAL GROUNDWATER FLOW ANALYSES
PART 1 INITIAL CONDITIONS
PART 2 LONG TERM RESIDUAL CONDITIONS

Anthony Burgess
Hagconsult AB oktober 1977

I slutet av rapporten har bifogats en förteckning över av KBS hittills publicerade tekniska rapporter i denna serie.

TECHNICAL REPORT 3

REGIONAL GROUNDWATER FLOW ANALYSES

PART I

INITIAL CONDITIONS

KBS-Kärnbränslesäkerhet

GROUNDWATER MOVEMENTS AROUND A REPOSITORY

Technical Report 3: Regional Groundwater Flow Analyses
Part I: Initial Conditions

Hagconsult AB
in association with
Acres Consulting Services Ltd
RE/SPEC Inc.

FOREWORD

This report was prepared as one of a series of technical reports within a study of the groundwater movements around a repository for radioactive waste in the Precambrian bedrock of Sweden. It was written in two parts, (I) initial flow conditions and (II) long-term residual conditions. This part is Part I. The contract for this study was between KBS - Kärnbränslesäkerhet (Project Fuel Safety) and Hagconsult AB of Stockholm, Sweden. RE/SPEC Inc. of Rapid City, SD/USA and Acres Consulting Services Ltd of Niagara Falls, Ontario/Canada acted as subconsultants to Hagconsult AB.

The principal author of this report is Dr Anthony Burgess of Acres. Review was provided by Dr Ulf E. Lindblom of Hagconsult AB and Dr Robin Charlwood of Acres. Input to the study was provided by Dr Håkan Stille and Mr Joe L. Ratigan of the Study Group and by other contributors to the KBS project.

The opinions and conclusions in this document are those of the author and should not be interpreted as necessarily representing the official policies or recommendations of KBS.

Stockholm September 1977

Ulf E. Lindblom
Study Director
Hagconsult AB

TABLES OF CONTENTS

LIST OF FIGURES

Figure

Figure

LIST OF TABLES

1. INTRODUCTION AND SCOPE OF WORK

The detailed study of groundwater flow may be divided into 3 stages:

Discussion and definition of parameters to be used in the analyses. Assessment of initial groundwater flow under natural, undisturbed conditions typical of proposed candidate sites.

Study of the response of the groundwater flow during the short term due to construction, changes of in situ stress conditions, and thermal loading from the waste. The time span to be studied is from the start of construction to the end of significant heat generation by the waste. The latter will of course depend upon the type of waste emplaced. Based upon the types of waste presently being considered for disposal, the short-term period may extend to about 1000 years after emplacement for spent fuel and about 100 years after emplacement for reprocessed waste.

Study of the long-term period to investigate the flow regime for times beyond the short-term considered above, until radioactive decay of the nuclides within the waste is sufficiently advanced that they no longer consitute a hazard.

The ultimate objective of the complete study is to provide estimates of groundwater flow for incorporation into predictive transport and risk models for the repository-biosphere system. The effects of construction of the repository and emplacement of wastes may be considered as perturbations to the natural regime. Therefore, a necessary prerequisite for the prediction of repository performance is a complete understanding of the initial groundwater conditions. This report will describe the results of the Stage I study of the initial groundwater conditions.

The design of the repository is at present in the conceptual stage. Investigations are in progress to determine geological and geohydrological parameters typical of the rock in which a repository may be located. Data from two sites, Forsmark and Oskarshamn, have been used in this study (Figure 1).

2. SOURCES OF DATA AND REFERENCES

A compilation of relevant geological, geotechnical and geohydrological conditions was given in the Technical Report No. 1, (1)[x]. This has been used as a basic source throughout the study. Because of the time frame imposed for the study of waste disposal in Sweden, only a limited amount of field data is available at the time of writing. For that reason we have studied general condition, utilizing data obtained from the literature, together with field data when available. The choice of parameters and boundary conditions together with reliability estimates are discussed in section 4 of this report.

A detailed list of references is included at the end of this report.

[x] Numbers in parentheses refer to references at end of text.

3. GROUNDWATER FLOW MODELS

3.1 Reliability, Deterministic & Stochastic Models

In this study, deterministic methods of groundwater flow analysis have been employed; i.e., the values of functions are uniquely determined by the defined input parameters and boundary conditions. In fact, however, groundwater flow may be better represented by considering the input parameters and boundary conditions as random variables, that is, a stochastic process. In groundwater analysis, the use of stochastic models is in an early stage of development. Wu, (2) used at Monte Carlo method to develop probable seepage quantities for a deposit of silt and fine sand containing lenses of coarse sand and gravel. More recently Freeze (3) has applied stochastic methods to one dimensional flow, and Gelhar (4,5) has investigated two dimensional systems. Wilson & Witherspoon (6) have used Monte Carlo methods for assigning joint apertures to an orthogonal set of joints in a study of flow beneath a dam.

When considering transport problems, the phenomen of mechanical dispersion must be considered. Mechanical dispersion arises from the mixing in varying pathways and velocities taken by a fluid during flow through fractured or porous media. In regard to mechanical dispersion in fractured geological materials, the statement by Castillo (7) is a good indication of the current status of investigations:

"Although the basic theoretical aspects of --(dispersion)-- have been treated at length for the case where the permeable stratum is composed of granular material, the classical concept of flow through a porous medium is generally inadequate to describe the flow behaviour in jointed rock, and it becomes increasingly unsuitable for analysis of dispersion. Despite these limitations, little work has been directed toward extending these ideas to handle flow through jointed formations---".

Our review of the literature indicates that this statement is still applicable even though 4 years have passed since publication of the Castillo, et.al. paper. A stochastic approach to modelling dispersion may be appropriate, although at this time there is insufficient data to propose such a model.

When considering the concentrations of radionuclides being transported through a subsurface system, a conservative approach would be to assume that the concentrations will undergo no decrease because of dispersion. This approach is conservative from the point of view of concentration levels, but may give unconservative estimates of the extent of the contaminated zone. Dispersion in singular features may be the principal contaminant transport mechanism and will be discussed later although this topic is outside the scope of this study.

The groundwater from modelling requirement for the assessment of radioactive waste isolation at this time unavoidably involves recognition of uncertainty in flow predictions. These uncertainties may be viewed conceptually as arising from several distinct sources :

(a) Lack of knowledge at the site conditions. (Data unavailability)
(b) Errors in formulation of theoretical models of flow. (Model errors)
(c) Errors in measurement of parameters. (Measurement errors)
(d) Unhomogeneous variations in parameters at the site. (Spatial variability)

Stochastic models for variations of type (a) and (b) could be formulated in terms of a single random variables describing the process ignoring spatial structure and computational procedures for linear problems are avialable, Freeze (3). These are sometimes referred to, misleadingly, as one-dimensional analyses. This may also be true for type (c) variations.

The analysis of type (d), spatial variability requires 2 or 3 dimensional models. One dimensional modelling of spatial variability has been shown to give very poor estimates of the variance of flows. This is because, by definition, the one-dimensional model eliminates spatial variations which would permit alternative flow paths around locations with extreme values. For instance, a low permeability value at a point in the pipe flow would strongly control the flow while in a 2 or 3 dimensional situation the flow would run around it.

Two and three dimensional stochastic modelling of groundwater flow is a very complex procedure and since the data is sparse it is not thought to be justified in this study at this time. However, single - random variable models of uncertainties, particularly type (a) will be used for reliability assessments of key parameters in the following sections. The computation procedure used was a discrete numerical convolution .

Deterministic models will be used for the groundwater flow models and the reliability assessments developed as described above can be applied to these.

3.2 Input Parameters

3.2.1 Permeability

The usual methods of field permeability testing measure the discharge into or out of a section of drillhole. The rate of flow and the ambient pressure head for the test are then used to calculate the permeability, assuming that the medium around the drillhole is an isotropic permeable medium. Over short lengths of drillhole widely fluctuating values of permeability are recorded due to the varying number and apertures of fractures intersected. This is well illustrated in the results from Kråkemåla drillhole K 1, (1). The fluctuations can be smoothed by averaging the permeability values over longer sections of the drillhole. This is quite valid since the analytical method treats the rock as a continuum with fixed properties for the individual elements.

The permeability - depth data avialable for this study is discussed in (1). From this it can be seen that even after averaging results over sections of drillholes, there remains a range of possible values for permeability at a particular depth (Figure 2). The empirical function for permeability with depth used in these analyses represents an estimated log median value. For comparison, the empirical median and range of values at vaious depths are tabulated below.

Depth (m)	Permeability m/s		
	from	to	median estimate
0	2.8×10^{-5}	6.3×10^{-7}	2.7×10^{-6}
50	2.5×10^{-7}	2.2×10^{-8}	1.1×10^{-7}
100	1.4×10^{-7}	1.6×10^{-8}	3.8×10^{-8}
200			1.3×10^{-8}
500	insufficient data for		3.7×10^{-9}
1000	estimate of range		1.7×10^{-9}
2000			9.4×10^{-10}

In general, the recorded averaged permeability values at a particular depth range over about one order of magnitude, except near the surface where the range is over 1.5 orders of magnitude. For the purpose of this study, it has been assumed that the one magnitude range of values is maintained at depth.

It should be noted that the effect of singularities has not been included in these permeability range estimates.

In summary, the averaged permeability for a particular depth may range over about one order of magnitude. The actual permeability of a particular limited section of a drillhole, however, may vary from the limit of measurable permeability, about 10^{-9}, to 10^{-6} m/s, or even higher.

In order to completely describe the permeability of a continuum, it is necessary to define the principal values of permeability, and the direction of the principal axes in space. The analysis of most field tests assume the medium to be isotropic. However, as noted by Snow (8) isotropy is the exception rather than the rule in groundwater hydrology.

In situ stress measurements in the Baltic Shield show that the horizontal stress is greater than the vertical stress. Fracture aperture and hence permeability is inversely proportional to the normal stress on the aperture. Anisotropy of the permeability may therefore be expected. In general, permeability data is obtained from vertical drillholes, and hence preferentially measures the horizontal permeability (see (1) for further discussion).

In this study, three permeability depth relationships have generally been used (1):

Case 1: Permeability homogeneous isotropic constant

$$K = 1.0 \times 10^{-8} \text{ m/s}$$

Case 2: Permeability isotropic, decreasing with depth as per empirically derived function

$$\log K = -5.57 + 0.362 (\log Z) - 0.978 (\log Z)^2 + 0.167 (\log Z)^3$$

where Z = depth in metres

Case 3: Permeability anisotropic

$$K_Z = 1.0 \times 10^{-9} \text{ m/s}$$

$$\log K_R = -5.57 + 0.362 (\log Z) - 0.978 (\log Z)^2 + 0.167 (\log Z)^3$$

The object of using these distributions is to investigate, for a given set of boundary conditions, the sensitivity to decreasing permeability with depth and the effect of anisotropy. While the author believes that anisotropy is likely

it must be emphasized that this is based solely on circumstantial evidence (in situ stresses, observations of near surface excavations). Such existence in the prototype remains to be proven.

3.2.2 Porosity

The porosity of crystalline rocks is rarely measured in the field or laboratory. It is, however, a very important parameter in the determination of pore velocity. Empirically or theoretically derived relationships between porosity and permeability may be used to determine the porosity where only the permeability has been measured. These are briefly discussed below.

(1) Kozeny-Carmen relationship. The original work of Kozeny on the relationship between porosity and permeability was developed by Carmen (9). The initial formulation was for porous media, however, its applicability to fractured rock may be extended by considering the fractures as elongate pores. Fisher (10) reports the relationship as

$$D = \left(\frac{B\,k}{n^3}\right)^{1/2}$$

where: D = joint spacing
k = intrinsic permeability
B = coefficient ≃ 180 for this pore geometry
n = porosity
This therefore becomes

$$n = 5.646\left(\frac{k}{D^2}\right)^{1/3}$$

The relationship is shown graphically on Figure 3 for D = 0.5 and 5 m.

(2) Parallel plate model of Snow. This is fully described in the Technical Report (1). The relationship between porosity and permeability for 2-dimensional flow in equally spaced orthogonal joint sets is given by

$$n = 4.58\left(\frac{k}{D^2}\right)^{1/3}$$

This relationship is shown graphically on Figure 3 for D = 0.5 and 5 m. It may be noted, that for a cubical set of joints

$$n = 5.45 \left(\frac{k}{D^2}\right)^{1/3}$$

This expression closely approximates the Cozeny-Karmen relationship.

(3) Field and laboratory measurements. Porosity and permeability values of small granite samples were measured by Fisher (10) in connection with geothermal studies in the Los Alamos granite. Porosity values for Canadian crystalline rocks of 0.27% to 1.39% have been reported (11). No details of the method of measurement or of the corresponding permeability values are given.

Webster (12) measured travel times for radioactive traces in deep crystalline rocks in the Savannah Basin. The effective porosity value computed was 8×10^{-4} for a permeability estimated at between 1.633×10^{-6} and 7.424×10^{-6} m/s.

At Studsvik, in situ tests were carried out by AB Atomenergi and SGU on a joint at a depth of 60 m to determine pore velocities and retardation characteristics (13). These results are plotted in Figure 3 .

These field and laboratory results are plotted on Figure 3 . It may be noted that empirical porosities are higher than theoretical for the same permeability value.

For a given permeability, the computed porosity may vary over about three orders of magnitude. For this study, porosity values have been based upon Snow's parallel plate model for a constant joint spacing of 1.8 m. The joint spacing was based upon the only fully detailed information available at the beginning of the study ( ), and observations of personel familiar with excavations in the Swedish Precambrian rock. The application of this model will result in conservative (high) values of pore velocities. However, since the porosity has been calculated from the permeability in a consistent manner throughout the analyses, the reported pore velocities may be readily modified as further field data become available on site specific permeability - porosity relationships.

3.2.3 Boundary conditions

Because of the relatively high rainfall in Sweden compared to infiltration, the groundwater surface is, in general, within 3-4 m of the ground surface ( ).

For this study, we have assumed that the water table is coincident with the ground surface. For all models, the lower boundary has been taken as impervious; i.e., a flowline, at a depth of between 1000 and 2000 m, depending upon the model. Previous work by Freeze (6) has shown that the potential distribution is relatively insentitive to the elevation for the lower impervious boundary for models where horizontal flow predominates.

For the local models of flow around a repository, the definition of the limiting vertical boundaries is very important. The results of regional models (see section 4.2.1) and the existence of near vertical major structural features indicates that, in general, the equipotentials are near vertical. For these conditions, constant potential vertical boundaries may be employed. More field information (geological and geohydrological) is required to determine the natural permeability, potential and flow charactersitics of these features, before the boundary conditions can be defined with any certainty. In this study, both constant potential and zero flux (flowline) vertical boundaries have generally been used in the analyses for comparison.

3.3 Analysis

3.3.1 Validation

The finite element method has been validated with available analytical solutions during its development. For example, a comparison of results from the finite element method and an analytical solution for a sinusoidal constant potential boundary is given in Appendix B .

3.3.2 Assumptions

The finite element program used solves for parallel Darcian flow through a continuum. As discussed in (1), these conditions are violated to varying degrees for flow along fractures. The above assumptions will result in conservative estimates for pore velocities.

3.3.3 Conceptual model

The finite element method used in this study requires that the discrete fractures be replaced by an equivalent continuum (1). This is strictly acceptable only if the fracture spacing is small in comparison to the element size. At present, however, a more sophisticated model is not justified in view of the limited data available on fracture frequency, apertures and orientations.

3.3.4 2-dimensional and 3-dimensional flow

In nature, the groundwater flow is 3-dimensional. For computational ease and economy, the flow patterns have been simplified and considered 2-dimensional or axi-symmetric. This approximation is valid for sections parallel to flowlines, providing the flowlines themselves are neither converging or diverging markedly. Errors due to 2-dimensional or axi-symmetric flow assumptions may therefore be minimized by judicious choice of cross sections.

3.4.1 Primary results

The primary results from a steady state groundwater analysis are potential and flux fields. The potential distributions are a function of the relative permeability values at different locations. The flux, however, is a function of both the relative and absolute permeability values. On the premise that a better estimate is possible of the relative permeabilities than of the absolute permeabilities, the reliability of the potential distribution will be better than of the fluxes.

3.4.2 Derived results

The overall objective of the analysis is to determine the pore velocities and flow paths in the repository area. For classical porous media flow

$$V_{pore} = \frac{K}{n} i$$

This relationship may not be completely valid for fracture flow. In particular no account is taken of the variations in fracture aperture and connectivity resulting in flow tortuosity. A more complete expression for the effective pore velocity may therefore be

$$V_p = C_T \frac{K}{n} i$$

where $0 < C_T < 1$. Since there is no data available on C_T, for this study it has been conservatively assumed to be unity.

The porosity itself may be considered as comprising two parts. The flow takes place only through a portion of the porosity, n_f (specific yield). The remainder is dead space, n_s (specific retention). If the porosity is back calculated from travel times, n_f will be determined. If the porosity is computed by 'static'

methods (thin sections, volumetric displacement) then the total porosity,n, ($n_s + n_f$) will be determined.

In order to demonstrate the variability of computed pore velocities arising from limited avilability of data and measurement errors combined, but not including model errors or spatial variability which may be significant, probability distributions have been computed. The parameters have been assumed to have log-uniform distributions within the following ranges:

$K = 9.5 \times 10^{-9}$ to 9.5×10^{-8}

$n = 9 \times 10^{-6}$ to 6.0×10^{-5}

$i = 5 \times 10^{-4}$ to 8.0×10^{-3}

These values indicate the ranges of parameters expected to be encountered in a repository area. The resulting probability distribution for pore velocity is shown on Figure 4 . It can be seen that the computed pore velocities have a range of three orders of magnitude.

In summary, it is concluded that until more specific data are available on the permeability and porosity at a repository site, the pore velocity can only be predicted to within a range of about three orders of magnitude.

4. PHYSICAL ASPECTS

4.1 Site Geology

4.1.1 Topography

F o r s m a r k

The area around Forsmark exhibits subdued local relief of about 10 m. The major low lying areas are occupied by lakes. Drainage is generally poorly developed, with the principal drainage courses developed along glacially deepended tectonic features in the bedrock (see later). The proposed repository is located about 15 km from the Baltic coast. The existing ground surface is at about elevation 35 m. (figure 5).

Inland from the repository the terrain is similar with the average elevation rising about 1 m in 2 km. At a distance of about 100 km, between Sandviken and Avesta, the relief becomes more pronounced, typically 100 m and locally up to 300 m. This topography continues westwards to the Norrland mountains area.

O s k a r s h a m n

The area around Oskarshamn exhibits a highly dissected relief of about 20 m. The candidate repository site is located to the east of Götemar, at an elevation of about 20 m above sea level and about 5 km from the Baltic Sea coast (figure 6). Inland, the average ground elevation rises at about 1 m per km to the Götaland Highlands. Drainage from this upland area is principally to the south-south east along valleys sub-parallel to the Vättern graben. Relative relief in the Götaland Highlands is generally 20 to 50 m, and locally over 100 m.

4.1.2 Climate

Precipiation for both the Oskarshamn and Forsmark regions increases from about 500 mm per year at the coast to about 700 mm per year inland (17).

Infiltration measurements of typical terrain units in Central Sweden indicate an infiltration coefficient of 0.11 to 0.37 (18).

4.1.3 Geology

The detailed geology of the candidate areas is being studied by SGU for KBS. Only the salient points affecting groundwater flow are discussed below. It should be noted that a criterion for preliminary site selection required an area of uniform granitic bedrock adjacent to the Baltic coast.

F o r s m a r k

The bedrock of the Forsmark area comprises Precambrian Svecofennian gneisses and gneissic granites with some leptites and minor areas of younger granitic and basic intrusions. Offshore, to the north east, the Precambrian basement is overlain by Jotnian sandstones, Cambro-Ordovician shales and sandstones and Ordovician Limestone (19).

In the candidate repository area, the bedrock is an even grained weakly foliated granite. Leptites containing worked deposits of iron occur nearby. The extent of abandoned workings has not been investigated in this study. It is recommended however, that an effort be made to determine the location extent and nature of any nearby workings since they could have an effect on the groundwater regime.

The surficial deposits of the area comprise tills overlain by post-glacial clays in the valley bottoms.

The structural geology of the area is extremely complex, reflecting a tectonic history extending back to the Precambrian. First and second order lineaments in the region have been identified from air photographs and satellite imagery by Stephansson and Carlsson (19) and more recently by SGU. A semi-quantitative examination of the predictive capability of lineation identification from satellite imagery is given by Ehrenborg (20) based on a study of an area to the south west of Stockholm.

The major structural features deduced from field mapping and air photo interpretation are shown on fig. 7 . The nature of these zones in the immediate vicinity of the proposed site has not, as yet, been investigated by drilling. The following preliminary interpretation has been provided by Brotzen (21).

1. Dextral shear movement along N-S zones (Finnsjön and Gåvestbo linear features), resulting in secondary second-order shearing along NE-SW lines.
2. Reactivation of N-S features by normal faulting, with tilting of the block towards the west. A possible horst and graben structure has been identified along the Gåvestbo feature.

Surface mapping of the joints has been undertaken by SGU together with deep drilling. The extent of fracturing at depth is currently being investigated by vertical and inclined drillholes. The results, however, are not yeat available.

O s k a r s h a m n

The bedrock of the Oskarshamn region comprises Precambrian Gothian rocks known collectively as the Småland-Värmland intrusions, primarily granitic and grandodiori-tec in composition. Younger granites of subjotnian age have intruded the Småland-Värmland suite at some locations. The candidate repository site in the Oskarshamn area is located within such an intrusion, the Götemar massif. Petrographic and structural aspects are described in detail by Kresten and Chyssler (22).
The granite is primarily massive, coarse grained, with some medium, fine grained and porphyritic varieties.

Offshore, the Precambrian rocks are understood to be overlain by Cambrian and Silurian sandstones and limestones. Rocks of this age are exposed in Öland, some 25 km offshore from the Götemar area.

The principal lineaments in the Oskarshamn area have been identified from air photos and satellite imagery Figure 8 (23). The major joint directions in the granite massif have been interpreted by Kresten and Chyssler (op.cit) as representing classic joint patterns of granitic plutons. Four joint sets have been identified: radial, tangential (concentric) diagonal and flat lying. A north-south reverse fault with a proven lateral extension of more than 25 km is located about 500-600 m west of the area being studied.

4.2 Boundary Conditions and Material Properties Used

Because of modelling limitations and in order to identify relative parametric and boundary condition effects, the modelling study has been divided into regional and local models.

4.2.1 Regional models

Based on the information detailed in Technical Report 1 (1), the regional flow is considered to take place primarily in the major tectonic features, and possibly also in the upper portion of the bedrock where subhorizontal joints are well developed.

The major structural features were scoured by the ice and are now occupied by valleys with lakes. These lakes, in turn, reflect and/or control the groundwater

level in the underlying rock, and thus may be used as indicators of the regional groundwater level. The spot elevations of lakes marked on the 1:300 000 topographic maps of the Forsmark and Oskarshamn areas were therefore plotted and contoured (Figures 9 and 10. Judgement was exercised in some areas where perched lakes occurred. In these instances the higher elevations were neglected and only the lower ones used for preparation of the contours.

In the Upplands area there is a regional gradient from the hills in the Dalarna area, to the Baltic coast in the east, and to a lesser extent to Lake Mälaren in the south east. The valley of the Dalälven creates a noticeable perturbation to the regional contours. In the Forsmark Area, the regional groundwater gradient is estimated to be about 1:1000.

The topography of Oskarshamn area rises more rapidly than in Upplands. As a result, the regional groundwater gradient is steeper, being about 2:1000.

For both areas, stylized flow lines have been drawn orthogonal to the groundwater contours. The real flow paths however, will be along the major tectonic features. Two-dimensional vertical sections for use in regional flow modelling have been taken along representative flow lines. In these models no flow out of plane has been considered.

4.3 Local Models

For local models representative potential distributions and/or fluxes from the regional model are used to define the boundary conditions for smaller areas.

In particular, the major tectonic features have been used as model boundaries to enable the response of the intervening rock block to be studied for various material parameter values and boundary conditions.

5. RESULTS OF ANALYSIS

5.1 Regional models

Models for the Forsmark and Oskarshamn regions have been analyzed as two-dimensional vertical sections. The principal difference between the two regions is the slope of the upper defined potential boundary; for Forsmark it is 1 in 1000 and for Oskarshamn it is 2 in 1000. The main objectives of the regional modelling are:

- to define boundary conditions for local models
- to interface with local models to enable probable overall travel times through the repository area to be determined.

The following cases, as discussed in section 3.3, have been analyzed for Oskarshamn: The model is shown in Figure 11

Case 1. Isotropic permeability $K = 1.0 \times 10^{-8}$ m/s (see Figure 12)

Case 2. Isotropic permeability decreasing with depth as per empirical function (see Figure 13)

Case 3. Anisotropic permeability:
$K_z = 1.0 \times 10^{-9}$ m/s
K_r = decreasing with depth as per empirical function (see Figure 14)

For these cases the vertical boundary beneath the Baltic Sea has been treated as a constant potential boundary at zero potential. The inland vertical boundary has been considered as a flowline (impervious) boundary on the basis of symmetry in the recharge area.

For Forsmark the case 1 permeability distribution has been analyzed. For this case, both vertical boundaries have been treated as constant potential boundaries (Figures 15 and 16).

It can be seen that for permeability distributions 2 and 3 the flux is concentrated in the top 100 m or so. We will designate this zone as the active zone and the lower zone as the quiescent zone. In the isotropic case this feature does not occur.

5.2 Local Topography and Discontinuity Models

To study the effect of topographic variations and of singular discontinuities, two example models have been used.

5.2.1 Topography effects

Figure 17 shows the mesh used to study the effect of a high point on flow patterns. The relief is 50 m and base width of the feature is 1 km. The effect of lower (or higher) relief can be determined from the results by linear scaling of the equipotentials and/or pore velocities. Thus, for only 10 m relief

$$V_{p10} = (10/50) \cdot V_{p50}$$

for the pore velocity at the same point.

The following analyses have been undertaken:

- Isotropic permeability (Case 1)
  $K = 1.0 \times 10^{-8}$ m/s
  vertical boundaries impervious i.e. flowlines (see Figure 18)

- Anisotropic permeability (Case 3)
  $K_z = 1.0 \times 10^{-9}$ m/s
  K_r decreasing with depth as per empirically derived function, vertical boundaries impervious i.e. flowlines (see Figure 19)

- Isotropic permeability (Case 1)
  $K = 1.0 \times 10^{-8}$ m/s
  vertical boundaries constant potential = 0 (see Figure 20)

- Anisotropic permeability (Case 3)
  $K_z = 1.0 \times 10^{-9}$ m/s
  K_r decreasing with depth as per empirically derived function, vertical boundaries constant potential = 0 (see Figure 21)

It is apparent from a study of the equipotentials and fluxes that the groundwater flow is very sensitive to the permeability distribution. In particular, the Case 3 analyses show an quiescent layer which does not appear for the Case 1 analyses. The boundary conditions have a lesser effect, modifying the pore velocities by a factor of about wo.

It should be noted that permeability condtions in a major structural feature may be relatively isotropic in the vertical plane. Thus, flow patterns in these features would take a form similar to the Case 1 examples i.e. deeply penetrating flow. The bedrock blocks, however, between the major structural features may have horizontal anisotropic permeability. For these areas, therefore the flow penetration from the topographic features will not be as marked.

The magnitudes of the pore velocities resulting from topographic effects may be compared with those resulting from the regional gradient alone, from a comparison of the relative potential gradients. For illustration, the potential gradients at a depth of 350 m immediately below the break in slope of the feature, are given in Table 1 . The following should be noted:

1. For the homogeneous isotropic permeability distribution (Case 1) the horizontal potential gradients are of the same order of magnitude as the regional gradient even for only 5 m relief. In addition, there are significant upward vertical gradients, and hence flows, at 500 m depth.

2. For the anisotropic permeability distribution (Case 2), the horizontal potential gradients are reduced by a factor of about eight compared to the isotropic conditions. For a relief of 5 m they are thus 10 to 20% of the typical regional gradient. Vertical potential gradients at 500 m are all downwards.

5.2.2 Discontinuity effects

Most of the major structural features are near vertical in attitude. These will have very little effect upon the flow patterns since the equipotentials themselves are near vertical. The following example therefore is illustrative rather than typical. A 1 m thick discontinuity, dipping at 14^{o} has been analyzed. A regional gradient of 2 in 1000 and isotropic constant permeability of 1.0×10^{-8} m/s have been used for the following cases: The mesh is shown in Figure 22

- No discontinuity, baseline analysis for comparison (see Figure 23)
- Discontinuity K = 1.0×10^{-6} m/s dipping opposite to the direction of flow (see Figure 24)
- Discontinuity K = 1.0×10^{-6} m/s dipping in the direction of flow (see Figure 25)

  Discontinuity K = 1.0×10^{-5} m/s dipping in the direction of flow (see Figure 26)

For this discontinuity conductivity where the discontinuity is dipping opposite to the direction of flow, the effect on the equipotentials is negligible. Pore velocity vectors in the discontinuity are, however, higher than in the surrounding rock, sub parallel to the direction of the discontinuity inclination. For the case considered, the discontinuity causes an upward displacement of the flow path of about 100 m. The relative magnitude of flow up the discontinuity compared to cross flow will depend upon the permeability contrast and the extent of anisotropy within the discontinuity. Without further data on the nature of such discontinuities, if they exist, meaningful conclusions cannot be drawn.

Where the dip of the discontinuity is in the direction of flow, the effect is to increase the equipotentials at depth near the discontinuity compared with the homogeneous baseline case. That is, the discontinuity tends to attract flow at depth depending on discontinuity conductivity. This is illustrated in Figure 27, which is a plot of the head difference between nodal points on the discontinuity and boundary points vertically above. At a depth of 667 m, the vertical gradient above the discontinuity is as follows:

- homogeneous baseline case: $i_z = -1.76 \times 10^{-5}$
- discontinuity: $K = 1 \times 10^{-6}$ m/s $i_z = -2.85 \times 10^{-5}$
- discontinuity: $K = 1 \times 1^{-5}$ m/s $i_z = -10.92 \times 10^{-5}$

While the increase in gradient is up to an order of magnitude, the absolute values of the gradient are still small in comparison with typical regional horizontal gradients (1 to 2 $\times 10^{-3}$)

From these analyses it is concluded that the discontinuity dipping in the direction opposite to the regional flow is may be more critical since it can cause a vertical displacement in a flow path. If dispersion (mixing) is strong then this could provide a preferential pathway to the surface. It may be noted, however, that the presence of a discontinuity appears to have little disturbing effect on the quiescent zone.

5.3 Site Model: Forsmark

The objective of this part of the study was to evaluate the relative strengths of the regional flow compared to that due to topographic effects. The models were designed to study the flow in the intact repository zone. The flow conditions in the bounding discontinuities may be representative of flow in singular features, but are very uncertain. Because of this, pore velocities in these zones are not shown on the figures. A plan of the site showing the major geological features is given in Figure 5. The mesh used to model the groundwater flow for the presently existing natural conditions is shown in Figure 28.

The groundwater surface and hence upper boundary potentials have been assumed coincident with the ground surface. The relief of the ground surface itself, however, has not been included in the model.

Inspection of the topography of the area indicates a regional gradient from Finnsjön (elevation 28.1) to Södra and Norra Åsjön (elevation 11.9) over a distance of about 5 km. This represents an overall gradient of 3.24×10^{-3}.

The surface potential of the Finnsjön linear feature has been taken equal to the surface elevation of 28.1 at Finnsjön. The surface potential of the Gåvestbo tectonic feature has been taken at elevation 24.5 m, which is the average ground surface estimated from the 1:500 000 topographic map.

The bounding discontinuities have been represented by 10 m wide zones with an isotropic permeability of 1.0×10^{-5} m/s. Two types of boundary conditions for these discontinuities have been considered.

1. Constant potential with depth. This corresponds to a regional vertical equipotential
2. Constant potential defined only at ground surface. The vertical boundary under these conditions is a streamline.

The field potential distribution is expected to lie between these two extreme assumptions.

Three permeability assumptions have been combined with the two possible boundary conditions above for the following analysis:

- Case 1. Isotropic permeability, K = 1.0 x 10^{-8}m/s vertical flowline boundaries (see Figure 29)

- Case 2. Isotropic permeability decreasing with depth as per empirically derived function (see Figure 30)

- Case 3. Anisotropic permeability, K_z = 1.0 x 10^{-9} m/s K_r decreasing with depth as per empirically derived function (see Figure 31)

- As for 1. above except with constant potential vertical boundaries (see Figure 32)

- As for 2. above except with constant potential vertical boundaries (see Figure 33)

- As for 3. above except with constant potential vertical boundaries (see Figure 34)

The following conclusions should be noted:

- For the same material properties, the change of boundary conditions has only a slight effect on the pore velocity magnitudes. The directions are modified, especially near to the bounding discontinuities.

- The pore velocities at 500 m depth decrease successively for the cases of isotropic constant permeability, isotropic permeability decreasing with depth, and anisotropic permeability decreasing with depth, respectively. For the constant potential vertical boundary simulations, the computed horizontal potential gradients at elevation - 500 m are shown on Figure 35. The average gradient between the two boundaries is shown for comparison. Divergence from the average gradient is a measure of the residual effect at depth of the upper boundary constant potential variations due to topographic relief. The anisotropic cases thus show that a quiescent zone could be expected.

6. SUMMARY AND CONCLUSIONS

Based on regional models of groundwater flow, the regional hydraulic gradient at depth in equal to the regional topographic gradient. As a result, the equipotentials are near vertical.

The permeability distribution with depth influences the groundwater flow patterns. A zone of sluggish flows, the quiescent zone is developed when the permeability decreases with depth.This feature is accentuated when horizontal anisotropy, with the horizontal permeability higher then the vertical permeability, is included. The presence of an inactive zone till be a prerequesite for a satisfactory repository site.

The effect of an inclined discontinuity representing a singular geological feature such as a fault plane or shear zone has been modelled. The quiescent zone does not appear to be unduly disturbed by such a feature. However, meaningful quantitative predictions related to the flows in a typical singular feature cannot be made without more specific data on their hydraulic properties (permeability, anisotropy, fracture spacing).

The effect of relief of the ground surface and hence the water table was studied using a simple model. The influence of anisotropy and boundary conditions was evaluated. With horizontal anisotropy and horizontal permeability decreasing with depth, the potential gradients due to the topographic relief decrease rapidly with depth. Perturbations to the quiescent zone under these conditions would be markedly reduced, compared to the effects for isotropic permeability.

Two dimensional analysis has been made for a site specific section of a candidate reository site at Forsmark. The lateral extent of the model was defined by major tectonic features, assumed vertical.

Potential gradients and pore velocities have been computed for a range of boundary conditions and assumed material properties. The potential gradients for the models with anisotropic permeability approach the average potential gradient between the boundaries.

The result of this study of the initial groundwater conditions will be used as input data for the analyses of the thermomechanical perturbations of the groundwater regime. In the long term, the groundwater flow will return to the initial conditions. The residual effects of the repository on the flow will be discussed in part 2 of this report.

REFERENCES

1. Stille, H., Burgess, A.S. and Lindblom, U.E. 1977. "GROUNDWATER MOVEMENTS AROUND A REPOSITORY, Phase 2, Technical Report 1, Geological and Geotechnical Conditions". To be submitted to KBS - Kärnbränslesäkerhet, Stockholm, Sweden.

2. Wu, T.H., Vyas, S.K. and Chang, N., 1973, "PROPABILISTIC ANALYSIS OF SEEPAGE" ASCE J. Soil Mech. and Found. Division, SM4 pp 323 - 340.

3. Freeze, R.A., 1975, "A STOCHASTIC-CONCEPTUAL ANALYSIS OF ONE-DIEMENSIONAL GROUNDWATER FLOW IN NONUNIFORM HOMOGENEOUS POROUS MEDIA" Water Resources Research vol 11 no 5 pp 725 - 741.

4. Gelhar, L.W., 1976 "EFFECTS OF HYDRAULIC CONDUCTIVITY VARIATIONS ON GROUNDWATER FLOWS" 2nd Int. Symp. on Stochastic Hydraulics, Lund, Sweden.

5. Gelhar, L.W., 1976, "STOCHASTIC ANALYSIS OF FLOW IN AQUIFERS" Advances in Groundwater Hydrology, American Water Resources Association.

6. Wilson, C.R., and Witherspoon, P.A., 1970, "AN INVESTIGATION OF LAMINAR FLOW IN FRACTURED POROUS ROCK" Depth of Civil Engineering, Institute of Transportation and Traffic Engineering, Publication No 70 - 6 University of California, Berkeley.

7. Castillo, E., Krizek, R.J., and Karadi, G.M. 1972. "COMPARISON OF DISPERSION CHARACTERISTICS IN FISSURED ROCK" Proc. 2nd Int. Symp. on Fundamentals of Transport Phenomena in Porous Media, Guelph, Canada, vol 2 pp 778 - 797.

8. Snow D.T. 1968 "FRACTURE DEFORMATION AND CHANGES IN PERMEABILITY AND STORAGE UPON CHANGES IN FLUID PRESSURE" Q. Colorado School of Mines vol 63 no 1 pp 201 - 244.

9. Scheidegger, A.E., 1957, "THE PHYSICS OF FLOW THROUGH POROUS MEDIA" University of Toronto Press.

10. Fisher, H.N., 1977 "AN INTERPRETATION OF THE PRESSURE AND FLOW DATA FOR THE TWO FRACTURES OF THE LOS ALAMOS HOT DRY ROCK (HDR) GEOTHERMAL SYSTEM" Energy resources and excavations technology, Proc. 18th U.S. Symposium on Rock Mechanics, Keystone, Colorado pp. 1B4 - 1 to 1B4 - 8.

11. Jessop, A.M., Robertson, P.B., Lewis, T.J., 1976 "A BRIEF SUMMARY OF THERMAL CONDUCTIVITY OF CRYSTALLINE ROCKS" Canadian Dept of Energy, Mines and Resources Report 76 - 4.

12. Webster, D.S., Proctor, J.F., and Marine I.W., 1970, "TWO WELL TRACER TEST IN FRACTURED CRYSTALLINE ROCK" U.S. Geol. Surv. Water Supply Paper 1544 - 1.

13. Häggblom, H., 1977. "CALCULATIONS FOR NUCLIDE TRANSPORT IN ROCK AND POROUS MEDIA" AB Atomenergi Report AE-RF-77-3253 Submitted to KBS - Kärnbränsle-säkerhet Stockholm, Sweden.

14. Carlsson Martna and Olssen 1977. Drillhole DBT-1 Private communication.

15. Gustafsson, Y., 1968, "THE INFLUENCE OF TOPOGRAPHY ON GROUNDWATER FORMATION" in Groundwater Problems, ed. Eriksson, E., Gustafsson, Y., Nilsson, K. Pergamon Press, pp 3 - 21.

16. Freeze, R.A., 1969, "THEORETICAL ANALYSIS OF REGIONAL GROUNDWATER FLOW" Inland Waters Branch Scientific Series 3, Dept of Energy Mines & Resources, Ottawa, Canada.

17. Sømme, A. 1960, The Geography of Norden, J.W. Cappeleus Forlag, Olso.

18. von Brömssen, F.V. "INFILTRATION COEFFICIENTS FOR GROUNDWATER INVESTIGATIONS IN MORAINE CLAY DISTRICTS IN CENTRAL SWEDEN" Nordisk Hydrologisk Konferens, Lund, Sweden, vol 2 pp 241 - 249. 1970

19. Stephansson, O. and Carlsson, H., 1976, Seismotektonisk analys av Fennoskandias berggrund, Luleå Tekniska Högskolan, Sweden.

20. Ehrenborg, J., 1977, "GEOLOGICAL INTERPRETATION OF BEDROCK FROM A LANDSAT COLOUR COMPOSITE" Geologiska Föreningens i Stockholm Förhandlingar vol 99 pp 58 - 62.

21. Brotzen, O., 1977, Private Communication.

22. Kresten, P. and Chyssler, J., 1976, "THE GÖTEMAR MASSIF IN SOUTH EASTERN SWEDEN: A RECONNAISSANCE SURVEY". Geologiska Föreningen i Stockholm Förhandlingar vol 98 pp 155 - 161.

23. Brotzen, O., Magnusson K-Å, and Ehrenborg J., 1976. "OSKARSHAMN, GEOLOGISK ÖVERSIKT" SGU 1976-11-01.

24. Gustafsson, I, 1977 Private Communication

25. Snow, D.T. 1968 Hydraulic character of the fractured metamorphic rocks of the front range and implications to the Rocky Mountain Arsenal wells. Q. Colorado School of Mines vol 63 no.1 pp 167 - 1999.

26. Carlsson, A and Olssen, T., 1977 Permeabilitetens variation i det svenska urberget, SGU

27. SGU 1977 Investigation for KBS Kråkemåla drillhole K1.

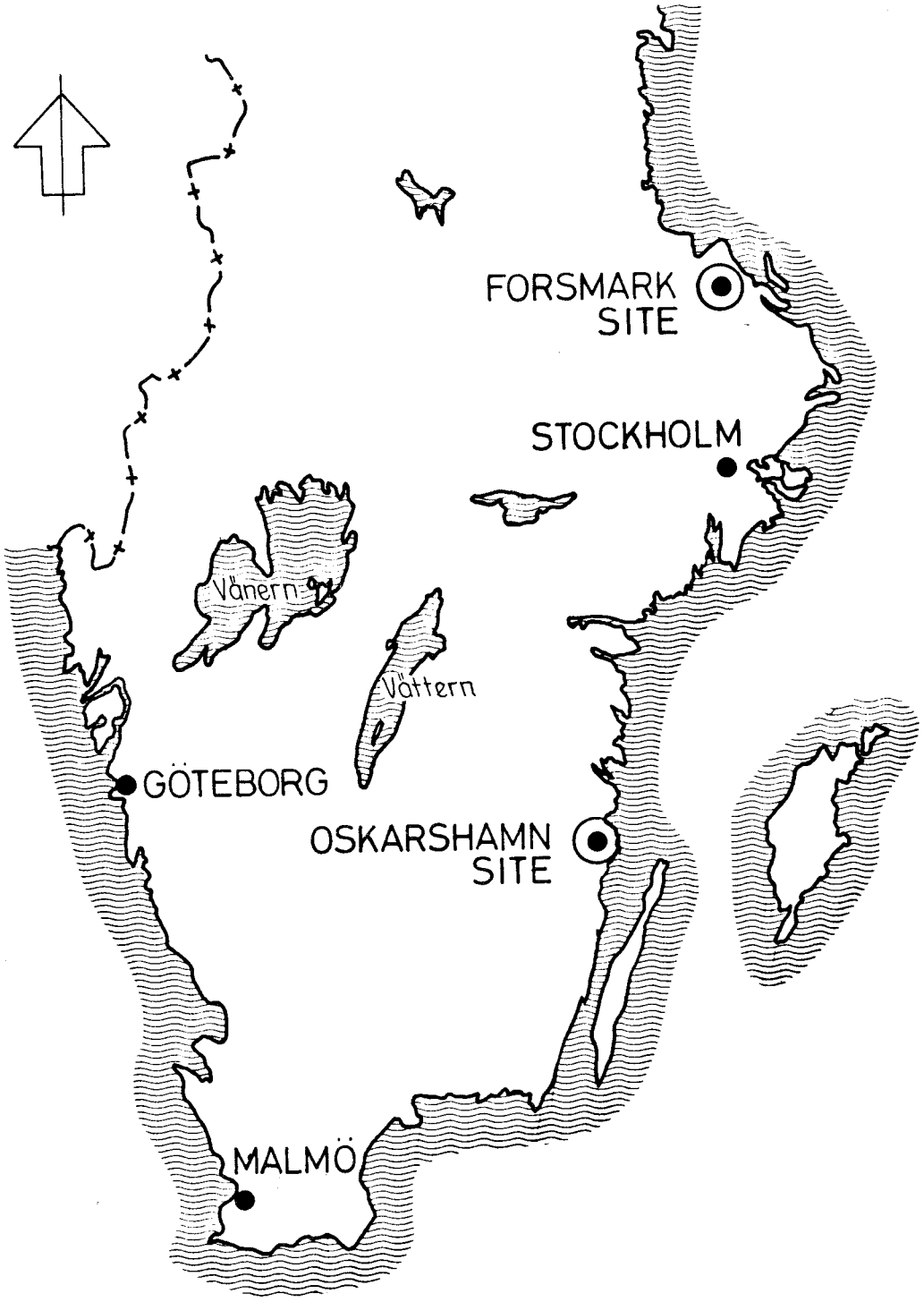

FIGURE 1. LOCATIONS OF INVESTIGATED SITES CONSIDERED IN THIS STUDY

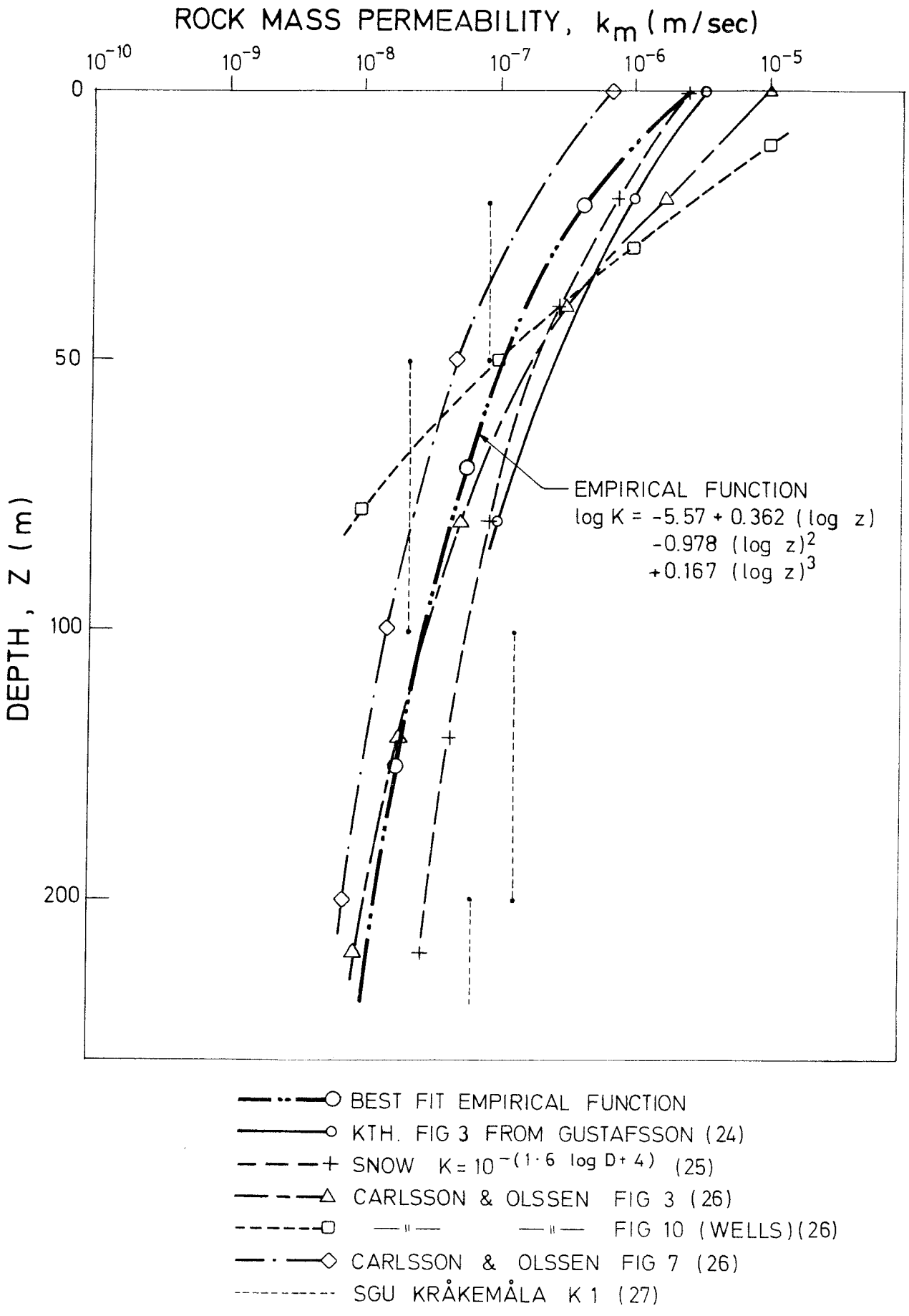

FIGURE 2. PERMEABILITY V DEPTH

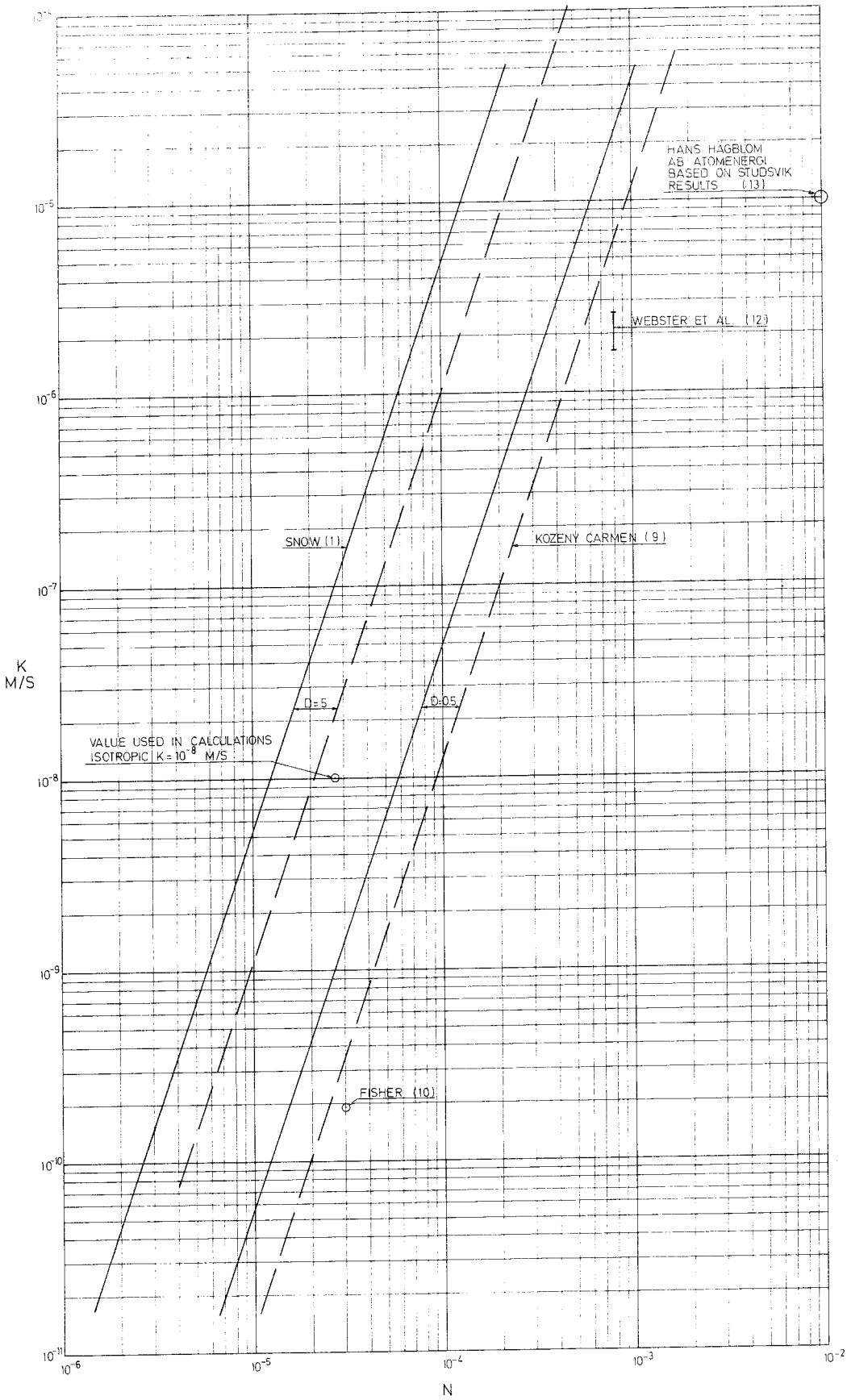

FIG. 3 POROSITY - PERMEABILITY RELATIONSHIPS

PARAMETER	VALUE RANGE		UNITS
K	7.9×10^{-10}	3.2×10^{-9}	m / s
n	1.0×10^{-5}	6.3×10^{-5}	
i	5.0×10^{-4}	8.0×10^{-3}	

$$Vp = \frac{K}{n} \cdot i$$

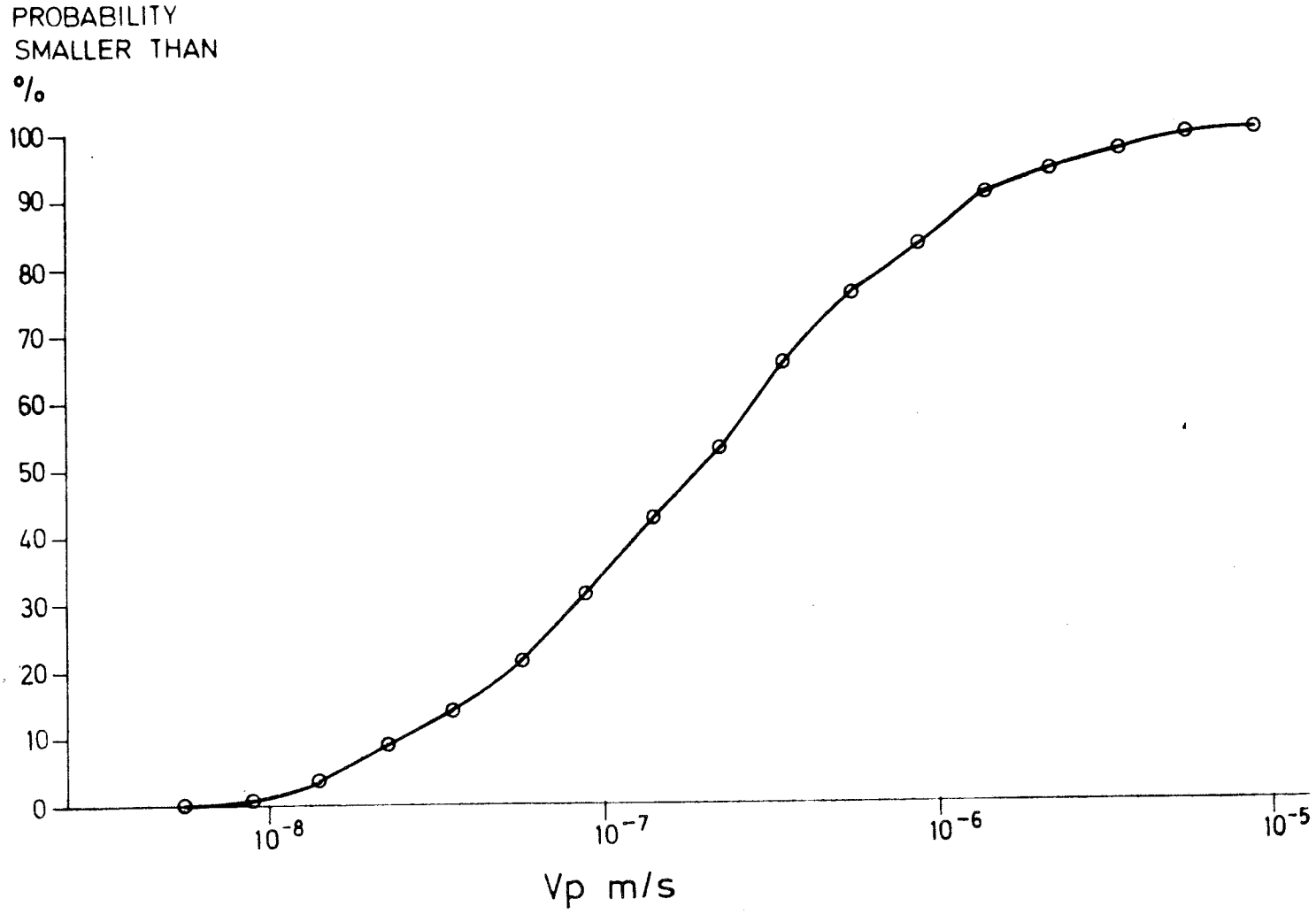

FIGURE 4 PORE VELOCITY RELIABILITY ANALYSIS

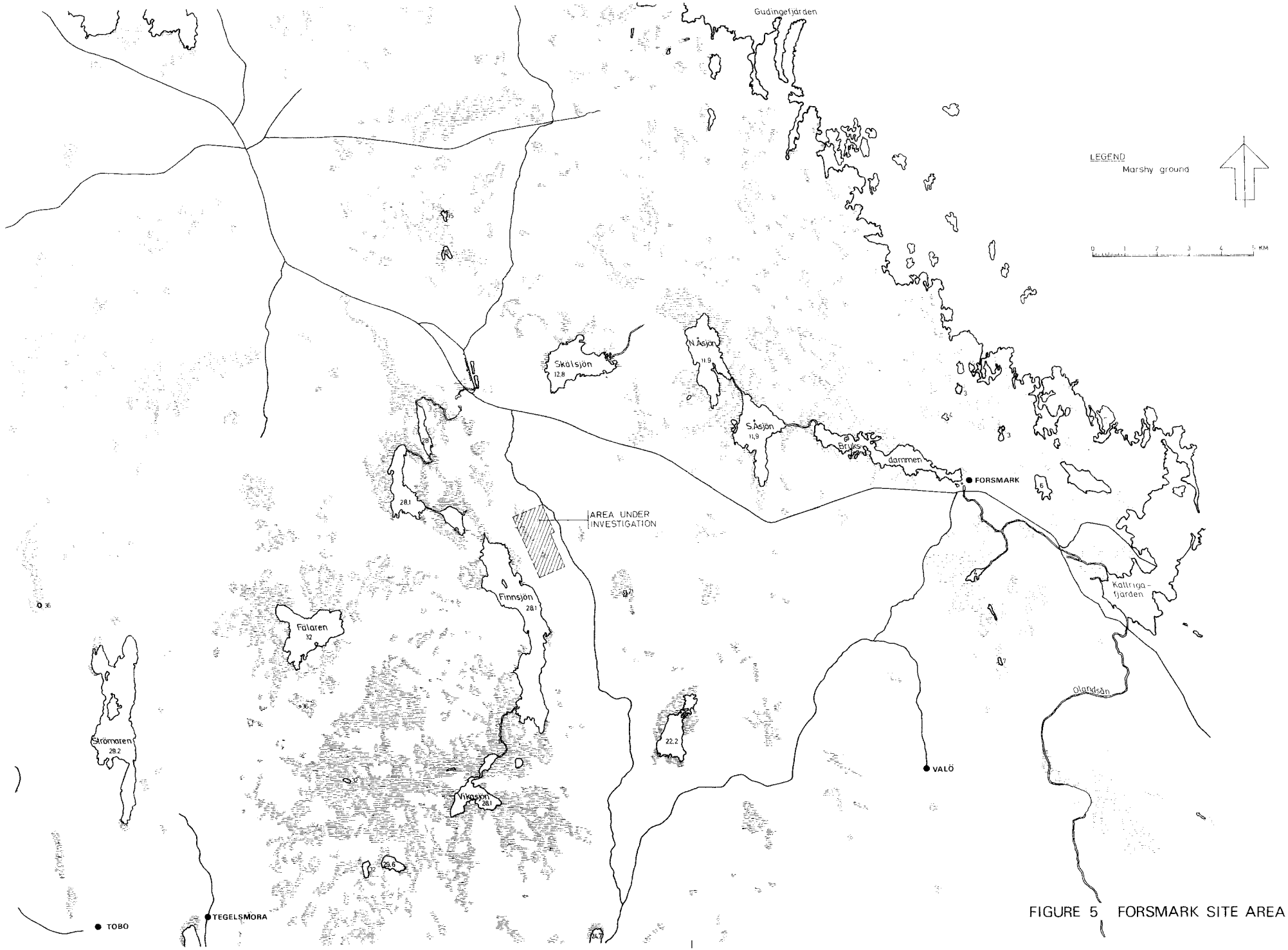

FIGURE 5 FORSMARK SITE AREA

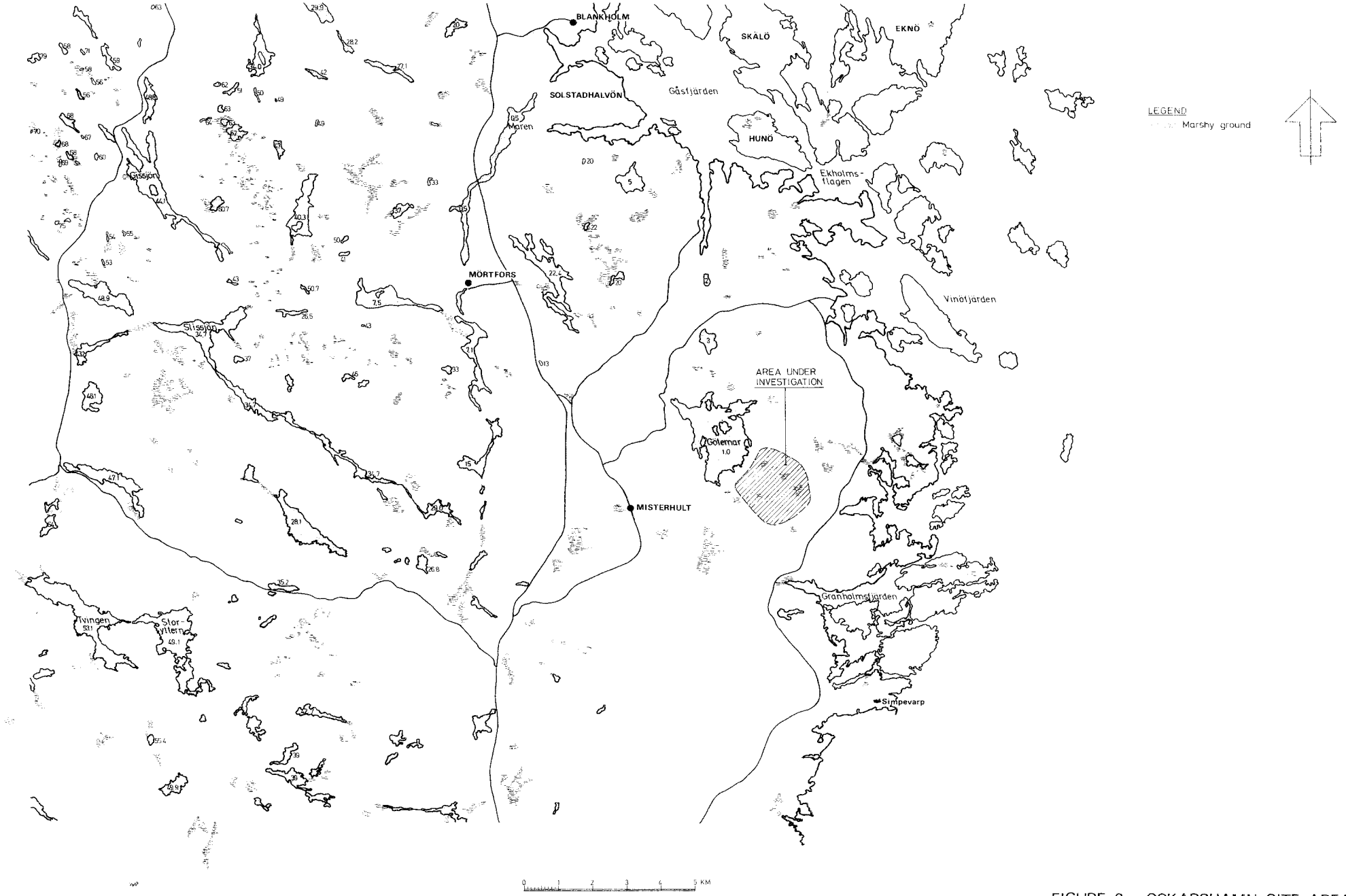

FIGURE 6 OSKARSHAMN SITE AREA

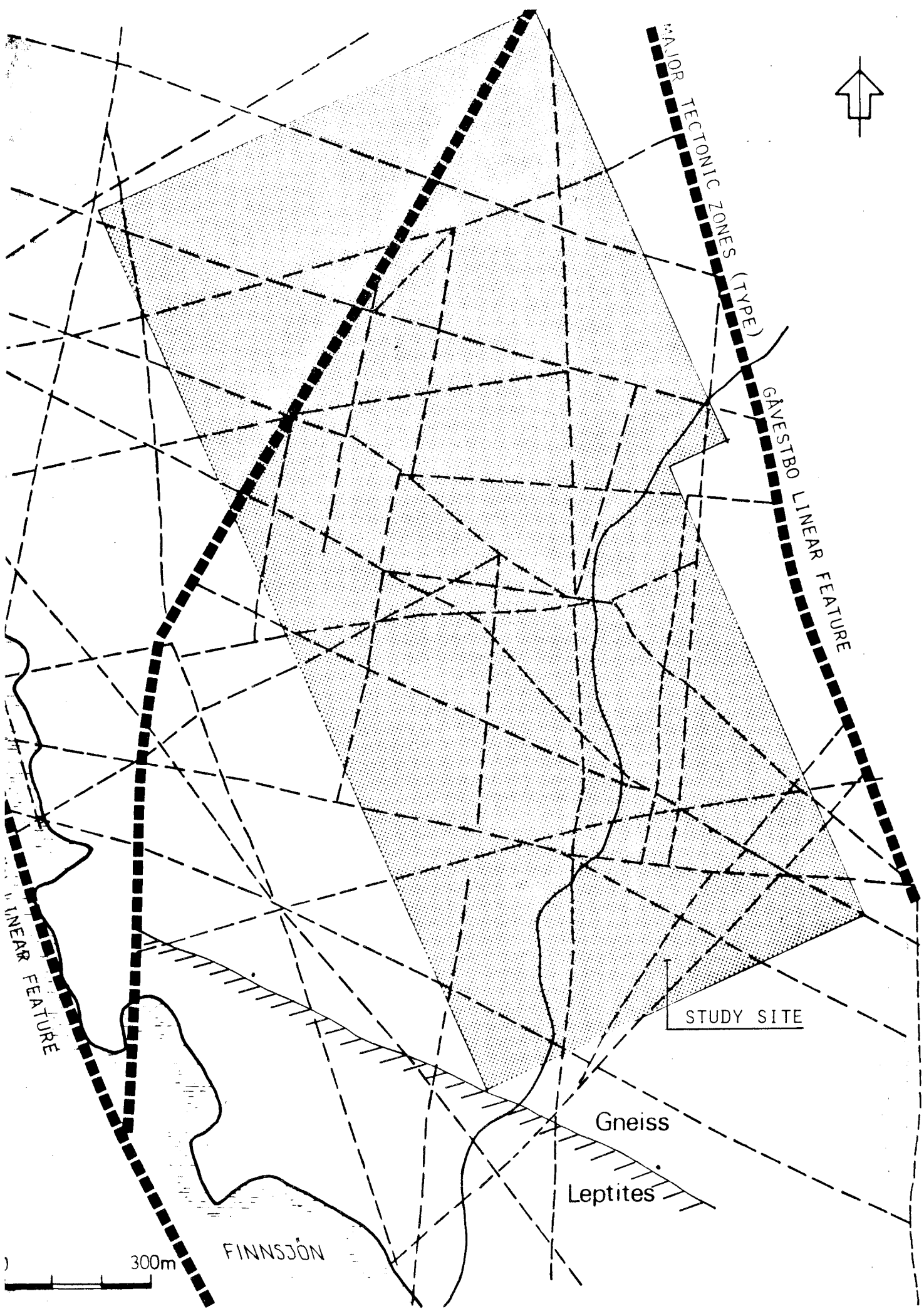

FIGURE 7 MAJOR STRUCTURAL FEATURES AT THE FORSMARK STUDY SITE.

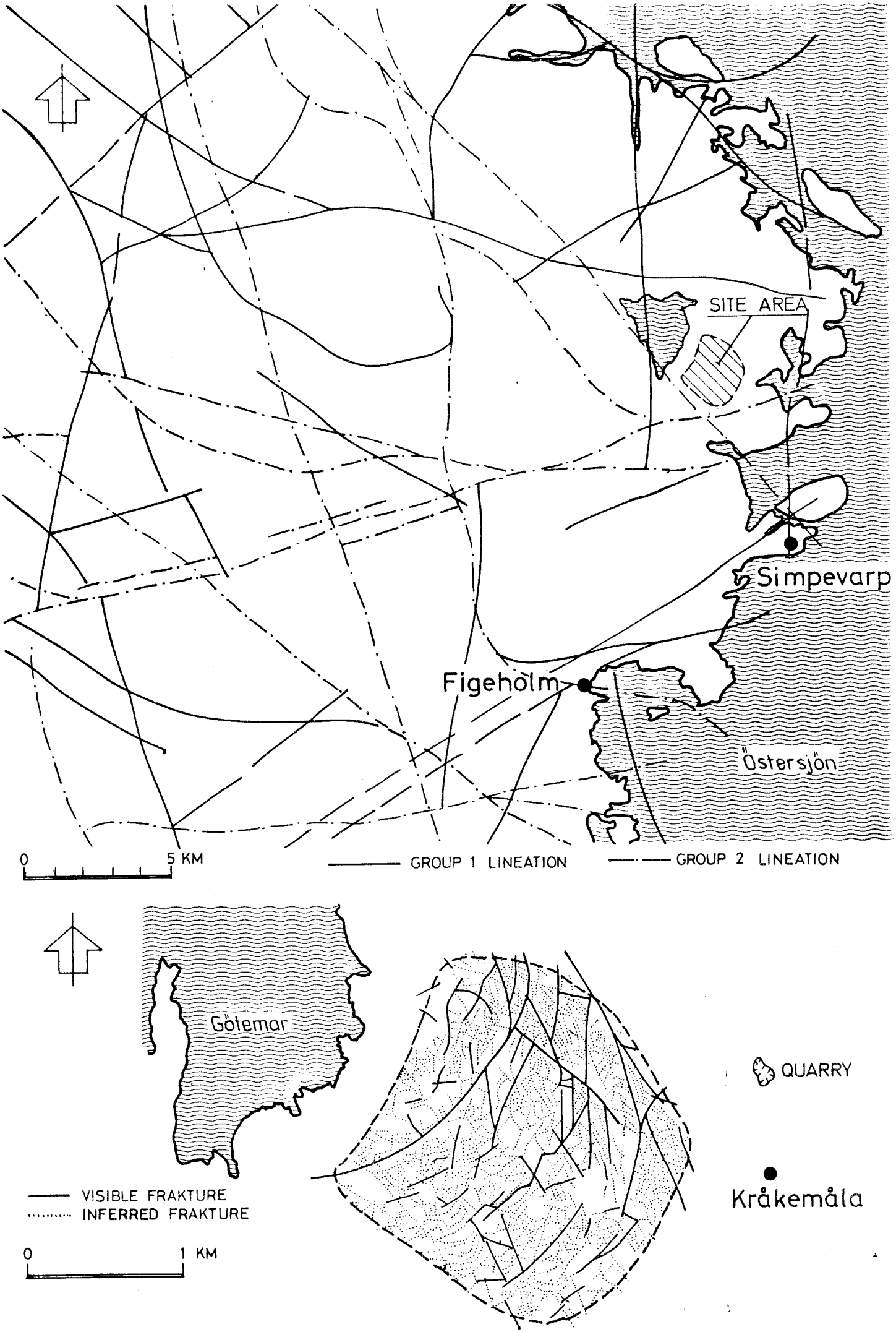

FIGURE 8. OSKARSHAMN - STRUCTURAL GEOLOGY ( )

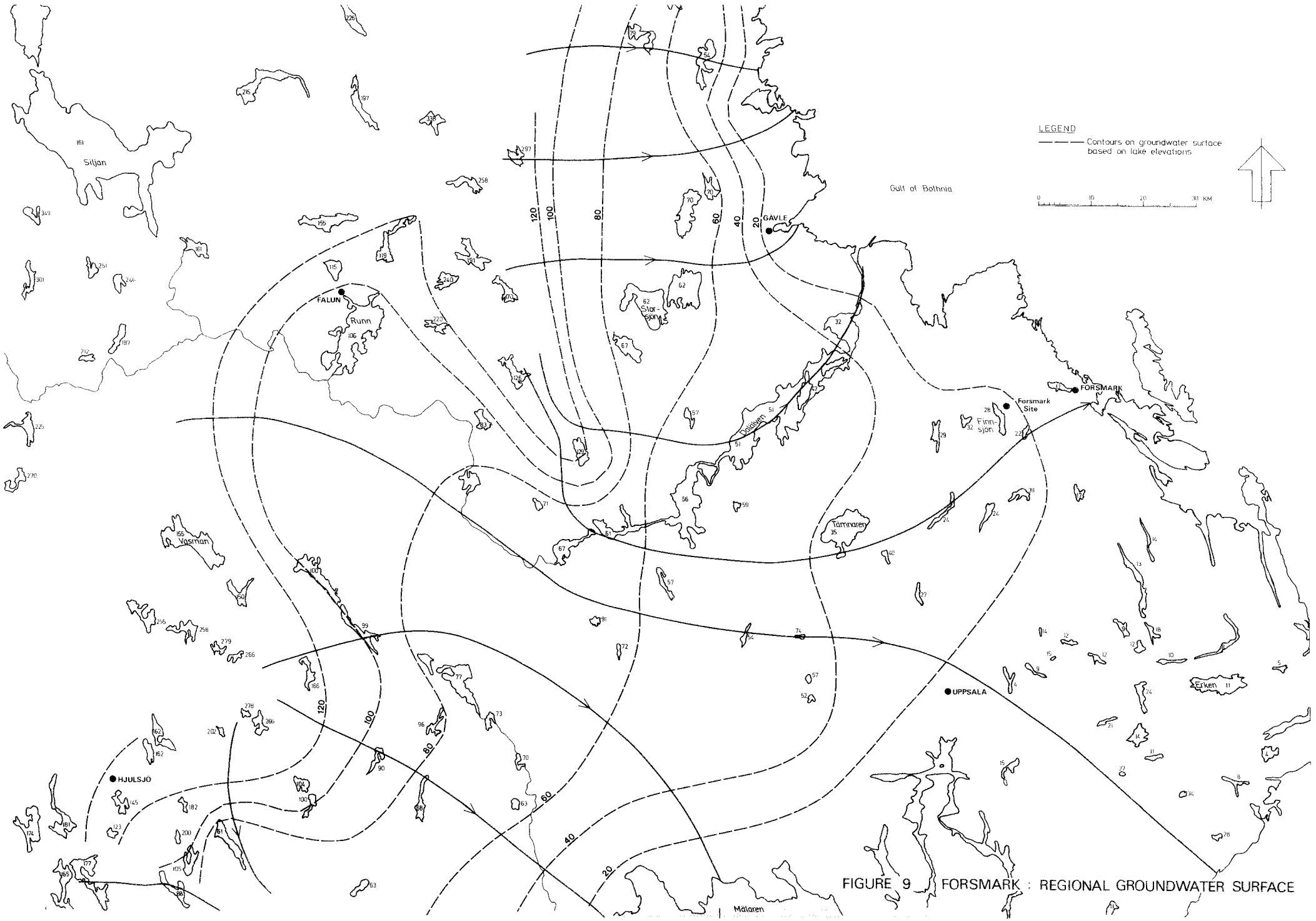

FIGURE 9 FORSMARK : REGIONAL GROUNDWATER SURFACE

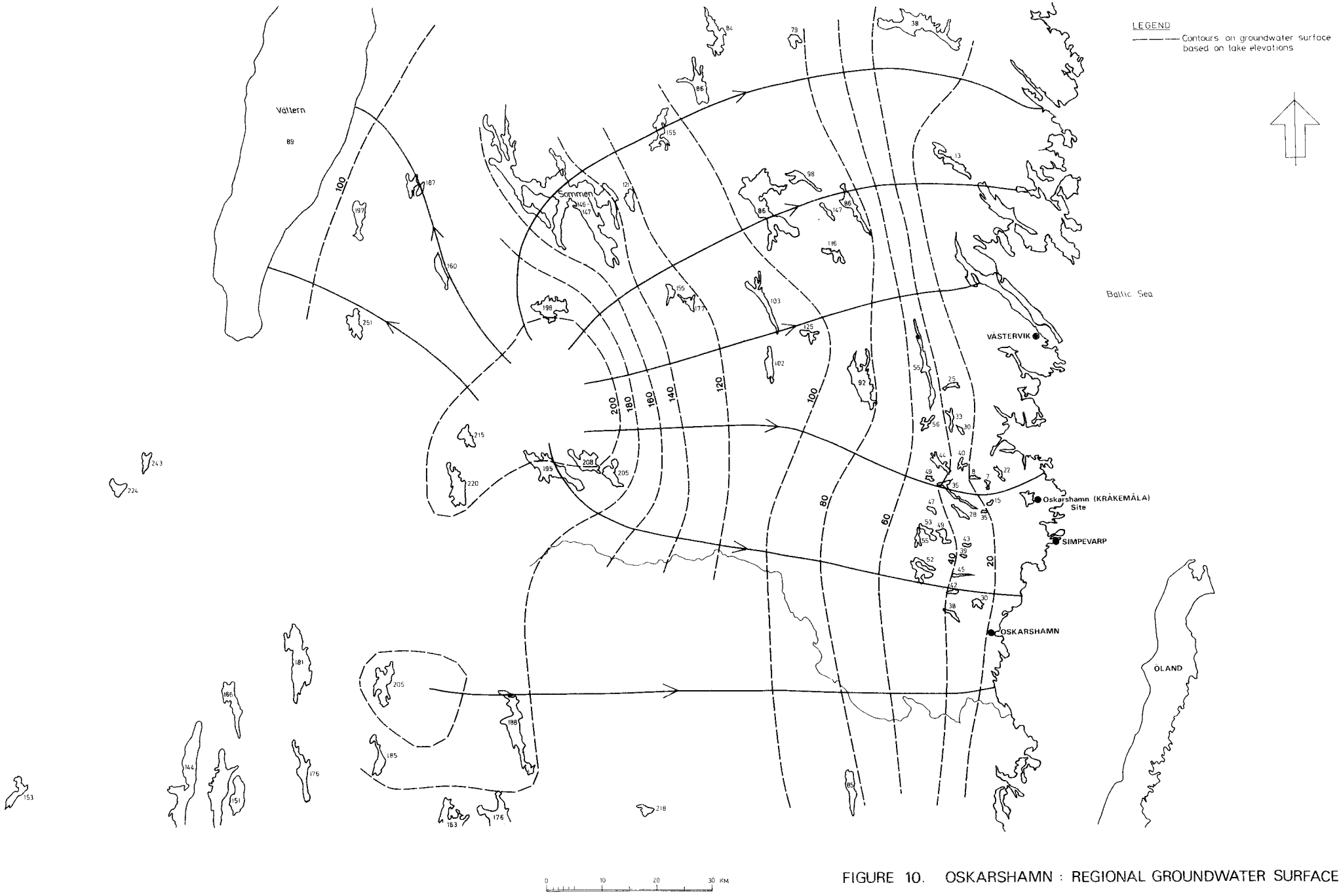

FIGURE 10. OSKARSHAMN : REGIONAL GROUNDWATER SURFACE

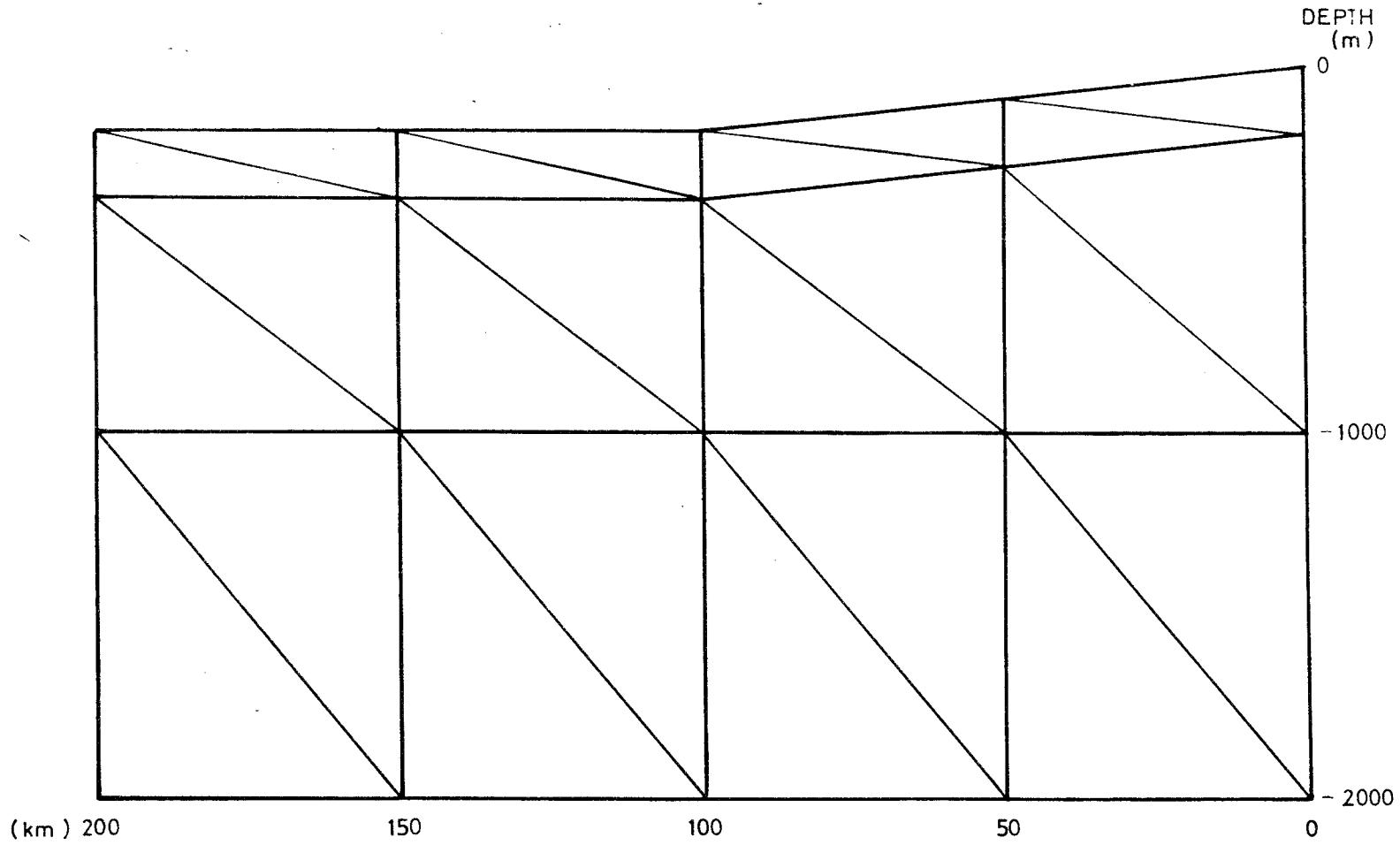

FIGURE 11. OSKARSHAMN: FINITE ELEMENT MESH FOR REGIONAL FLOW

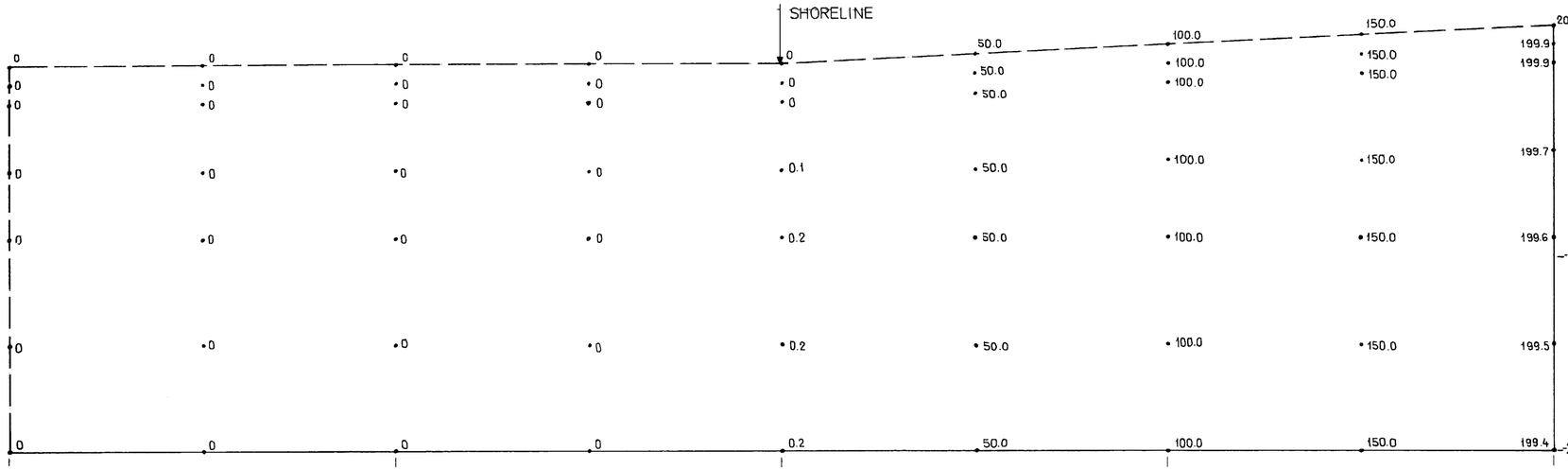

EQUIPOTENTIALS

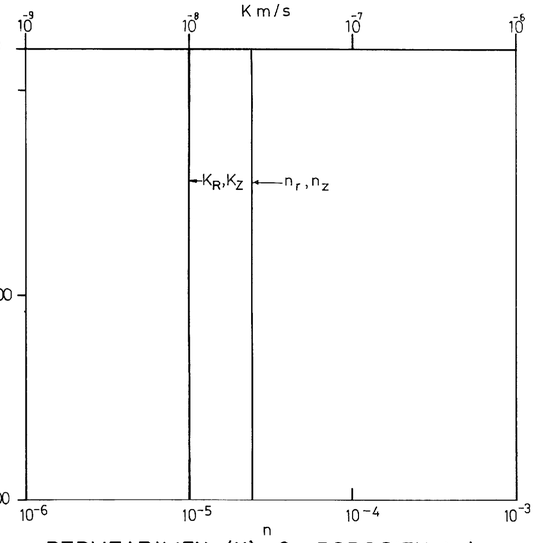

PERMEABILITY (K) & POROSITY (n)

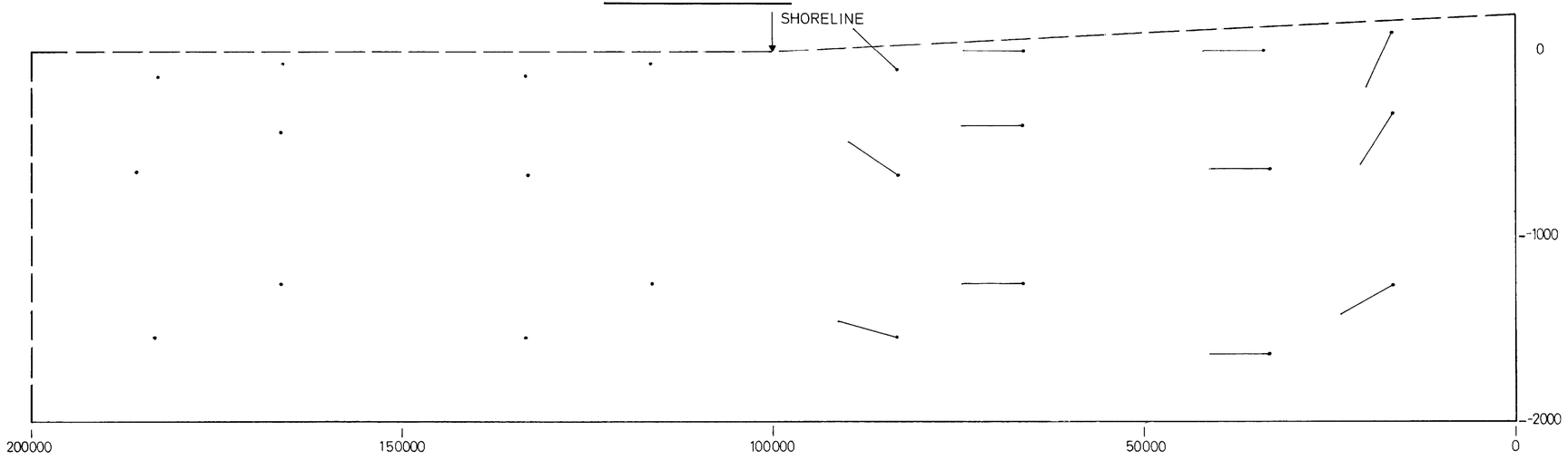

PORE VELOCITY VECTORS

Scale 0 1×10^{-6} m/s

BOUNDARY CONDITIONS

——— Zero flux boundary

– – – – Fixed potential boundary

KBS – Kärnbränslesäkerhet

GROUNDWATER MOVEMENTS AROUND A REPOSITORY

INITIAL CONDITIONS

OSKARSHAMN: REGIONAL FLOW, CASE 1

Hagconsult ab Stockholm Sept. 1977

FIGURE: 12

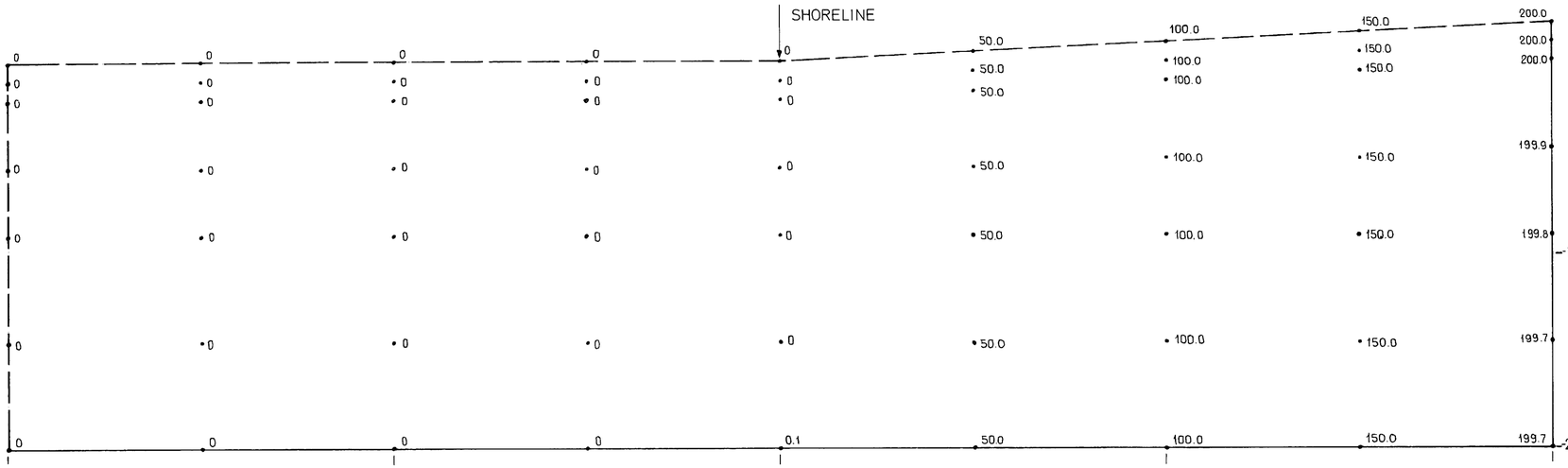

EQUIPOTENTIALS

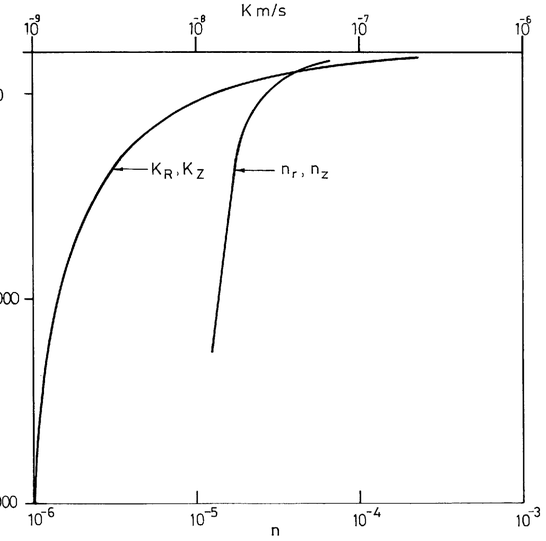

PERMEABILITY (K) & POROSITY.(n)

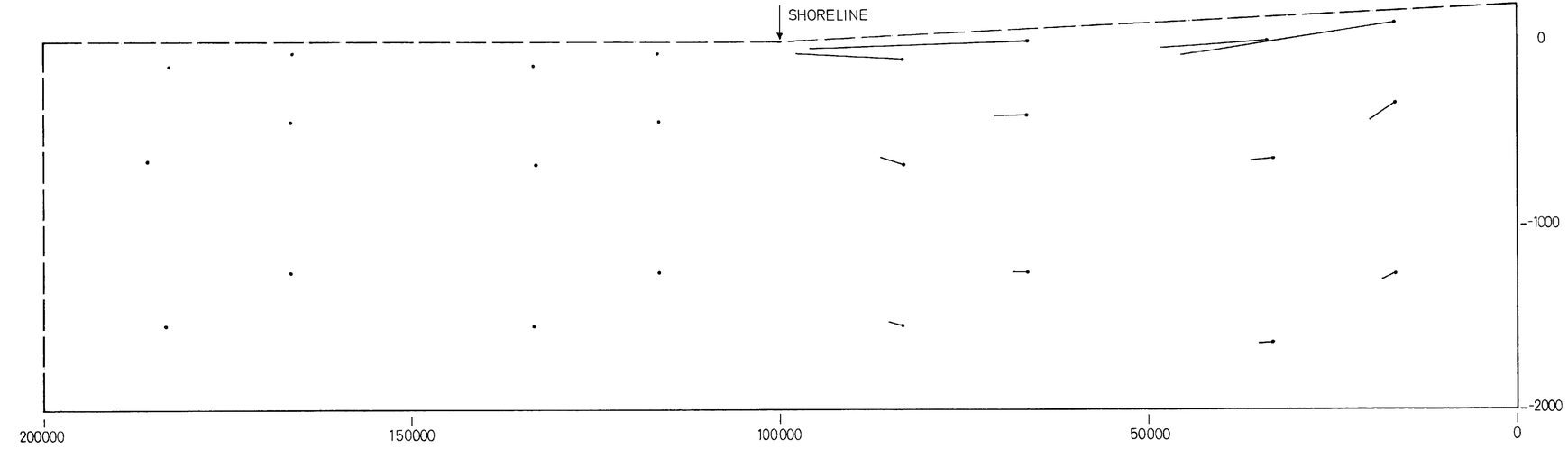

PORE VELOCITY VECTORS

Scale 0 1×10^{-6} m/s

BOUNDARY CONDITIONS

——— Zero flux boundary

– – – – Fixed potential boundary

KBS – Kärnbränslesäkerhet

GROUNDWATER MOVEMENTS AROUND A REPOSITORY

INITIAL CONDITIONS

OSKARSHAMN : REGIONAL FLOW, CASE 2.

Hagconsult ab Stockholm Sept. 1977

FIGURE: 13

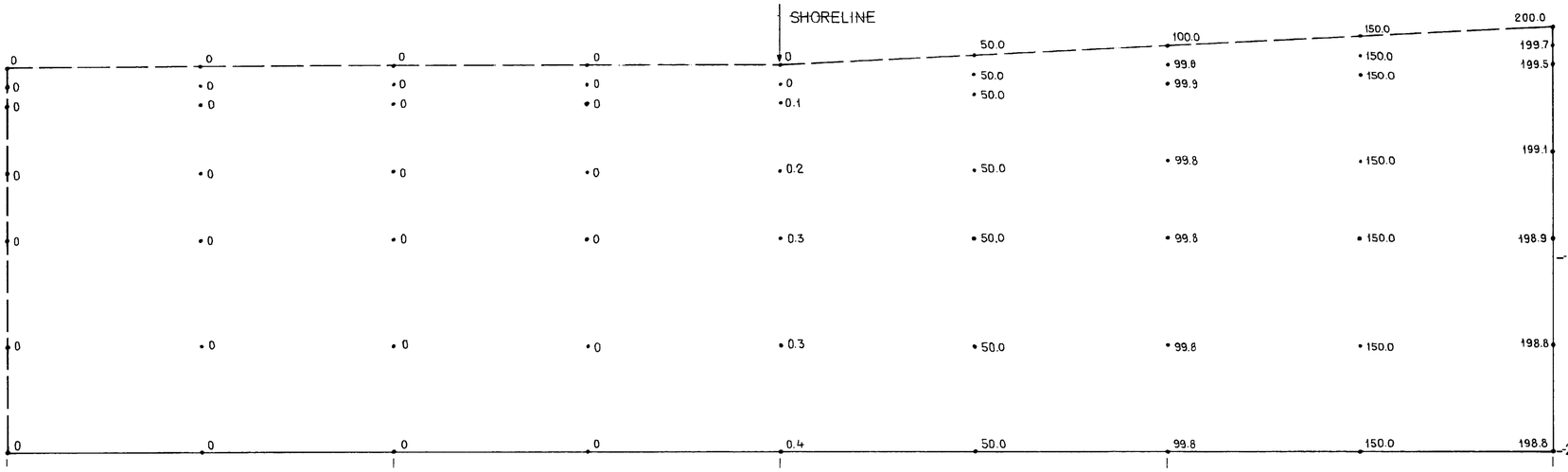

EQUIPOTENTIALS

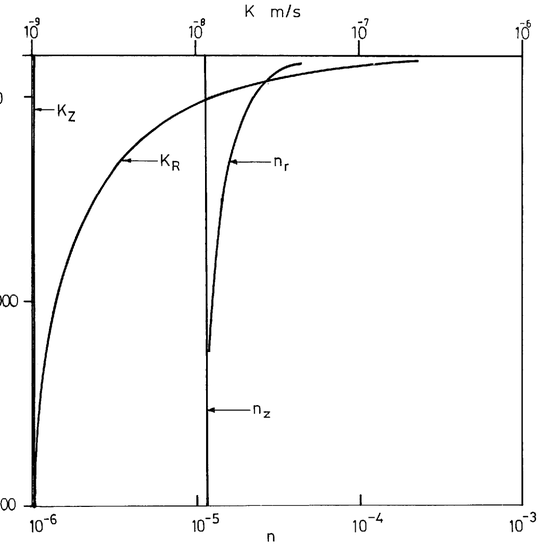

PERMEABILITY (K) & POROSOTY (n)

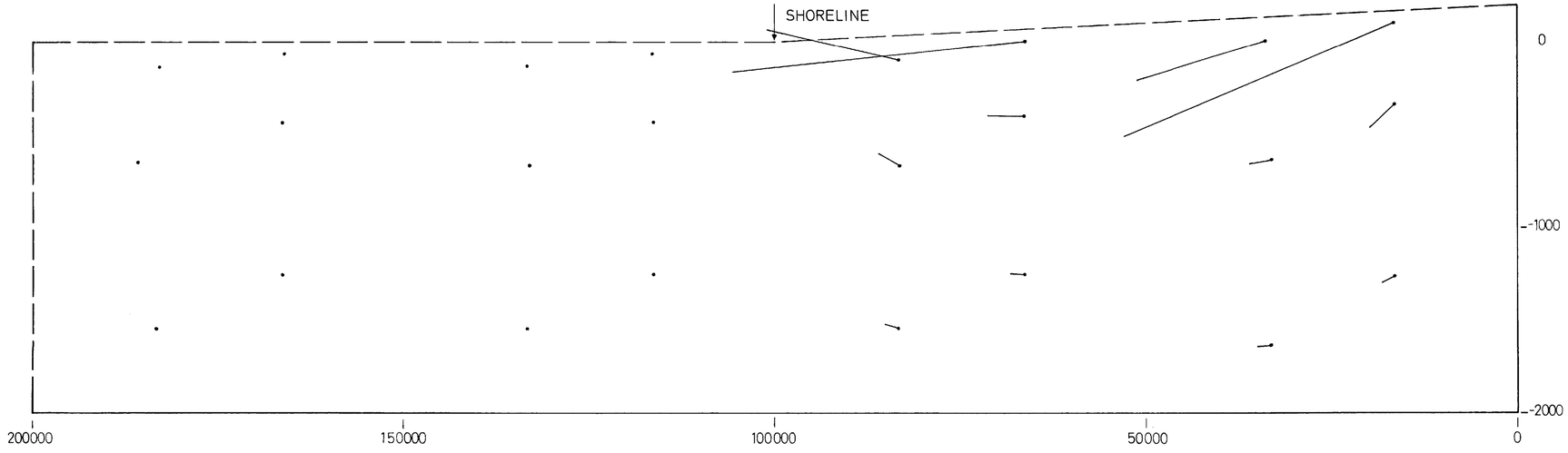

PORE VELOCITY VECTORS

Scale 0 1×10^{-6} m/s

BOUNDARY CONDITIONS

——— Zero flux boundary

– – – Fixed potential boundary

KBS – Kärnbränslesäkerhet

GROUNDWATER MOVEMENTS AROUND A REPOSITORY

INITIAL CONDITIONS

OSKARSHAMN: REGIONAL FLOW, CASE 3

Hagconsult ab Stockholm Sept. 1977

FIGURE: 14

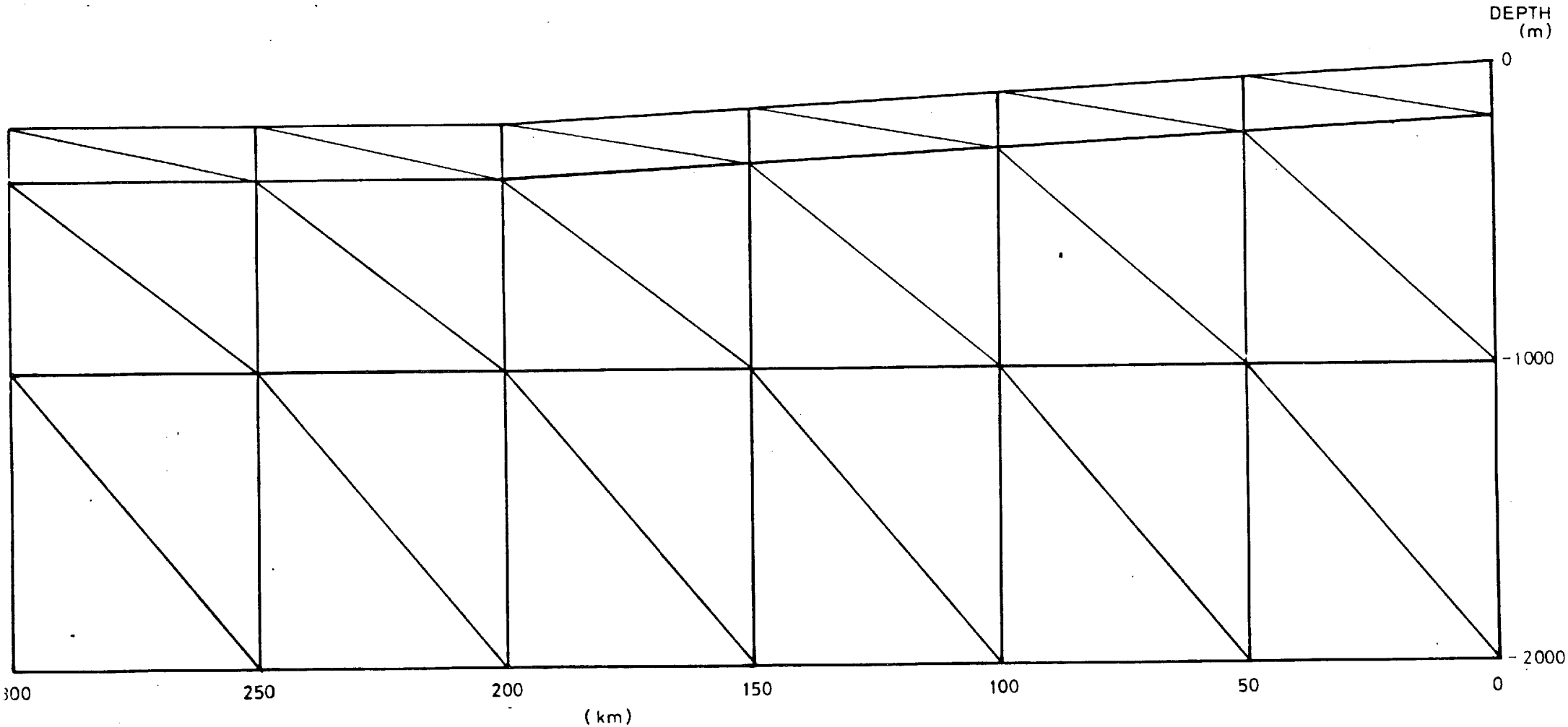

FIGURE 15. FORSMARK: FINITE ELEMENT MESH FOR REGIONAL FLOW

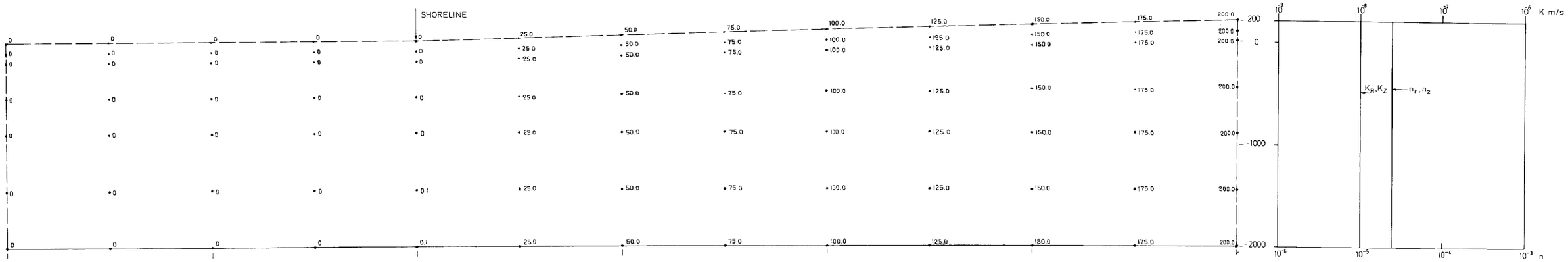

EQUIPOTENTIALS

PERMEABILITY (K) & POROSITY (n)

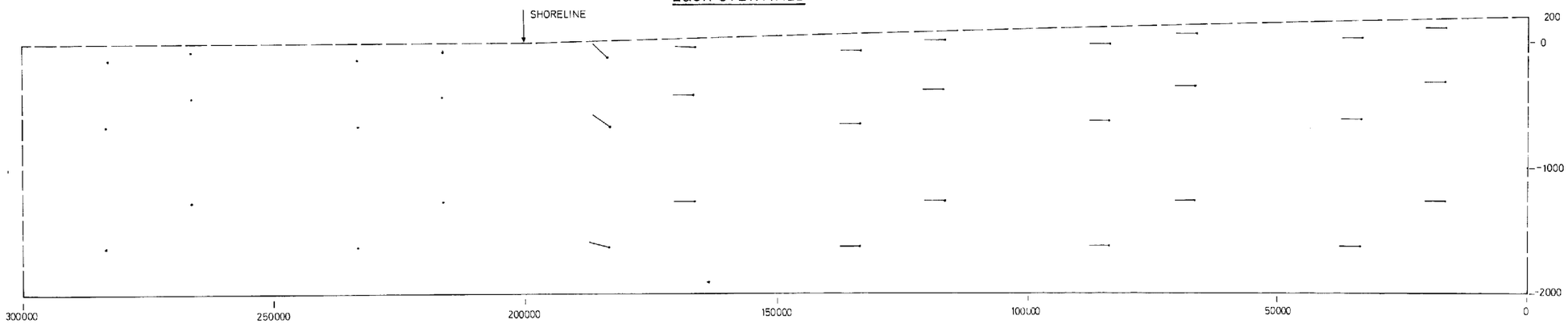

PORE VELOCITY VECTORS

Scale 0 $1 \cdot 10^{-6}$ m/s

BOUNDARY CONDITIONS

——— Zero flux boundary

– – – – Fixed potential boundary

KBS – Kärnbränslesäkerhet

GROUNDWATER MOVEMENTS AROUND A REPOSITORY

INITIAL CONDITIONS

FORSMARK : REGIONAL FLOW, CASE 1

Hagconsult ab Stockholm Sept. 1977 **FIGURE: 16**

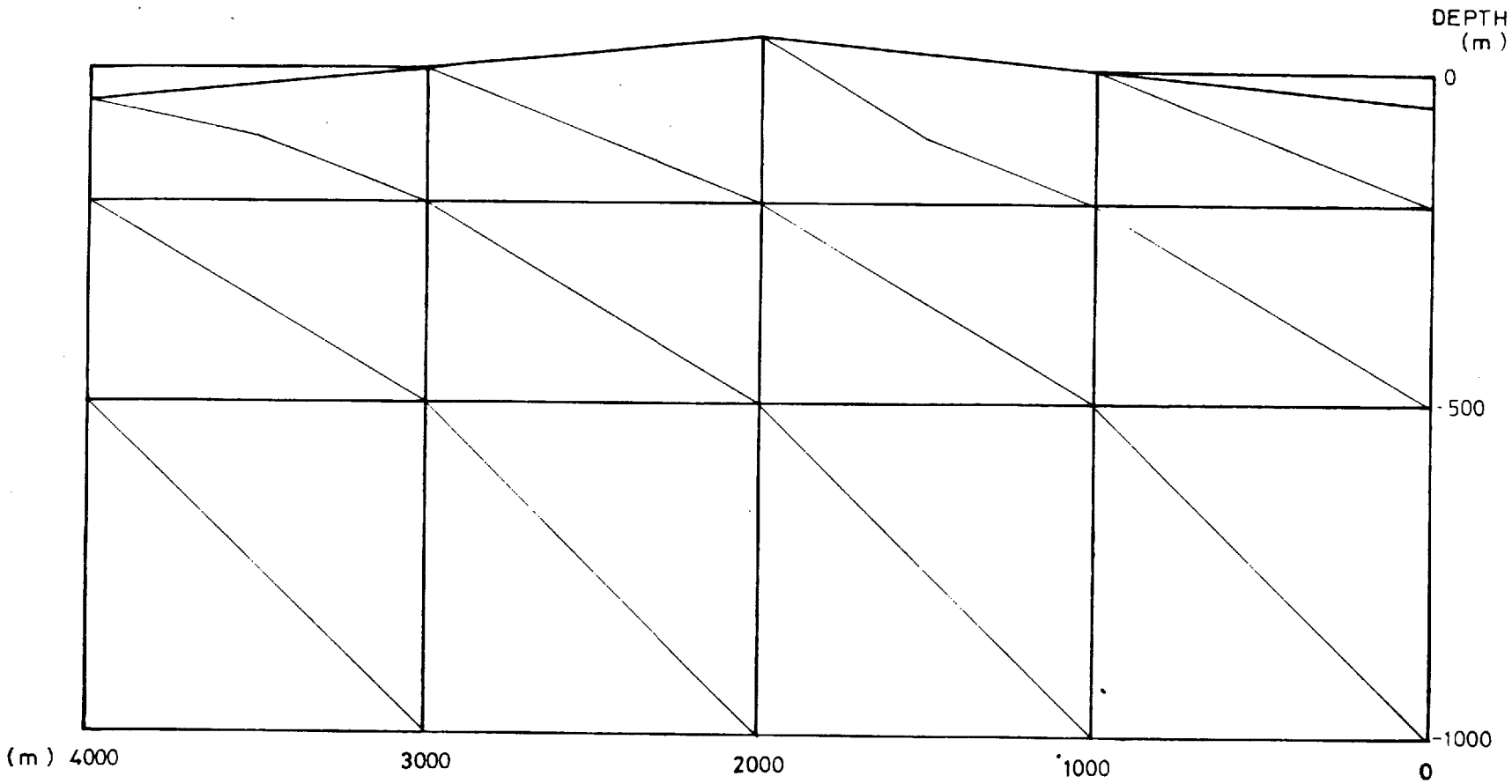

FIGURE 17. TOPOGRAPHY EFFECTS: FINITE ELEMENT MESH

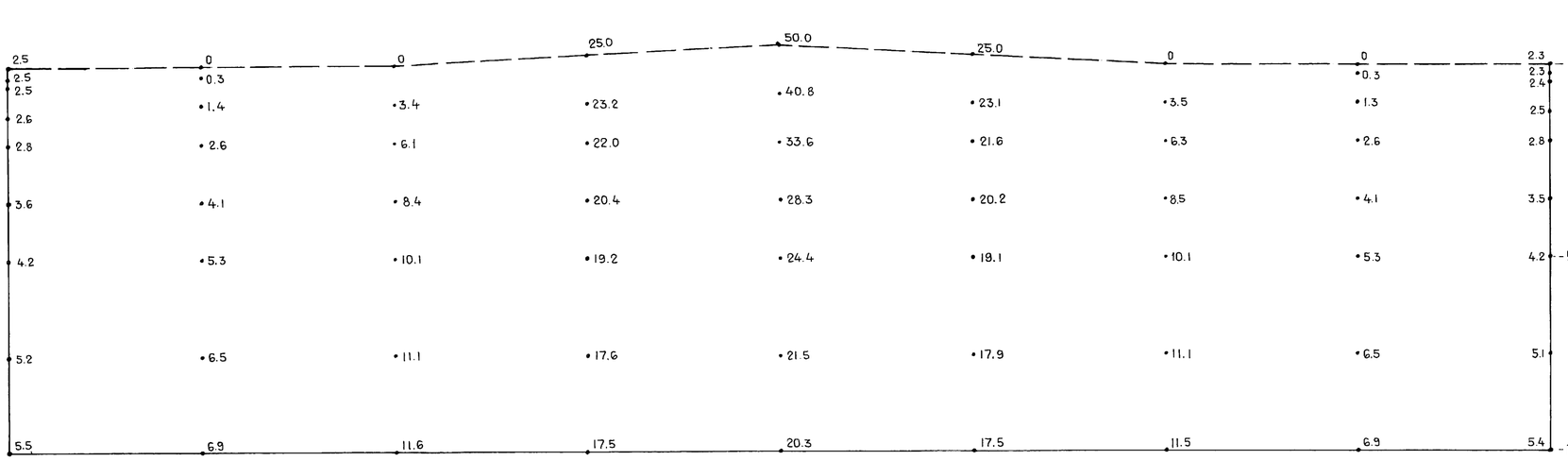

EQUIPOTENTIALS

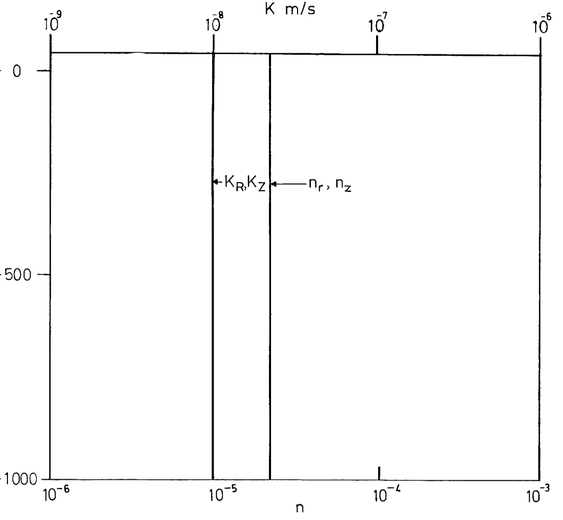

PERMEABILITY (K) & POROSITY (n)

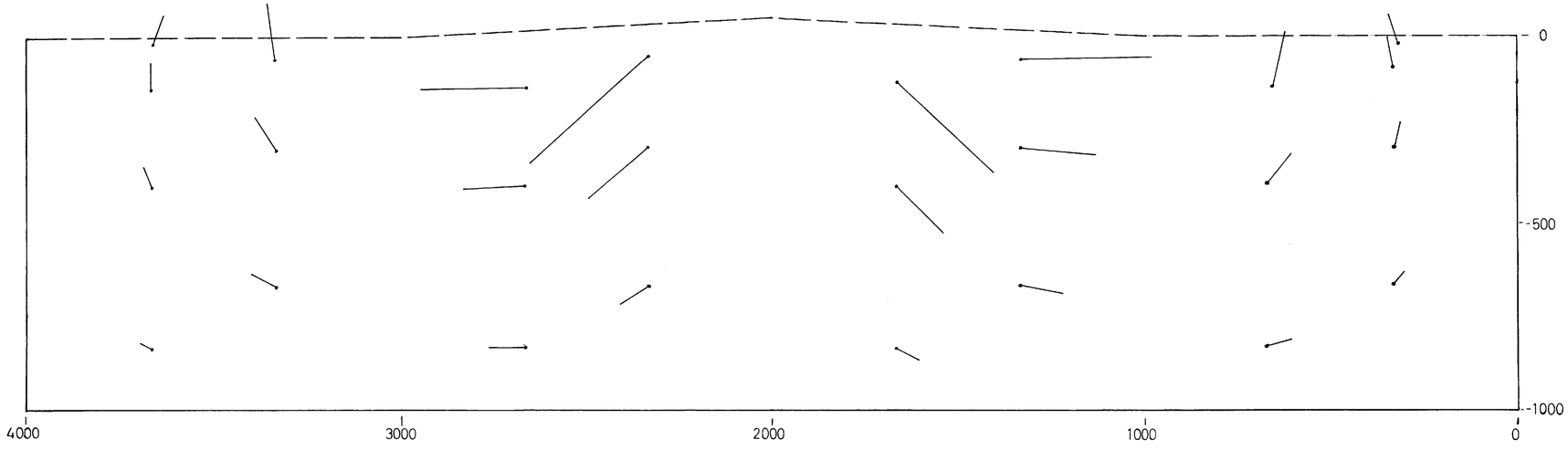

PORE VELOCITY VECTORS

Scale 0 10×10^{-6} m/s

BOUNDARY CONDITIONS

——— Zero flux boundary

– – – – Fixed potential boundary

KBS – Kärnbränslesäkerhet

GROUNDWATER MOVEMENTS AROUND A REPOSITORY

INITIAL CONDITIONS

TOPOGRAPHY EFFECTS : IMPERVIOUS BOUNDARY, CASE 1

Hagconsult ab Stockholm Sept. 1977 **FIGURE : 18**

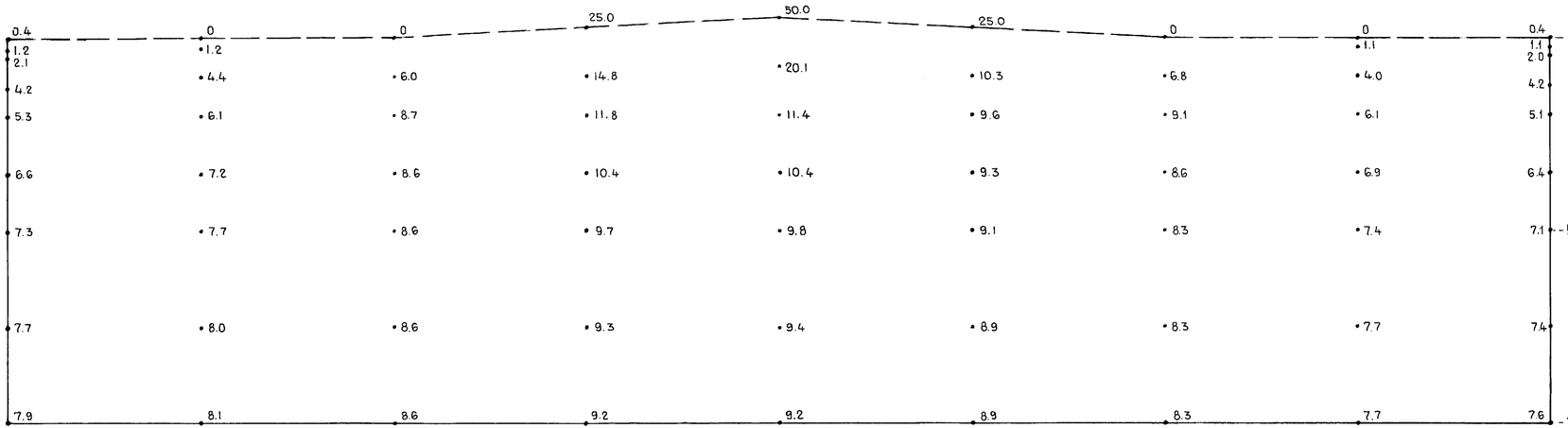

EQUIPOTENTIALS

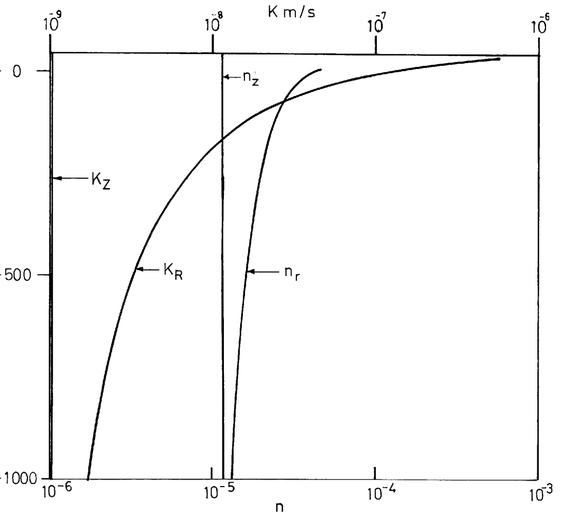

PERMEABILITY (K) & POROSITY (n)

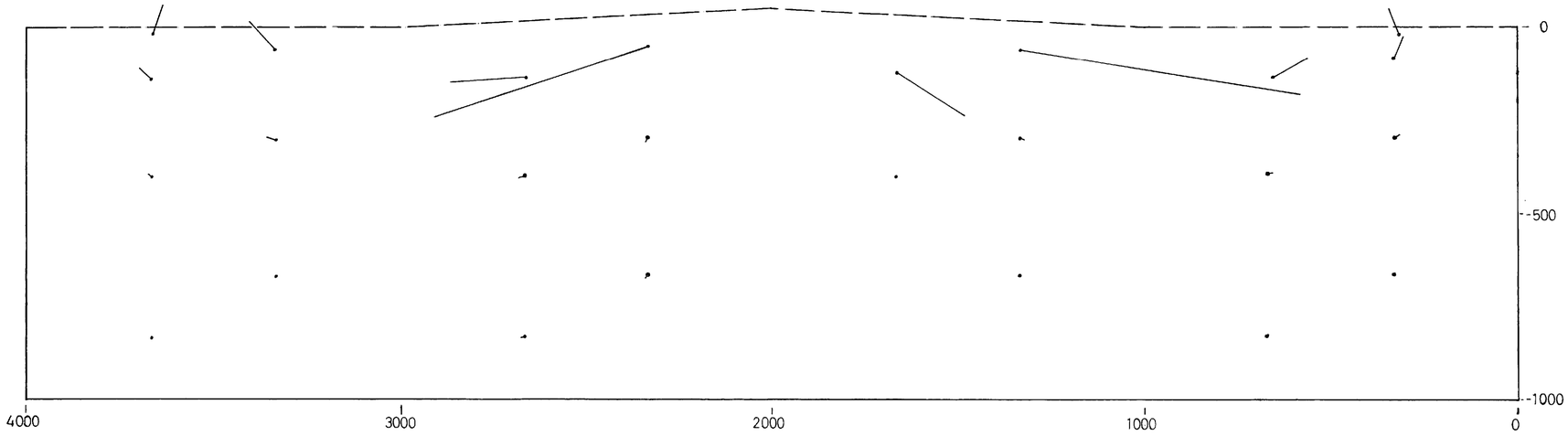

PORE VELOCITY VECTORS

Scale 0 10×10^{-6} m/s

BOUNDARY CONDITIONS

——— Zero flux boundary

– – – Fixed potential boundary

KBS – Kärnbränslesäkerhet

GROUNDWATER MOVEMENTS AROUND A REPOSITORY

INITIAL CONDITIONS

TOPOGRAPHY EFFECTS: IMPERVIOUS BOUNDARY, CASE 3

Hagconsult ab Stockholm Sept. 1977 **FIGURE: 19**

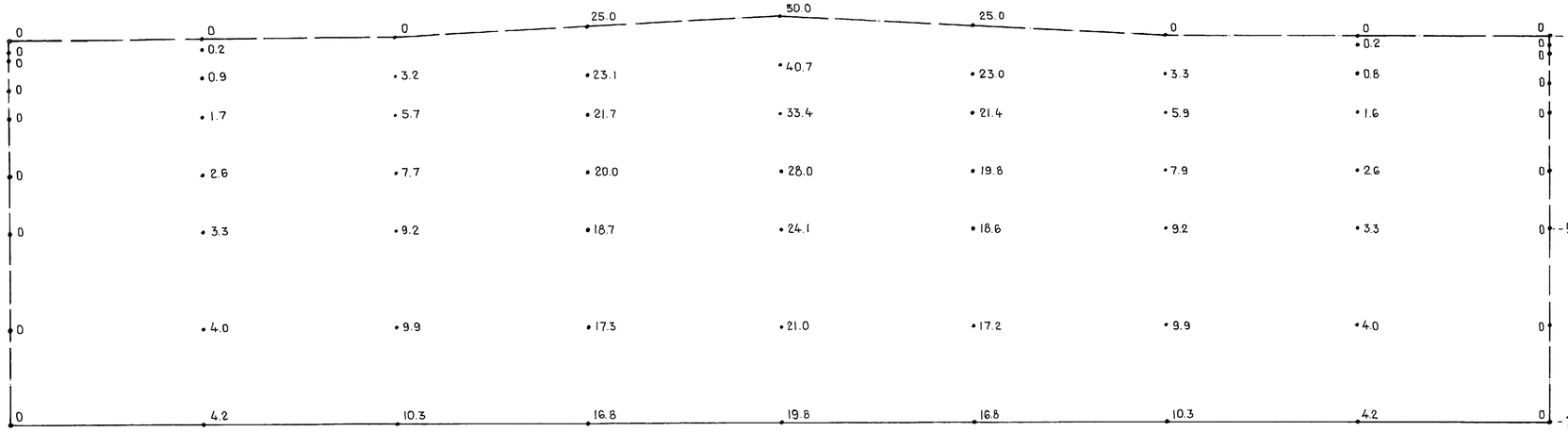

EQUIPOTENTIALS

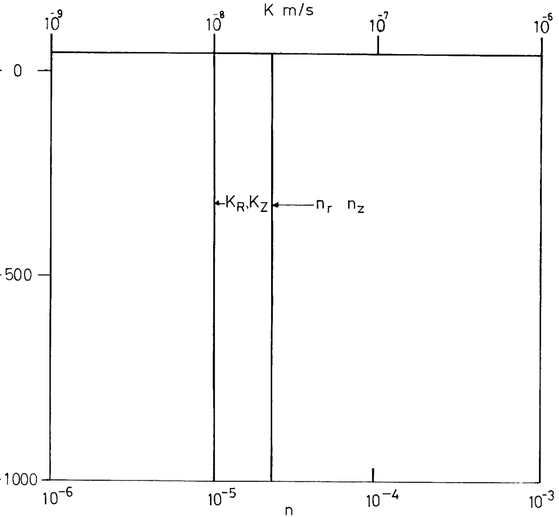

PERMEABILITY (K) & POROSITY (n)

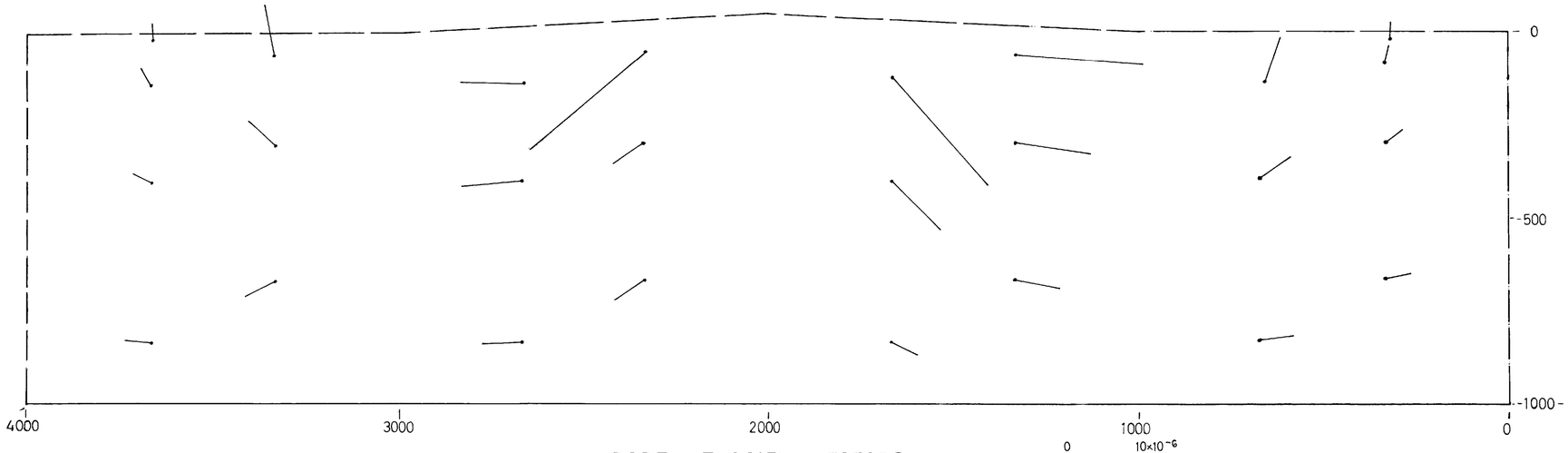

PORE VELOCITY VECTORS

Scale 0 10×10^{-6} m/s

BOUNDARY CONDITIONS

——— Zero flux boundary

– – – Fixed potential boundary

KBS – Kärnbränslesäkerhet

GROUNDWATER MOVEMENTS AROUND A REPOSITORY

INITIAL CONDITIONS

TOPOGRAPHY EFFECTS : CONSTANT POTENTIAL BOUNDARY , CASE 1

Hagconsult ab Stockholm Sept. 1977 **FIGURE : 20**

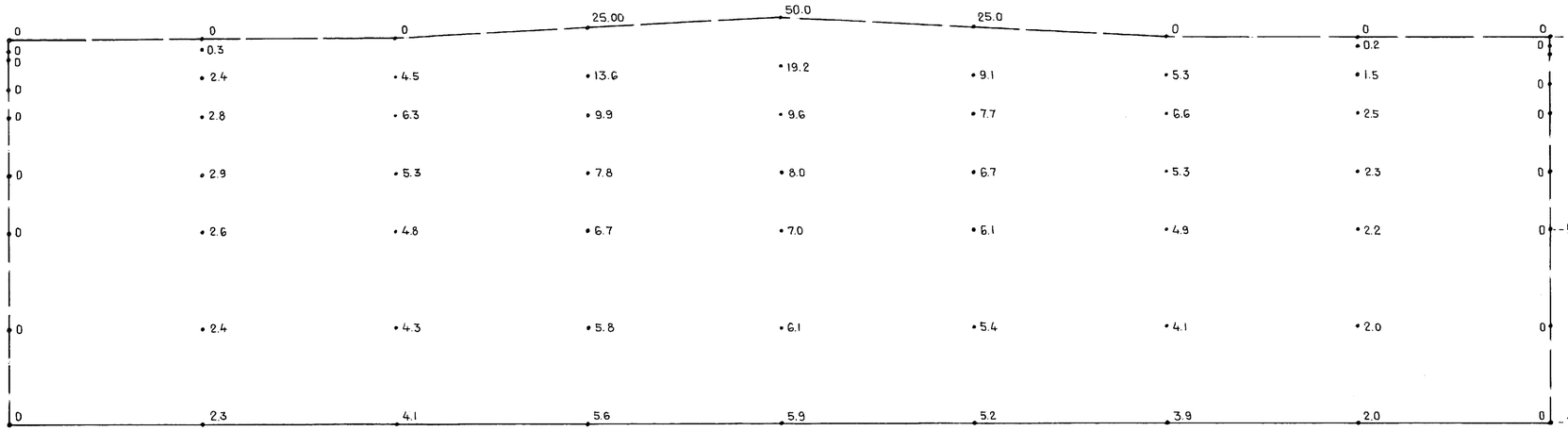

EQUIPOTENTIALS

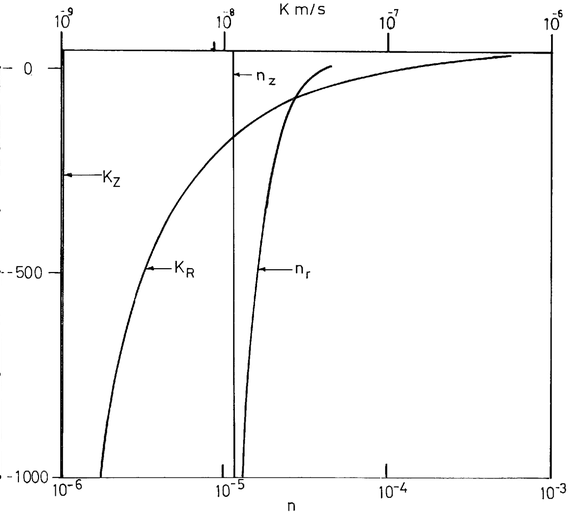

PERMEABILITY (K) & POROSITY (n)

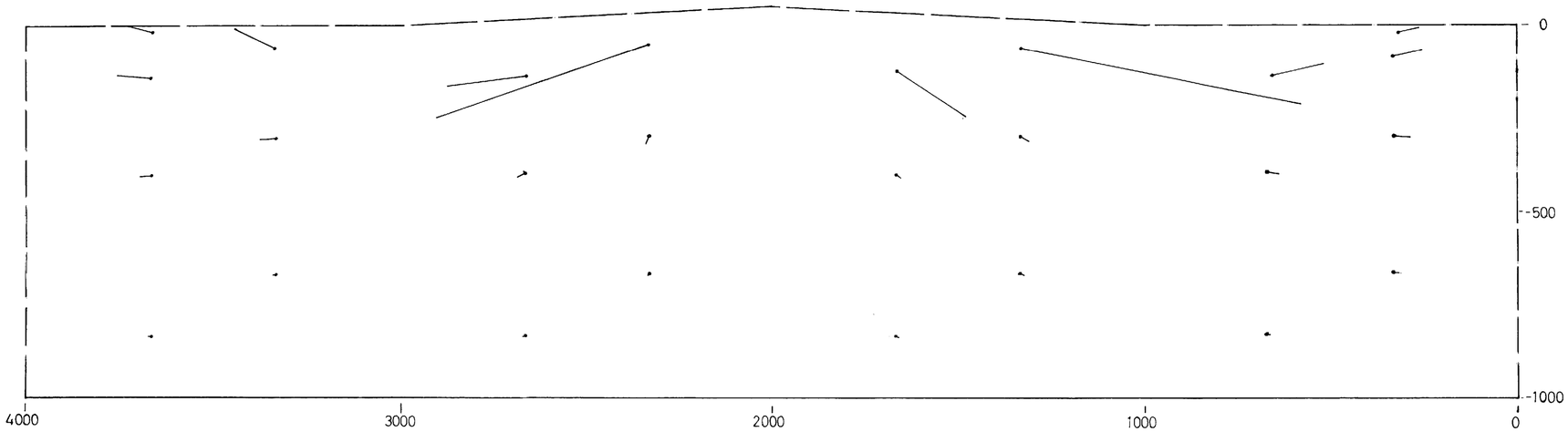

PORE VELOCITY VECTORS

Scale 0 10×10^{-6} m/s

BOUNDARY CONDITIONS

——— Zero flux boundary

— — — Fixed potential boundary

KBS – Kärnbränslesäkerhet

GROUNDWATER MOVEMENTS AROUND A REPOSITORY

INITIAL CONDITIONS

TOPOGRAPHY EFFECTS : CONSTANT POTENTIAL BOUNARY , CASE 3

Hagconsult ab Stockholm Sept. 1977 **FIGURE: 21**

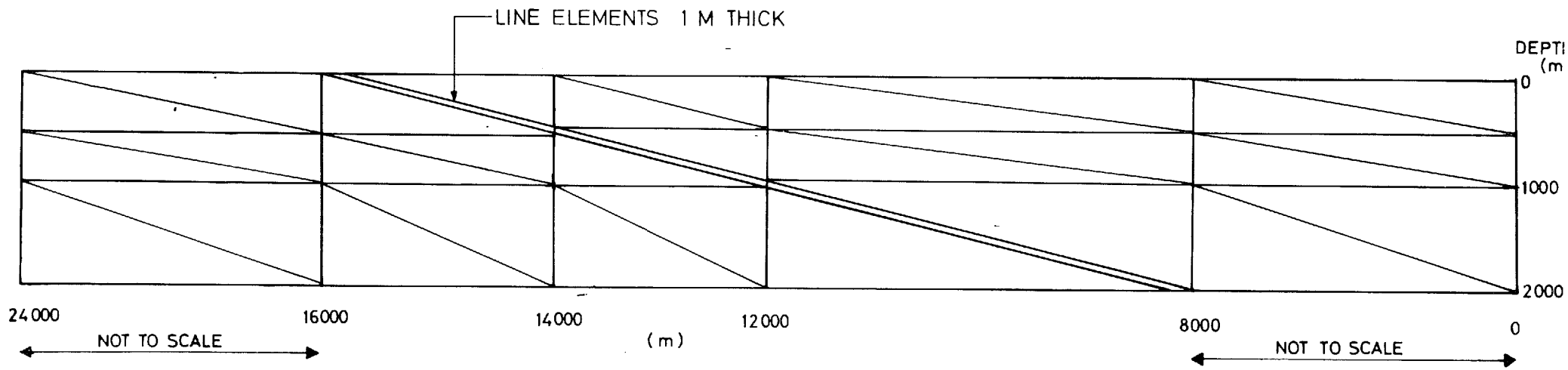

FIGURE 22. DISCONTINUITY EFFECTS: FINITE ELEMENT MESH

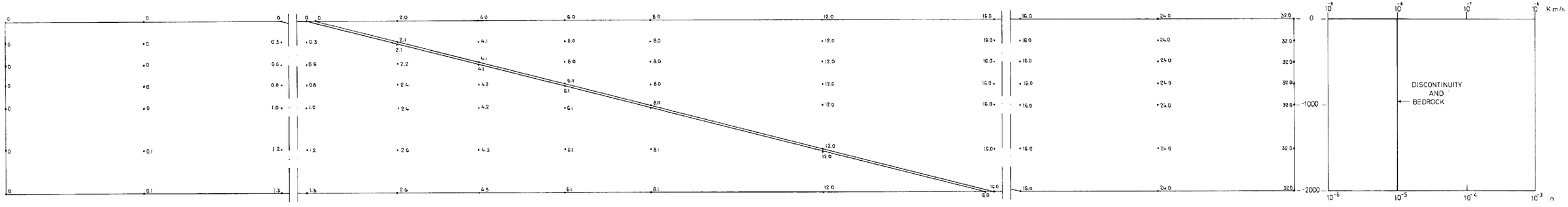

EQUIPOTENTIALS

PERMEABILITY (K) & POROSITY (n)

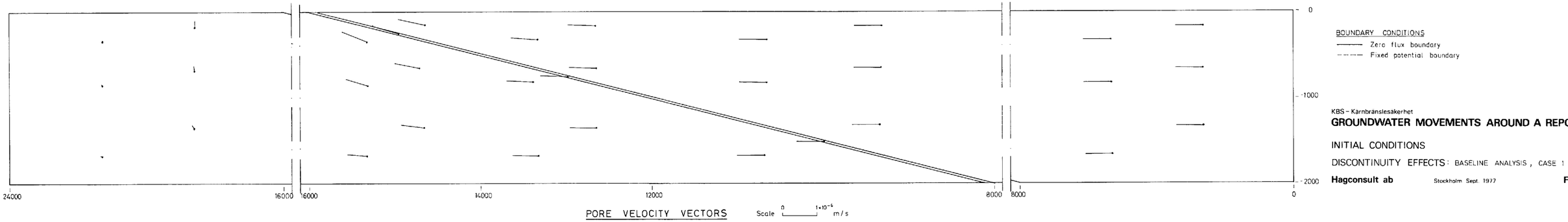

PORE VELOCITY VECTORS Scale 0 $1\cdot10^{-6}$ m/s

BOUNDARY CONDITIONS
Zero flux boundary
Fixed potential boundary

KBS – Kärnbränslesäkerhet

GROUNDWATER MOVEMENTS AROUND A REPOSITORY

INITIAL CONDITIONS

DISCONTINUITY EFFECTS: BASELINE ANALYSIS, CASE 1

Hagconsult ab Stockholm Sept. 1977 **FIGURE: 23**

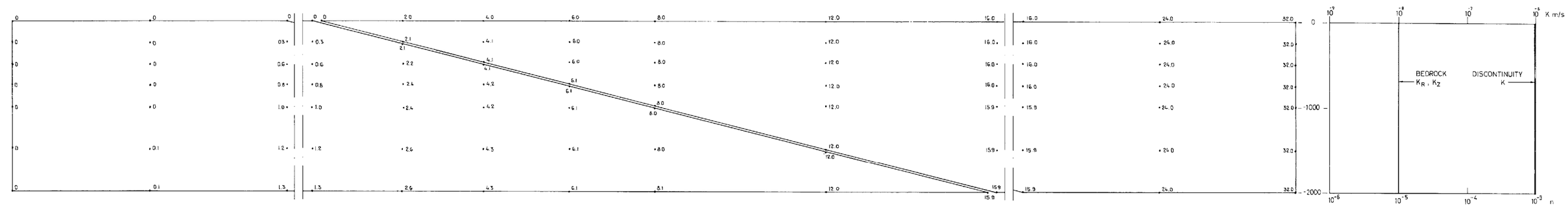

EQUIPOTENTIALS

PERMEABILITY (K) & POROSITY (n)

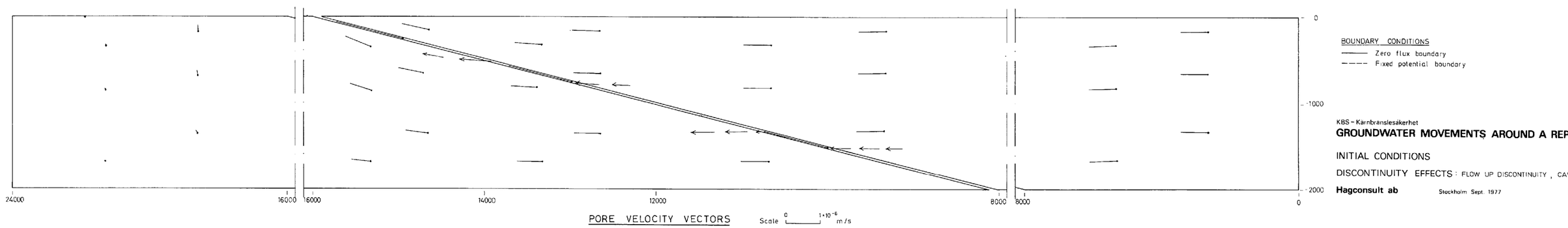

PORE VELOCITY VECTORS Scale 0 $1\cdot10^{-6}$ m/s

BOUNDARY CONDITIONS
Zero flux boundary
Fixed potential boundary

KBS – Kärnbränslesäkerhet

GROUNDWATER MOVEMENTS AROUND A REPOSITORY

INITIAL CONDITIONS

DISCONTINUITY EFFECTS: FLOW UP DISCONTINUITY, CASE 1

Hagconsult ab Stockholm Sept. 1977 **FIGURE: 24**

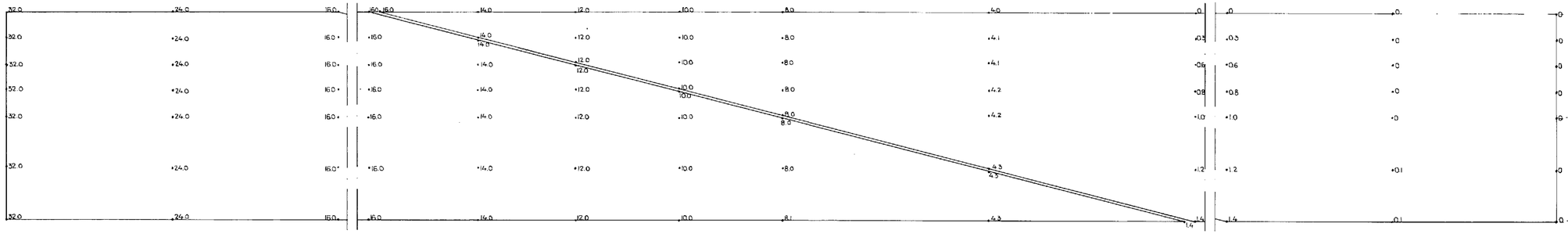

EQUIPOTENTIALS

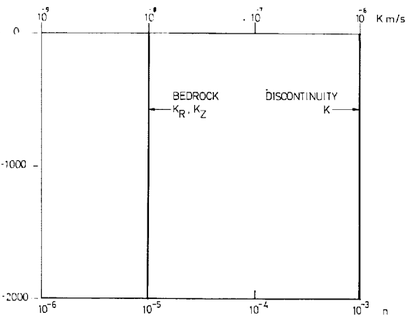

PERMEABILITY (K) & POROSITY (n)

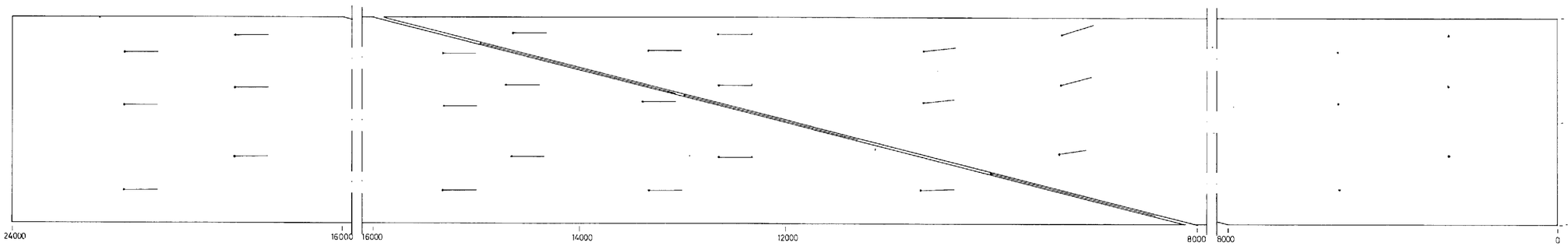

BOUNDARY CONDITIONS
——— Zero flux boundary
– – – – Fixed potential boundary

PORE VELOCITY VECTORS Scale 0 1×10^{-6} m/s

KBS – Kärnbränslesäkerhet

GROUNDWATER MOVEMENTS AROUND A REPOSITORY

INITIAL CONDITIONS

DISCONTINUITY EFFECTS : FLOW DOWN DISCONTINUITY , CASE 1

Hagconsult ab Stockholm Sept. 1977 **FIGURE : 25**

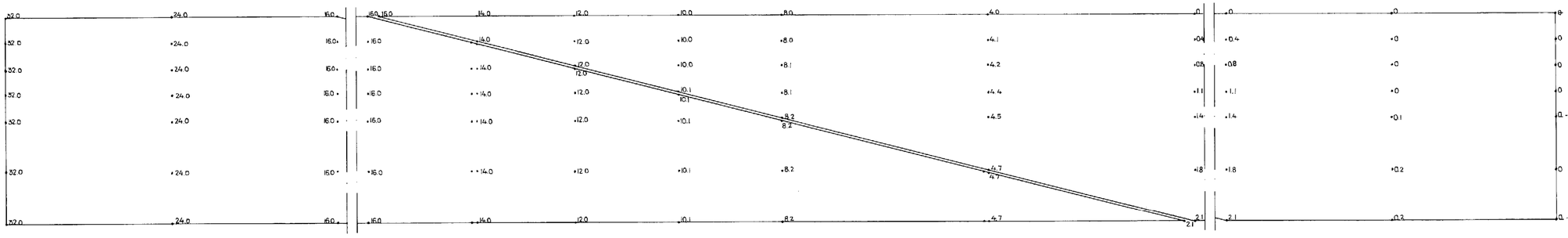

EQUIPOTENTIALS

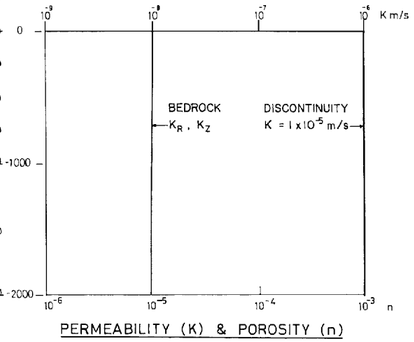

PERMEABILITY (K) & POROSITY (n)

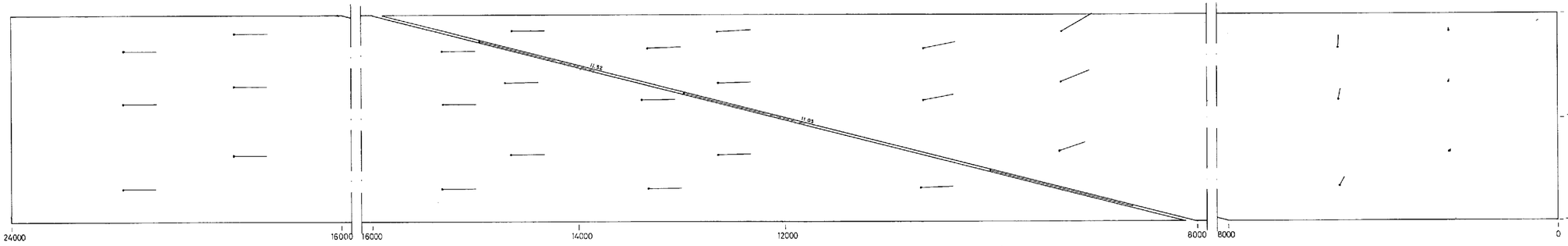

BOUNDARY CONDITIONS
——— Zero flux boundary
– – – – Fixed potential boundary

PORE VELOCITY VECTORS Scale 0 1×10^{-6} m/s

KBS – Kärnbränslesäkerhet

GROUNDWATER MOVEMENTS AROUND A REPOSITORY

INITIAL CONDITIONS

DISCONTINUITY EFFECTS : FLOW DOWN DISCONTINUITY , CASE 1

Hagconsult ab Stockholm Sept. 1977 **FIGURE : 26**

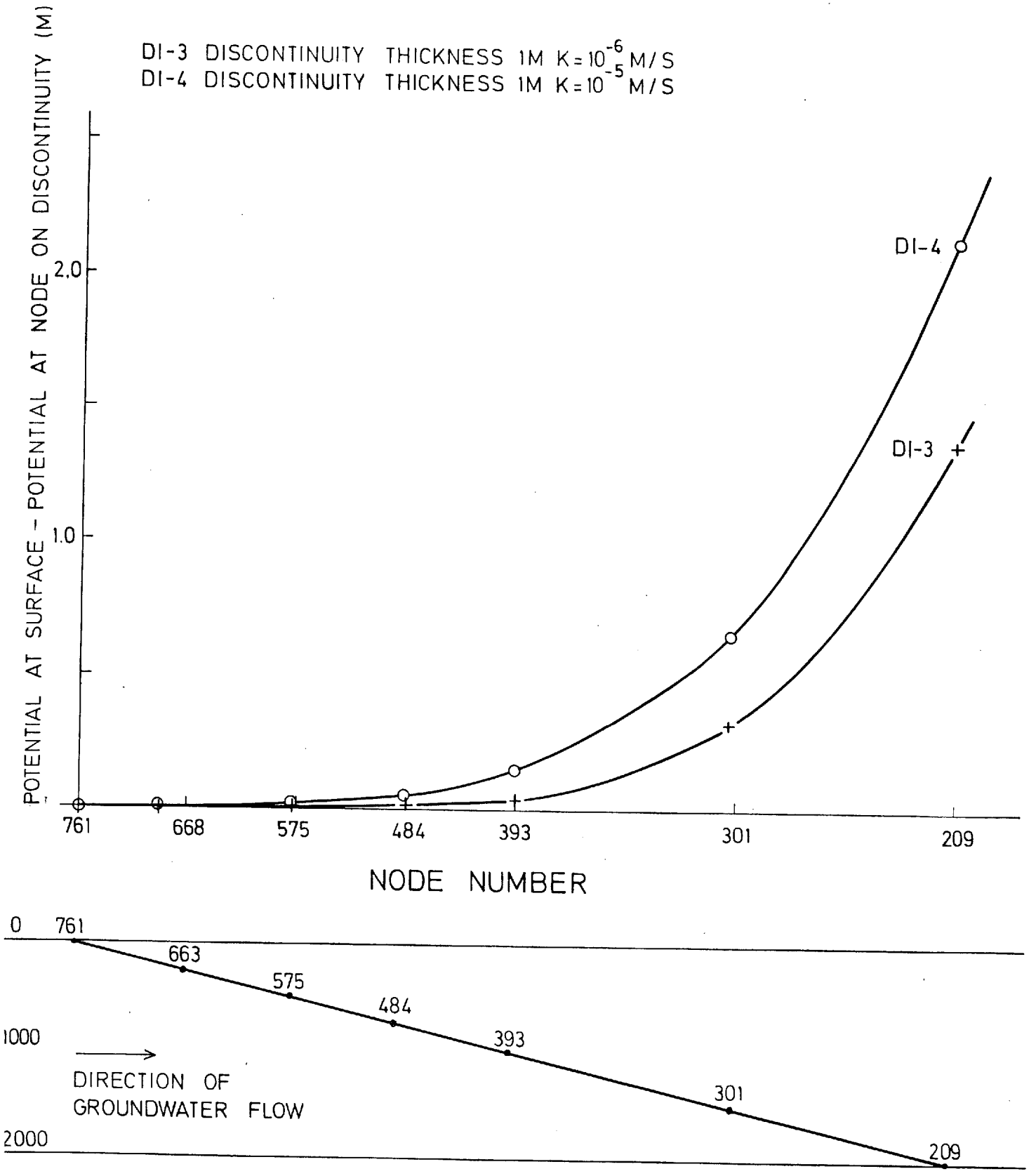

FIGURE 27. POTENTIALS ALONG DISCONTINUITY

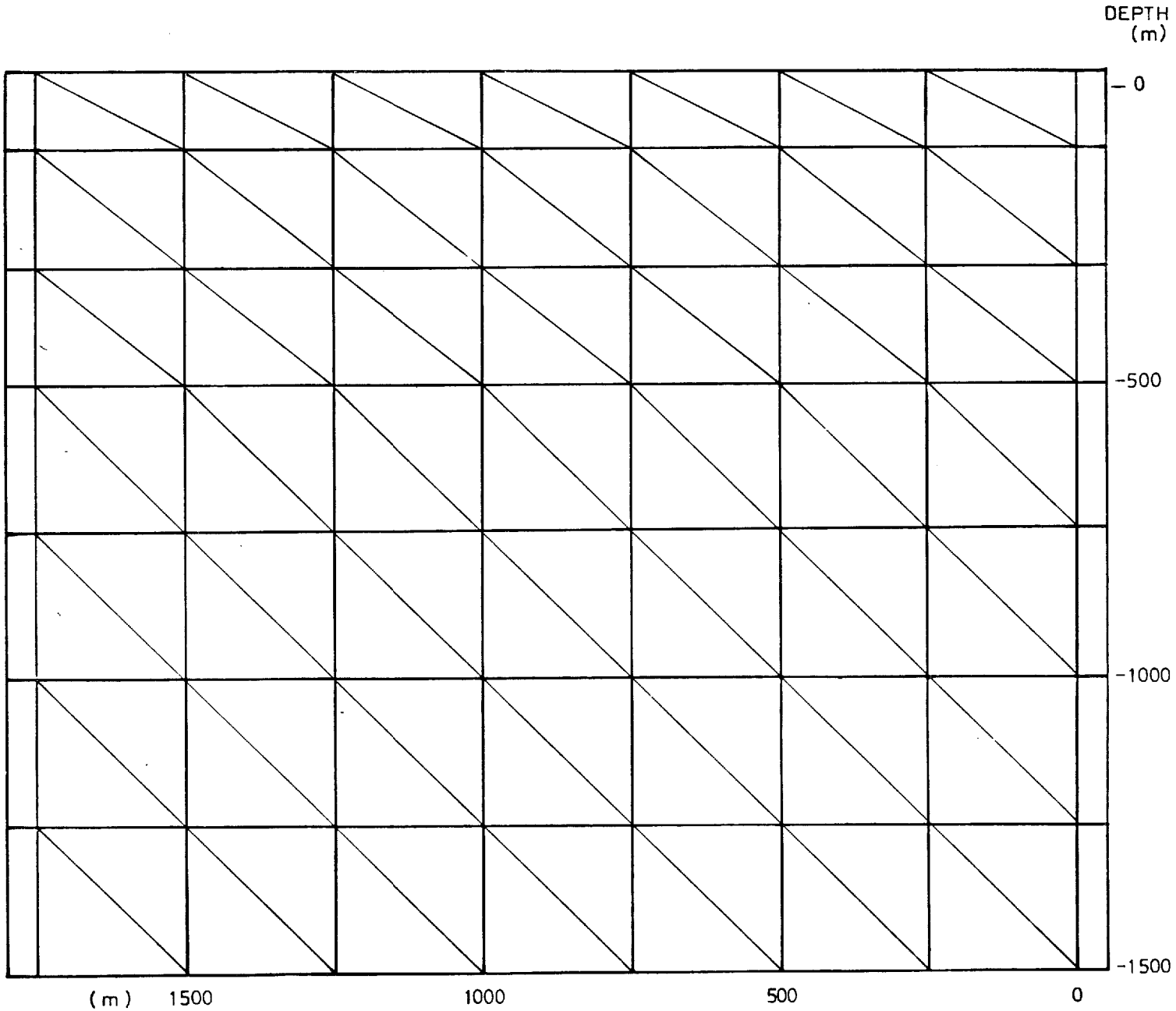

FIGURE 28. FORSMARK: SITE MODEL, FINITE ELEMENT MESH

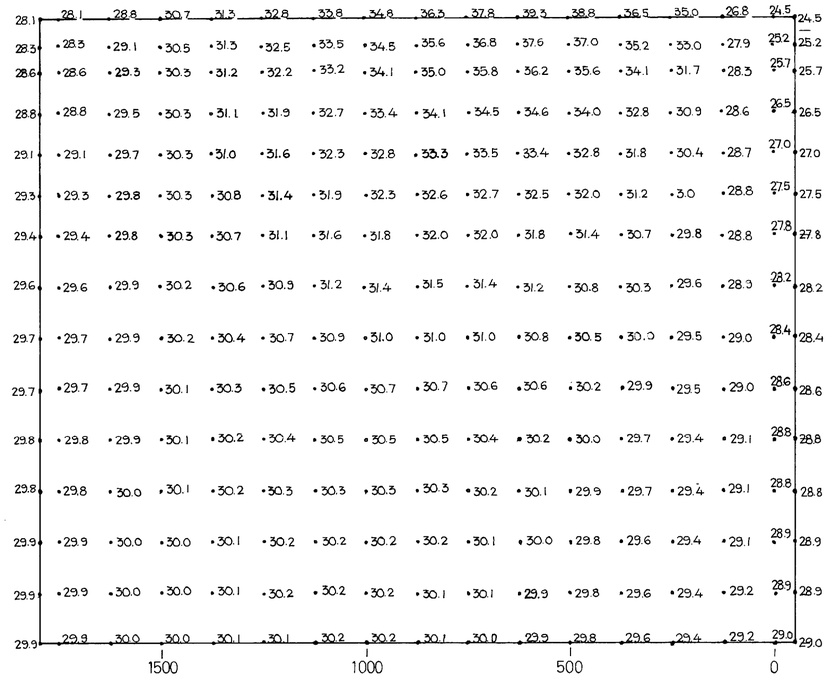

EQUIPOTENTIALS

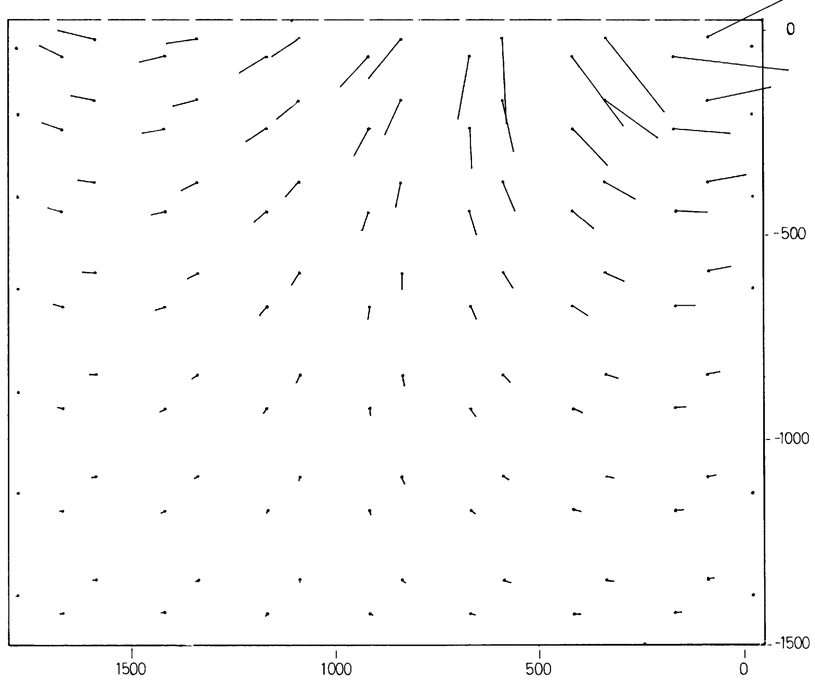

PORE VELOCITY VECTORS

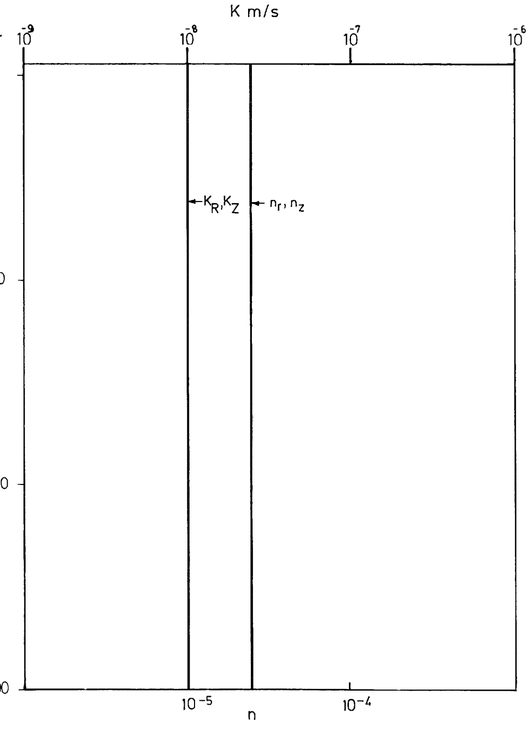

PERMEABILITY (K) & POROSITY (n)

BOUNDARY CONDITIONS

——— Zero flux boundary

– – – – Fixed potential boundary

Scale 0 10×10^{-6} m/s

KBS – Kärnbränslesäkerhet

GROUNDWATER MOVEMENTS AROUND A REPOSITORY

INITIAL CONDITIONS

FORSMARK : SITE MODEL , IMPERVIOUS BOUNDARIES , CASE 1

Hagconsult ab Stockholm Sept. 1977 **FIGURE:29**

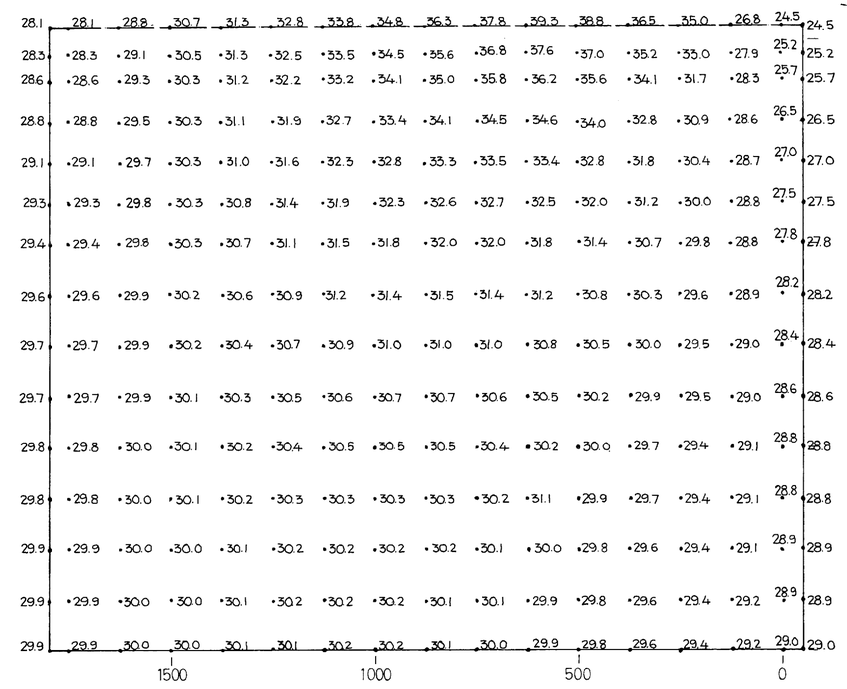

EQUIPOTENTIALS

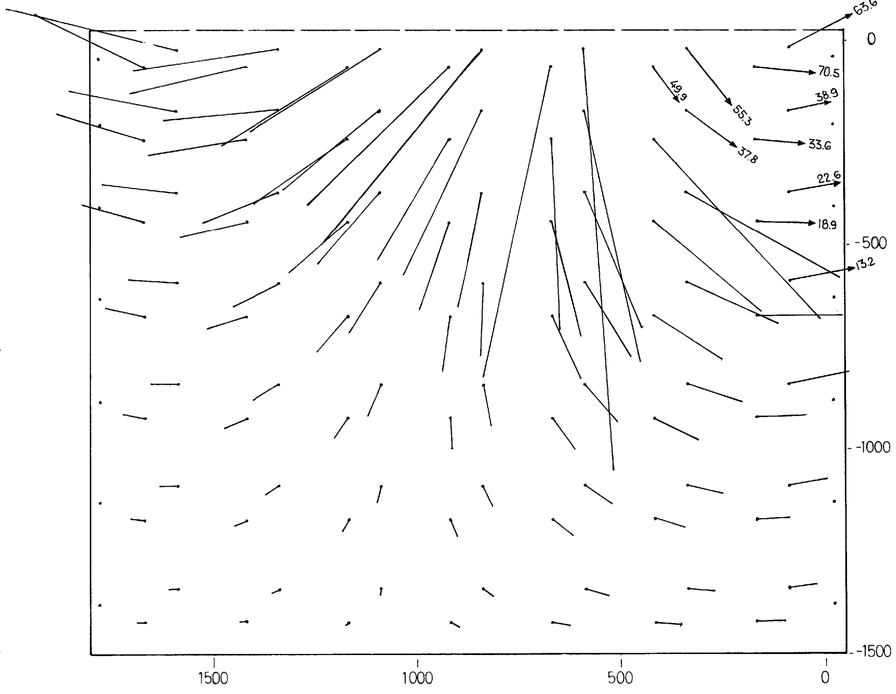

PORE VELOCITY VECTORS

Scale 0 10×10^{-6} m/s

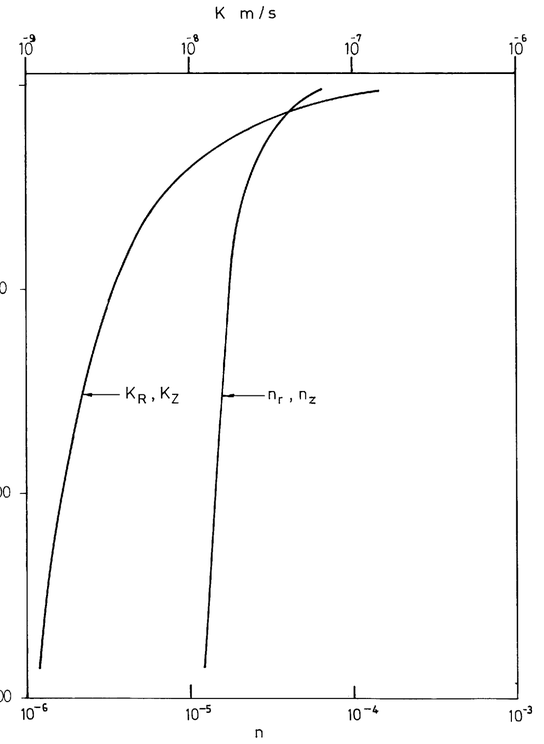

PERMEABILITY (K) & POROSITY (n)

BOUNDARY CONDITIONS

——— Zero flux boundary

– – – – Fixed potential boundary

KBS – Kärnbränslesäkerhet

GROUNDWATER MOVEMENTS AROUND A REPOSITORY

INITIAL CONDITIONS

FORSMARK : SITE MODELL , IMPERVIOUS BOUNDARIES, CASE 2

Hagconsult ab Stockholm Sept. 1977 **FIGURE : 30**

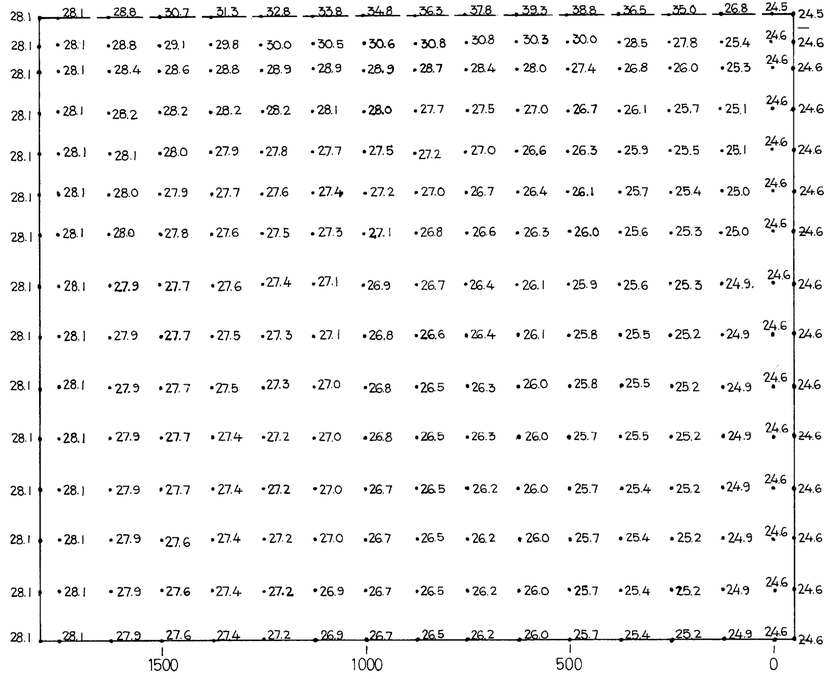

EQUIPOTENTIALS

BOUNDARY CONDITIONS

——— Zero flux boundary

— — — Fixed potential boundary

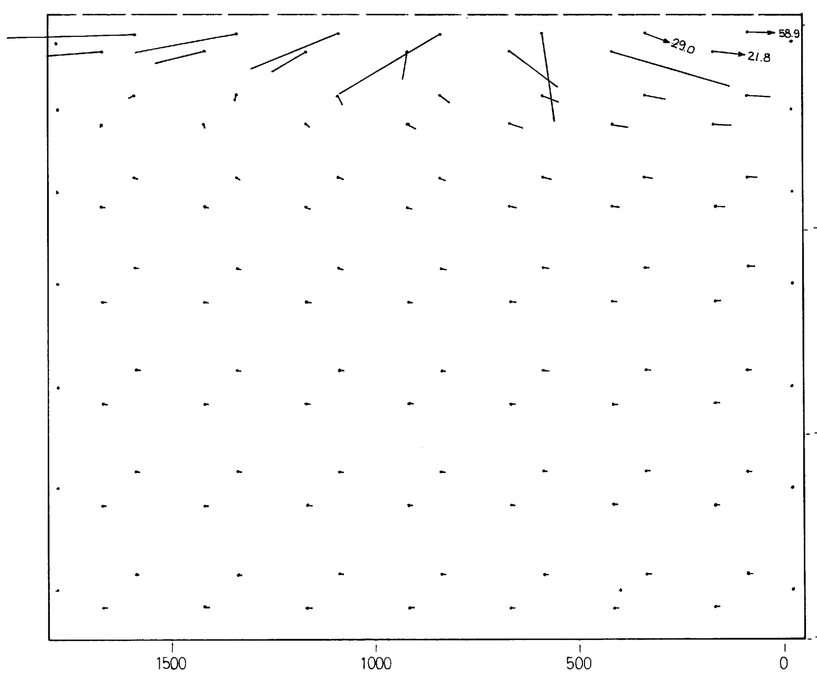

PORE VELOCITY VECTORS

Scale 0 10×10^{-6} m/s

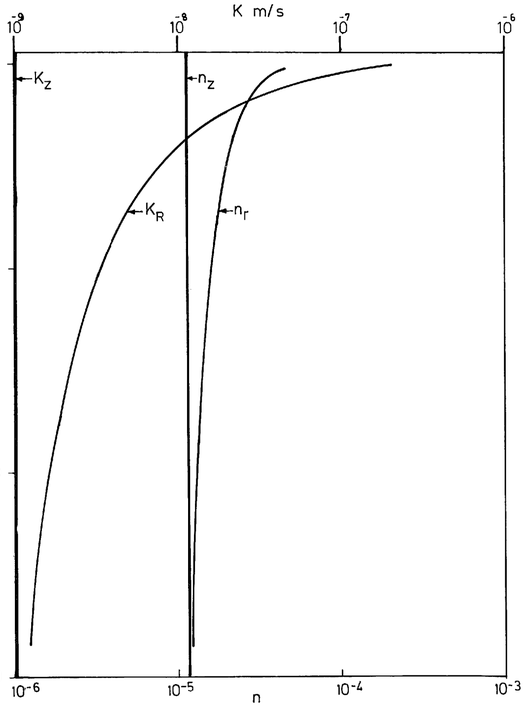

PERMEABILITY (K) & POROSITY (n)

KBS – Kärnbränslesäkerhet

GROUNDWATER MOVEMENTS AROUND A REPOSITORY

INITIAL CONDITIONS

FORSMARK : SITE MODEL, IMPERVIOUS BOUNDARIES , CASE 3

Hagconsult ab Stockholm Sept. 1977 **FIGURE: 31**

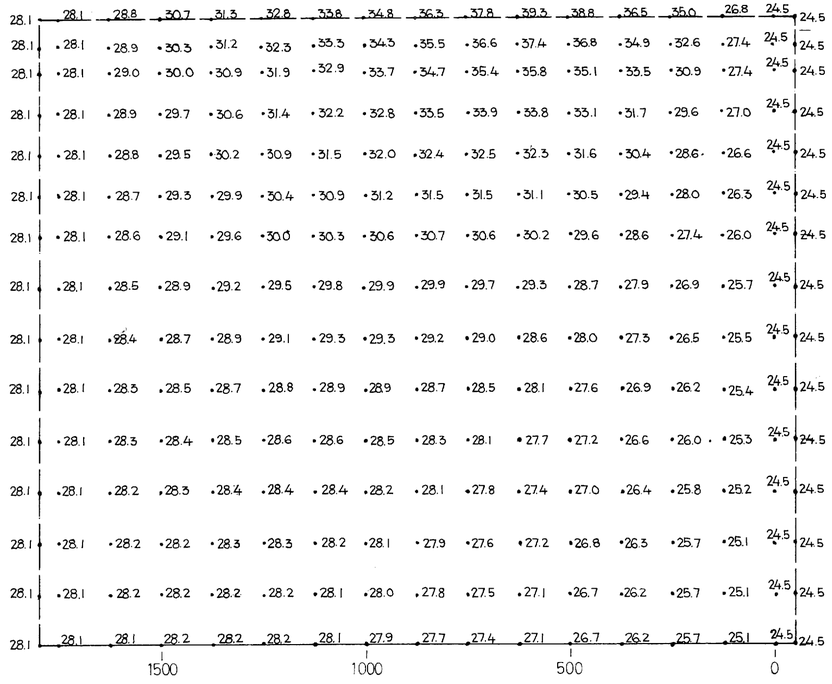

EQUIPOTENTIALS

BOUNDARY CONDITIONS

——— Zero flux boundary

– – – – Fixed potential boundary

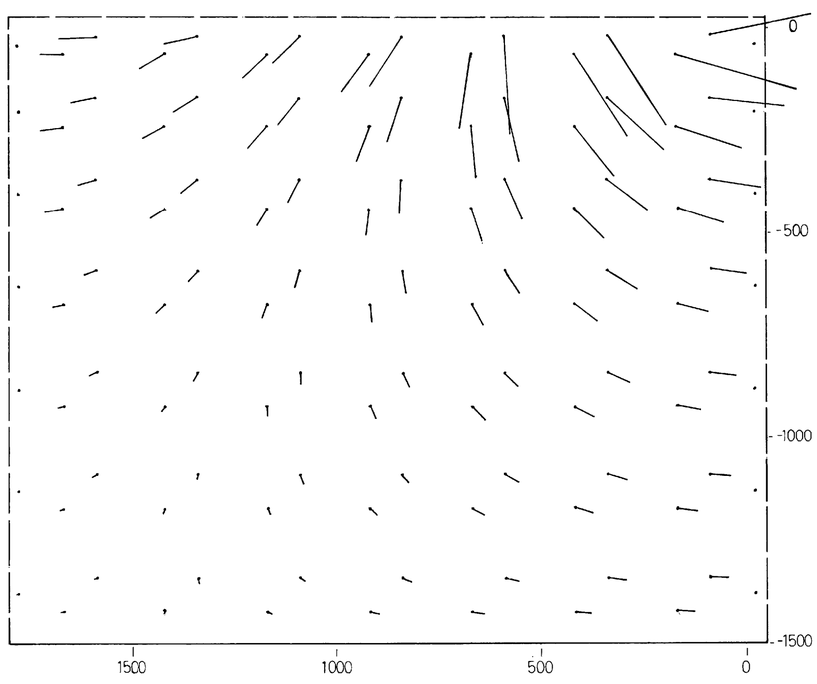

PORE VELOCITY VECTORS

Scale 0 10×10^{-6} m/s

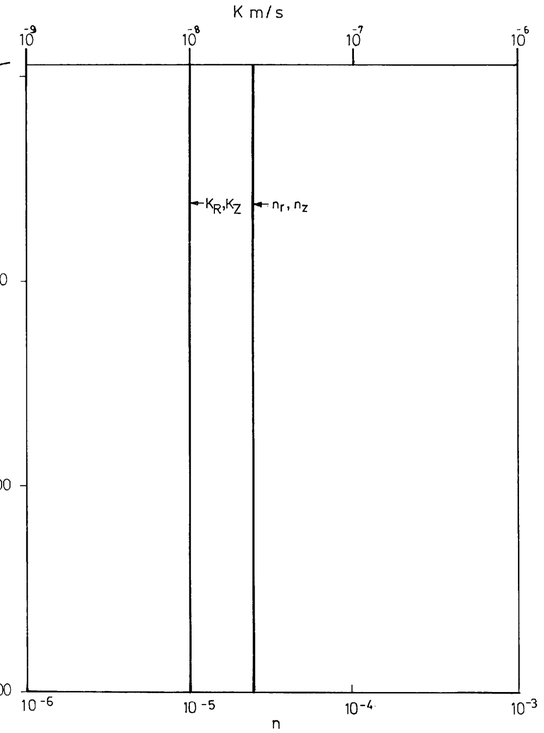

PERMEABILITY (K) & POROSITY (n)

KBS – Kärnbränslesäkerhet

GROUNDWATER MOVEMENTS AROUND A REPOSITORY

INITIAL CONDITIONS

FORSMARK : SITE MODEL , CONSTANT POTENTIAL BOUNDARIES, CASE 1

Hagconsult ab Stockholm Sept. 1977 **FIGURE: 32**

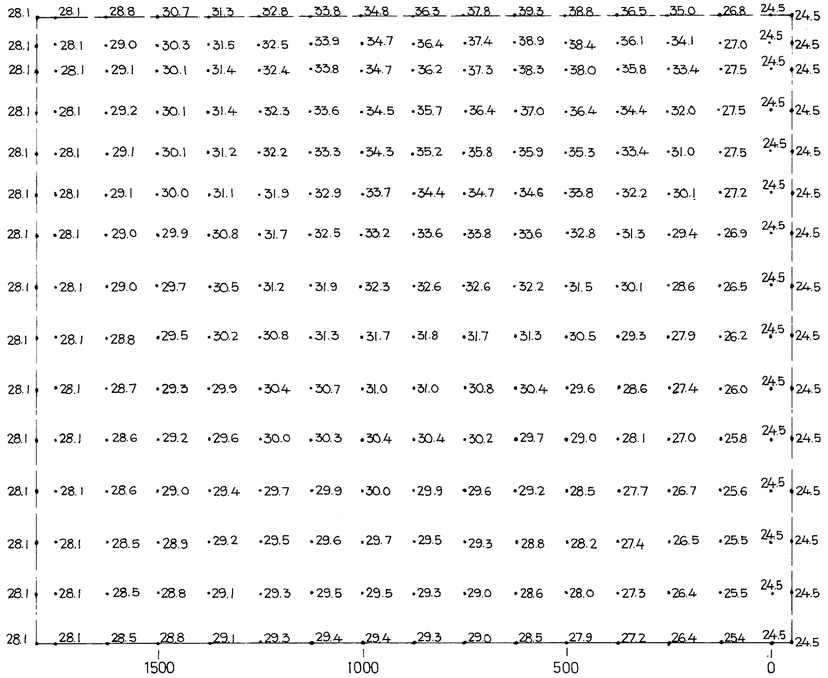

EQUIPOTENTIALS

BOUNDARY CONDITIONS

——— Zero flux boundary

– – – – Fixed potential boundary

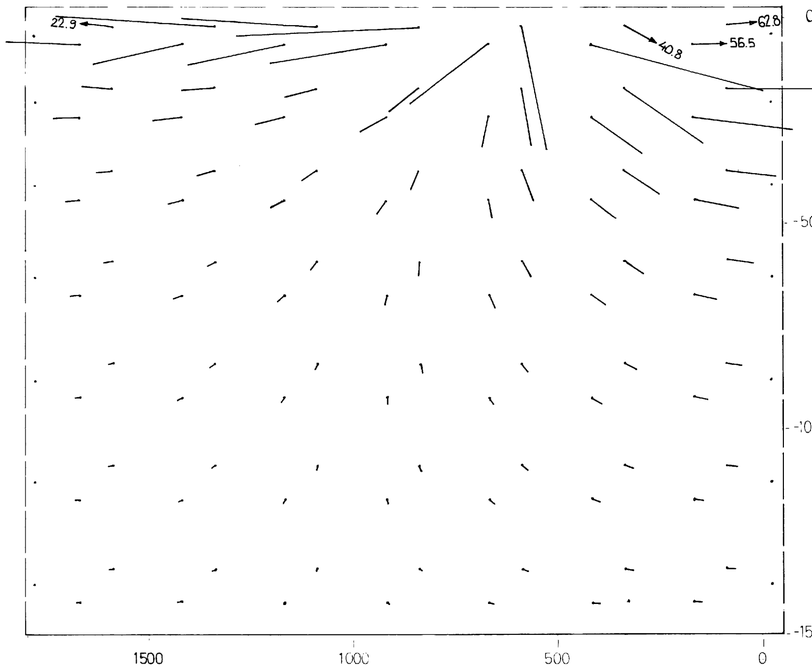

PORE VELOCITY VECTORS

Scale 0 10×10^{-6} m/s

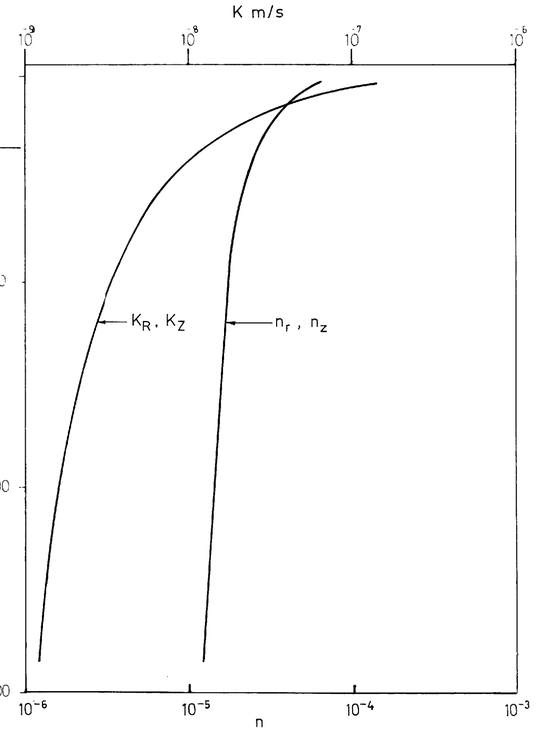

PERMEABILITY (K) & POROSITY (n)

KBS – Kärnbränslesäkerhet

GROUNDWATER MOVEMENTS AROUND A REPOSITORY

INITIAL CONDITIONS

FORSMARK : SITE MODEL , CONSTANT POTENTIAL BOUNDARIES , CASE 2

Hagconsult ab Stockholm Sept. 1977 **FIGURE: 33**

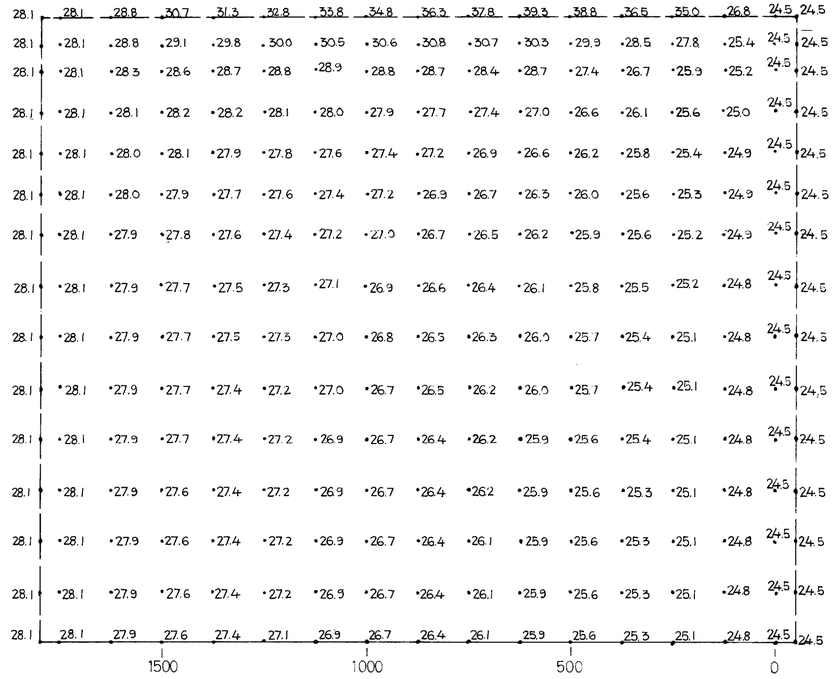

EQUIPOTENTIALS

BOUNDARY CONDITIONS

——— Zero flux boundary

– – – – Fixed potential boundary

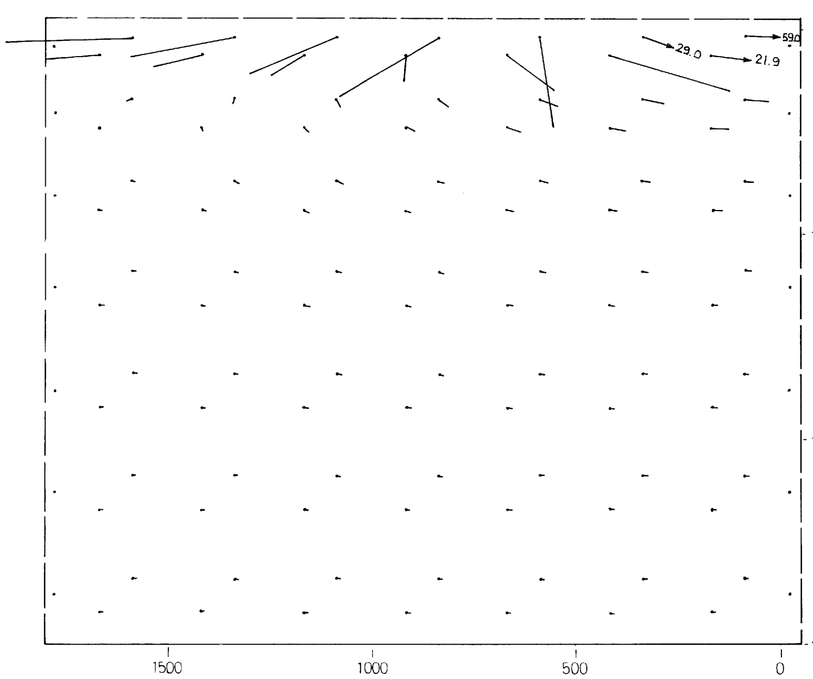

PORE VELOCITY VECTORS

Scale 0 10×10^{-6} m/s

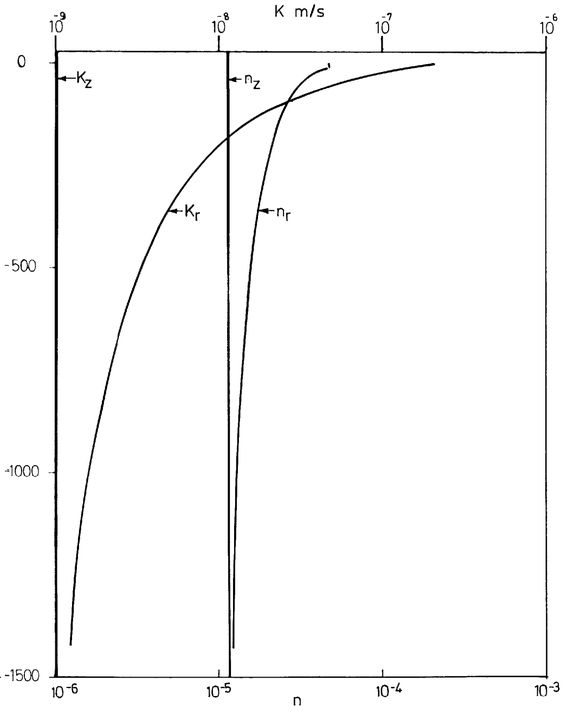

PERMEABILITY (K) & POROSITY (n)

KBS – Kärnbränslesäkerhet

GROUNDWATER MOVEMENTS AROUND A REPOSITORY

INITIAL CONDITIONS

FORSMARK : SITE MODELL , CONSTANT POTENTIAL BOUNDARIES , CASE 3

Hagconsult ab Stockholm Sept. 1977 **FIGURE: 34**

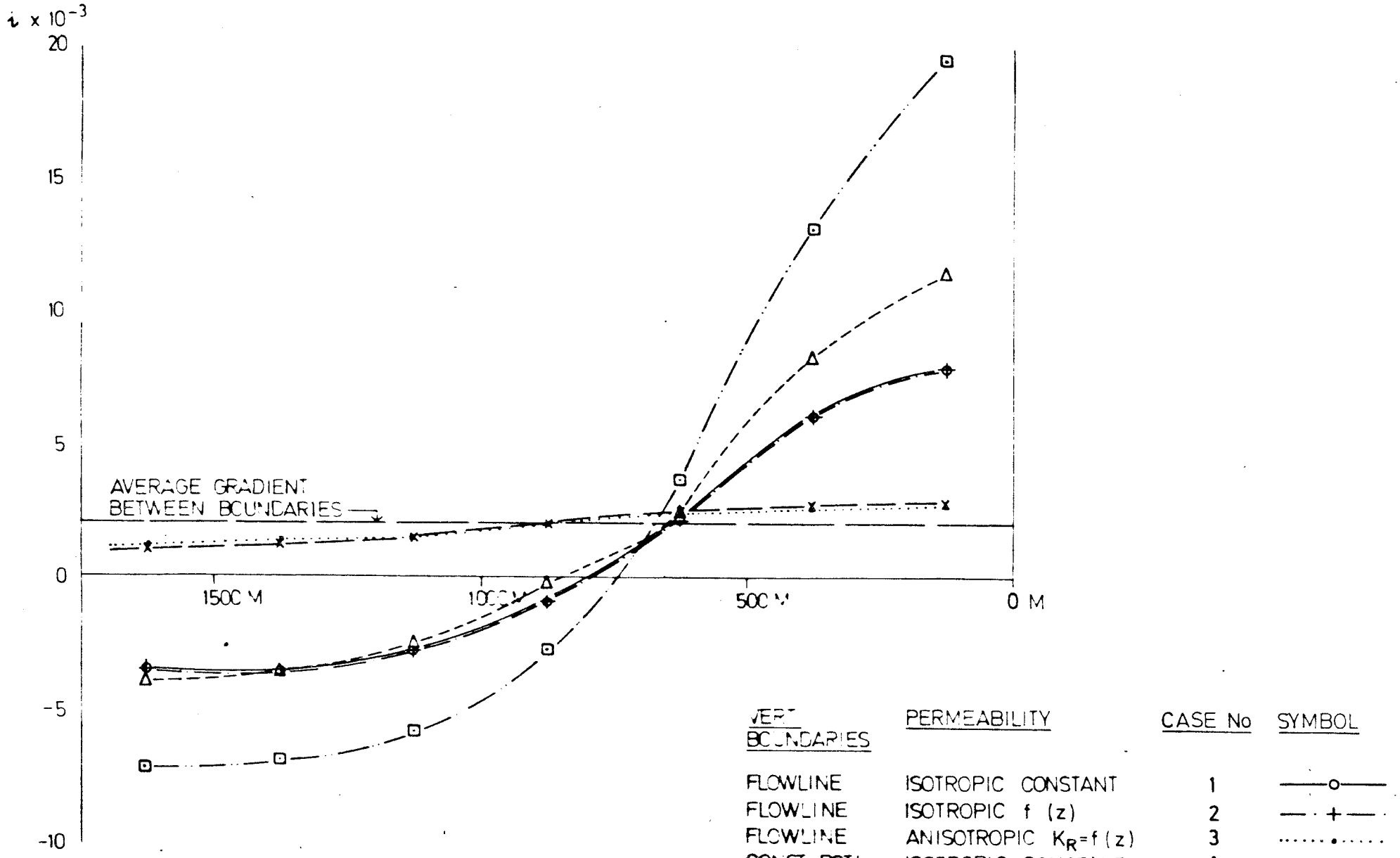

FIGURE 35 FORSMARK SITE MODEL HORIZONTAL POTENTIAL GRADIENTS AT ELEVATION - 500 M.

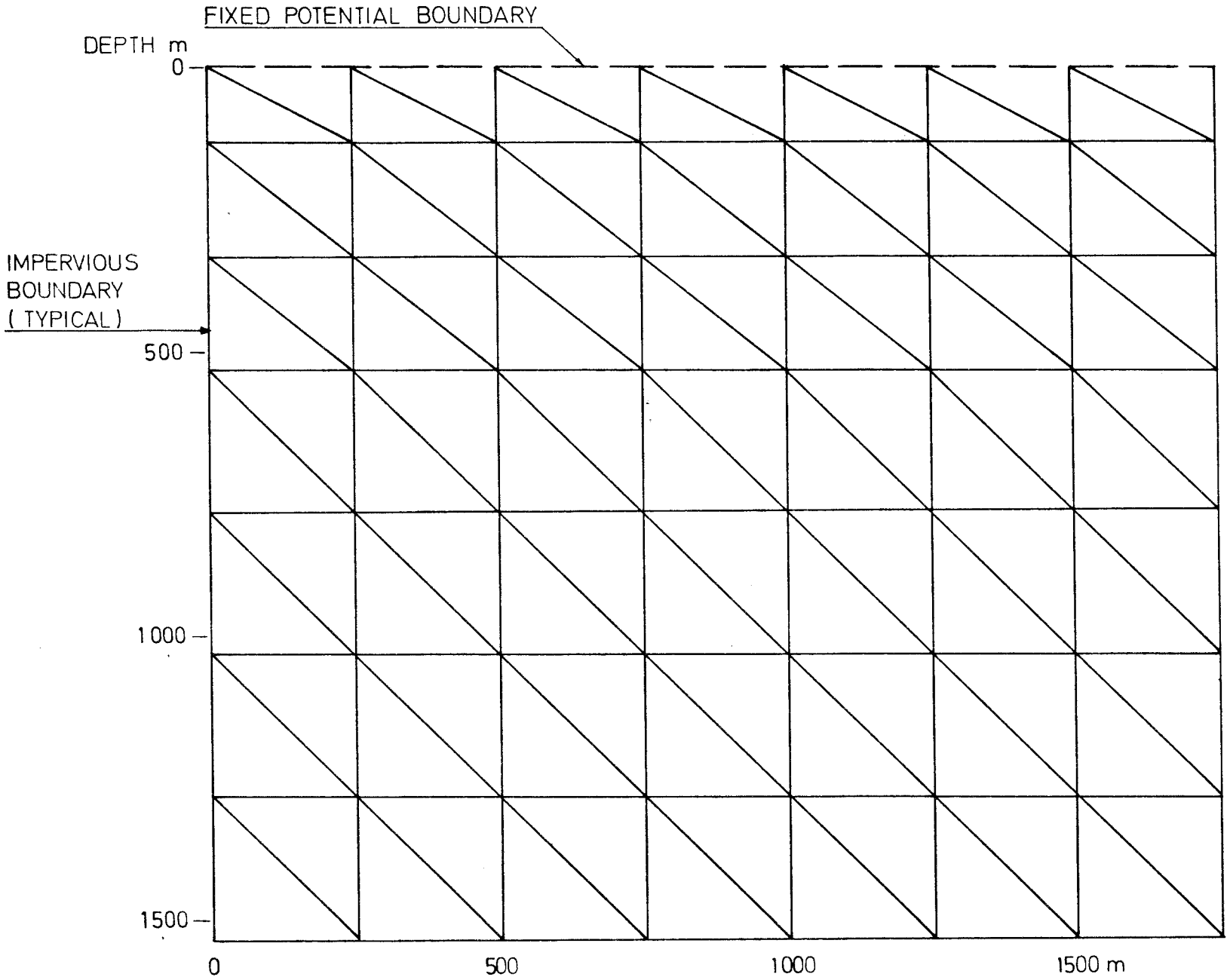

FIGURE B-1. FINITE ELEMENT MESH: VALIDATION

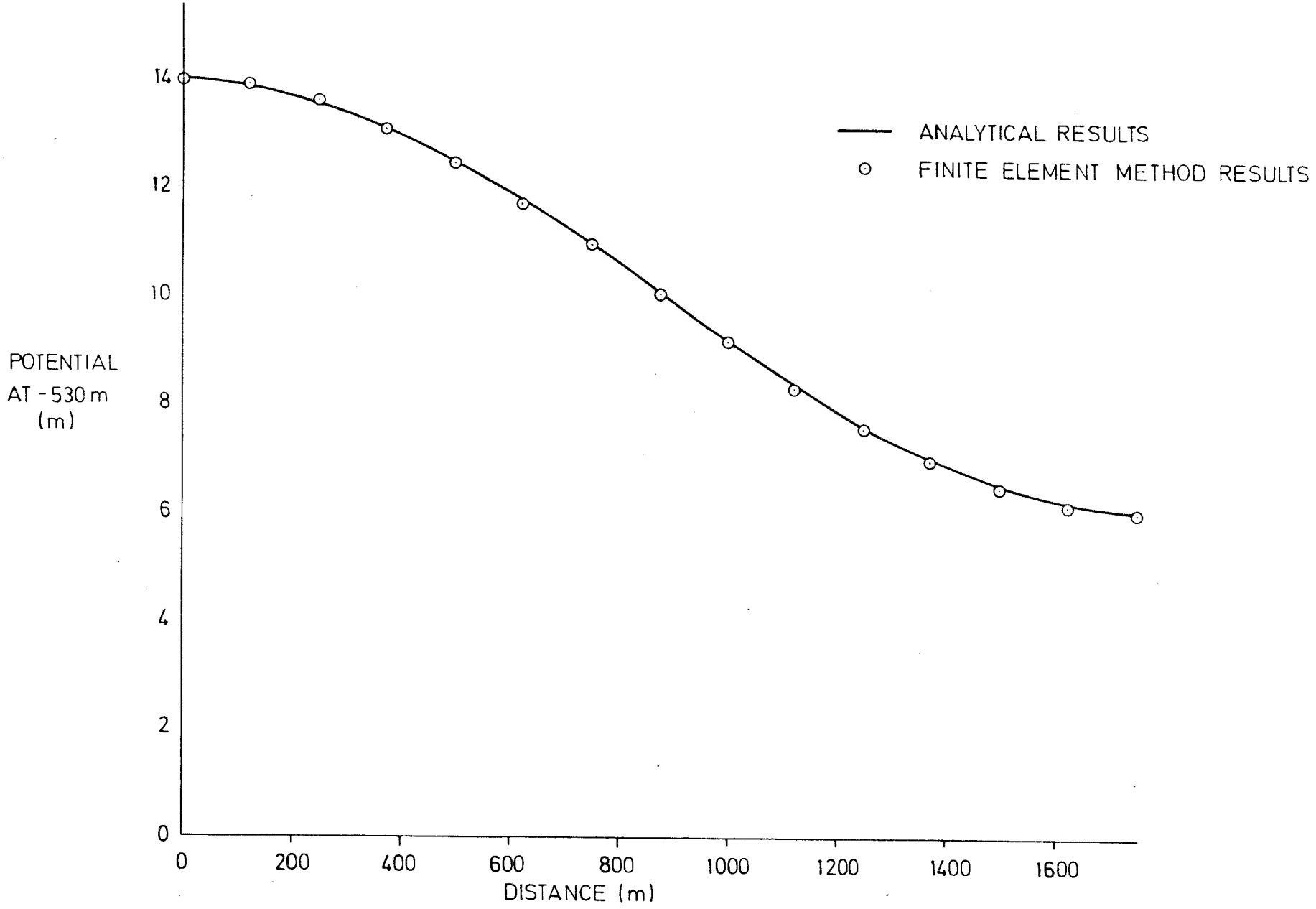

FIGURE B-2. FINITE ELEMENT METHOD - VALIDATION WITH ANALYTICAL SOLUTION FOR SINUSOIDAL FIXED POTENTIAL BOUNDARY

TABLE I

COMPARATIVE POTENTIAL GRADIENTS	i_z	i_r
Regional Gradient 2 in 1000		2.0×10^{-3}
Isotropic K, flowline boundaries, relief 50 m	-3.57×10^{-3}	16.32×10^{-3}
Isotropic K, constant potential boundaries, relief 50 m	-1.67×10^{-3}	17.60×10^{-3}
Isotropic K, flowline boundaries, relief 5 m	-0.36×10^{-3}	1.63×10^{-3}
Isotropic K, constant potential boundaries relief 5 m	-0.17×10^{-3}	1.76×10^{-3}
Anisotropic K, flowline boundaries, relief 50 m	0.45×10^{-3}	2.21×10^{-3}
Anisotropic K, constant potential boundaries, relief 50 m	4.67×10^{-3}	4.21×10^{-3}
Anistropic K, flowline boundaries, relief 5 m	0.05×10^{-3}	0.22×10^{-3}
Anisotropic K, constant potentail boundaries, relief 5 m	0.47×10^{-3}	0.42×10^{-3}

Note 1. Pore velocity may be calculated from

$$V_p = \frac{K}{n} \cdot i$$

Note 2. Sign convention

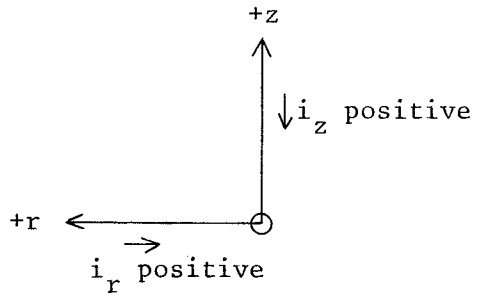

A P P E N D I X A

FINITE ELEMENT METHOD

APPENDIX A

FINITE ELEMENT METHOD

A2.1 INTRODUCTION

This appendix describes FINI 5-0, a two-dimensional, planar and axisymmetric transient (or steady state) finite element saturated groundwater flow code, developed at Acres Consulting Services limited, Niagara Falls, Canada, in early 1976.

The available anisotropic isoparametric elements are a quadratic head (total potential) triangle (6 nodes), a quadratic head gap (fracture) element (6 nodes), and a boundary loading element (3 nodes). Matrics and vectors are computed by numerical quadrature.

Required material properties are principal values of anisotropic conductivity and principal angle (tangential to gap elements) porosity and specific capacity.

The model starts from a specified arbitrary set of initial conditions and proceeds steppwise through a number of solutions during the course of a transient run. Boundary conditions include specified head at a node, nodal fluid load (source or sink), element internal fluid source and surface loads. The surface loads are specified normal seepage velocity and specified head outside a film. All specified values and loads are variable linearly over time spans consisting of one to several time steps and can be started and stopped independently whenever desired.

Gradient, fluxes and pore velocities are computed in a post-processor attached to the main program itself and plotting of meshes, equipotential lines and pore velocities is accomplished by a follow-up program, FINI 510, that accesses several of the disc files produced by the main code.

The program is divided into several overlay segments to minimize core storage requirements. (Within each overlay, the coding is broken into subroutines.) In addition, extensive use is made of disc storage and all data passed from overlay to overlay is written to disc and reread in the newly loaded overlay. This not only minimizes storage but facilitates restarts during long runs or multiple runs and simplifies debugging.

A2.2 FORMULATION AND DEVELOPMENT

The basic equation for two-dimensional saturated groundwater flow, as used in the model, is:

$$K_{km} \frac{\partial^2 \phi}{\partial x_k \partial x_m} + Q - nc \frac{\partial \phi}{\partial t} = 0, \qquad (1)$$

where ϕ = total potential (head),

x = linear dimension,

n = porosity (fractional),

K = hydraulic conductivity = $\rho g \frac{k}{\mu}$,

ρ = fluid density, k = intrinsic permeability,

g = gravitational constant, μ = dynamic viscosity,

Q = volumetric source rate,

c = specific capacity or storage = $\rho g (\beta_f + \alpha_s/n)$,

β_f = fluid compressibility, α_s = solid compressibility

t = time.

In the finite element discretization of the modeled region, the physical space is broken up into elements, in each of which the potential field is described by a simple relationship:

$$\phi = \phi_i N_i . \qquad (2)$$

The ϕ_i are the solution values at specified discretization points or nodes and the N_i are distribution functions associated with each node.

The ϕ_i are also assumed to vary linearly over time steps so that accounting for the time variation expands equation (2) into:

$$\phi = \phi_i^k M_k N_i \qquad (3)$$

in which the M_k are time distribution functions associated with the old and new solutions spanning the time interval in question.

A weighted-residual method may be used with finite elements to formulate a set of linear algebraic equations representative of the modeled system. In this model we use Galerkin weighting in which the residual, multiplied by the distribution functions previously mentioned, is integrated and set equal to zero over the whole region of study.

The form of the Galerkin pseudo-functional is:

$$\chi_G = \int_R \left(K_{km} \frac{\partial^2 \phi}{\partial x_k \partial x_m} + Q - nc \frac{\partial \phi}{\partial t} \right)^* \phi \, dR \qquad (4)$$

*The residual is not varied in the derivation of the matrix equation below. Integration-by-parts and the divergence theorem yield a quadratic formulation:

$$\chi_G = \int_R \left(- K_{km} \frac{\partial \phi^*}{\partial x_k} \frac{\partial \phi}{\partial x_m} + Q^* \phi - nc \frac{\partial \phi^*}{\partial t} \phi \right) dR + \int_S \left(K_{km} \frac{\partial \phi}{\partial x_k} \phi \, i_m \right) dS, \qquad (5)$$

where the second term is a boundary flux term used to express natural boundary conditions impermeable or imposed seepage velocities and specified head outside a film. i_m is the outward facing normal to the surface S. This term is omitted for impermeable boundaries or boundaries with fixed potential and is replaced for other boundaries by:

$$\int_S \left[q - \alpha (\phi - \phi_a) \right]^* \phi \, dS, \qquad (6)$$

where the imposed seepage velocity q is positive for water inflow. α is the film transfer coefficient and ϕ_a is the ambient potential outside the film. The impermeable condition requires that the boundary be a streamline.

The load film with transfer coefficient α and specified external potential may be used for very thin layers of resistance to groundwater flow e.g. shallow (surface) grouting in a cavity with specified head. It may also be used for a type of substructured model wherein a local model is constructed, but the boundary condition is specified head well outside the model boundaries. In this case, $\alpha = K * L$, where K is the conductivity of the external medium and L is the distance from boundary to point of specified head, ϕ_a. When this approximation can be applied, it eliminates the need to model all the flow region with a mesh.

An additional important boundary condition is the phreatic surface with specified infiltration (vertical seepage velocity), $q/\cos(\theta)$, where θ is the angle between the surface normal and vertical. In steady state runs, the phreatic surface may be determined by iteratively moving the mesh to approximations of the true surface until the solved vertical pore velocity at the surface point equals $q/\cos(\theta)/n$. At each iteration ϕ = vertical coordinate at each surface node. This mesh distortion must be performed manually between successive iterations, but may be automated in a future version of this program if use warrants.

In transient analysis, similar time steps with moving phreatic surface may be taken. The vertical velocity of the surface would be:

$$V_s = q/\cos(\theta)/n - V_y \qquad (7)$$

where V_y is the solved vertical pore velocity

Generally in unconfined transient flow of this type, the compression (storage) effects in equation (1) may be neglected compared to the storage occurring at the phreatic surface.

When the first variation of this pseudo-functional is taken:

$$\frac{\partial \chi_G}{\partial \phi_i} = 0 \tag{8}$$

the following matrix equations result at time step ℓ (Δt = step length):

(a) For fixed α

$$\left[\frac{2}{3} (\bar{\bar{K}} + \bar{\bar{\alpha}}) + \frac{\bar{\bar{C}}}{\Delta t} \right] \phi_j^{\ell} = \left[- \frac{1}{3} (\bar{\bar{K}} + \bar{\bar{\alpha}}) + \frac{\bar{\bar{C}}}{\Delta t} \right] \phi_j^{\ell-1} + \frac{1}{3} \left[\bar{Q} + \bar{q} + \bar{\bar{\alpha}} \phi_a \right]^{\ell-1} + \frac{2}{3} \left[\bar{Q} + \bar{q} + \bar{\bar{\alpha}} \phi_a \right]^{\ell} \tag{9a}$$

(b) For variable α

$$\left[\frac{2}{3} \bar{\bar{K}} + \frac{\bar{\bar{C}}}{\Delta t} \right] \phi_j^{\ell} = \left[- \frac{1}{3} \bar{\bar{K}} - \bar{\bar{\alpha}} + \frac{\bar{\bar{C}}}{\Delta t} \right] \phi_j^{\ell-1} + \frac{1}{3} \left[\bar{Q} + \bar{q} + \bar{\bar{\alpha}} \phi_a \right]^{\ell-1} + \frac{2}{3} \left[\bar{Q} + \bar{q} + \bar{\bar{\alpha}} \phi_a \right]^{\ell} \tag{9b}$$

(c) For steady-state solutions we have:

$$\left[\bar{\bar{K}} + \bar{\bar{\alpha}} \right] \phi_j = \bar{Q} + \bar{q} + \bar{\bar{\alpha}} \phi_a \, . \tag{9c}$$

The component matrices are:

$\bar{K} = \sum^{e} \int_e K_{km} N_{j,x_k} N_{i,x_m} dR$, where $\sum^{e}$ is a sum over all elements,

$\bar{\alpha} = \sum^{e} \int_e \alpha N_j N_i dS$, where S is the external boundary on the element,

$\bar{\bar{\alpha}} = \sum^{e} \int_e \alpha N_i dS$

$\bar{C} = \sum^{e} \int_e nc N_j N_i dR$,

$\bar{Q} = \sum^{e} \int_e Q N_i dR + Q_i$, where Q_i is a nodal load (source), and

$\bar{q} = \sum^{e} \int_e q N_i dS$.

These matrices are presented for the general case. In 2-D planar (dR) is (dxdy). For the axisymmetric, replace (dR) by $(2\pi r dz dr)$, (dS) by $(2\pi r dS)$ and (Q_i) by $(2\pi r Q_i)$.

A2.3 UNITS

The program is written in dimensionless form so that any compatible set of units for the input data will be acceptable.

As an example consider the following: In metric units, the desirable units of length and time may be the metre and second respectively. The value of K,n and c must therefore be given in input data so that the diffusivity K/nc has units m^2/sec or

length^2/time. K in [m/sec], n dimensionless and c in [m^{-1}] will achieve this and are compatible. The constituent units for K are: k in [m^2], μ in [kg/m sec], ρ in [kg/m^3] and g in [m/sec^2]. Similarly, the additional constituent units for c are: β_f and β_s in [Pa^{-1} or m sec^2/kg]. It is important to note that the nodal locations must be given in the length unit desired e.g. [m] in this example. Also, loading units must be compatible, e.g.: volumetric source Q in [sec^{-1}, actually m^3/m^3 sec], boundary normal seepage velocity q in [m/sec], film coefficient α in [sec^{-1}], film external potential ϕ_a in [m] and nodal source Q_i in [m^3/sec].

A P P E N D I X B

FINITE ELEMENT METHOD VALIDATION

APPENDIX B

FINITE ELEMENT METHOD VALIDATION

To confirm to validity of the finite element method used for this study, an analysis was performed for the using the mesh and boundary conditions shown in Figure B1. The constant potentials on the upper boundary are determined by

$$\rho_z = 0 \quad = a \cos \frac{2\pi}{b} \cdot r$$

The potential at any point is then given by: (1)

$$\rho_{r,z} = a \frac{\cosh \left(\frac{2\pi (d-z)}{b}\right) \cdot \cos \left(\frac{2\pi r}{b}\right)}{\cosh \left(\frac{2\pi d}{b}\right)}$$

For the conditions

a = 5 m

b = 1750 m

d = 1530 m

the numerically computed values of $\rho_{r,z}$ for z = -530 are plotted on Figure B2 together with the analytically calculated values. The maximum difference between analytical numerical values as a percentage of the total overall potential difference, is 0.62%.

The finite element method is therefore considered adequate by comparison with an exact analytical solution for representation of groundwater flow.

TECHNICAL REPORT 3

REGIONAL GROUNDWATER FLOW ANALYSES

PART II

LONG TERM RESIDUAL CONDITIONS

KBS-Kärnbränslesäkerhet

GROUNDWATER MOVEMENTS AROUND A REPOSITORY

Phase 2. Technical report 3: Regional Groundwater Flow Analyses
Part II: Long Term Residual Conditions

Hagconsult AB
in association with
Acres Consulting Services Ltd
RE/SPEC Inc.

FOREWORD

This report was prepared as one of a series of technical reports within a study of the groundwater movements around a repository for radioactive waste in the Precambrian bedrock of Sweden. It was written in two parts, (I) initial flow conditions and (II) long-term residual conditions. This part is Part II. The contract for this study was between KBS - Kärnbränslesäkerhet (Project Fuel Safety) and Hagconsult AB of Stockholm, Sweden. RE/SPEC Inc. of Rapid City, SD/USA and Acres Consulting Services Ltd of Niagara Falls, Ontario/Canada acted as subconsultants to Hagconsult AB.

The principal author of this report is Dr Anthony Burgess of Acres. Review was provided by Dr Ulf E. Lindblom of Hagconsult AB and Dr Robin Charlwood of Acres. Input to the study was provided by Dr Håkan Stille and Mr Joe L. Ratigan of the Study Group and by other contributors to the KBS project.

The opinions and conclusions in this document are those of the author and should not be interpreted as necessarily representing the official policies or recommendations of KBS.

Stockholm October 1977

Ulf E. Lindblom
Study Director
Hagconsult AB

TABLE OF CONTENTS

LIST OF FIGURES

Figure

LIST OF TABLES

Table

OBJECTIVES AND SCOPE

This part of the technical report considers the groundwater flow in the repository area for the period after the significant thermal cycle perturbations. The temperature as a function of time at the repository mid plane is shown in Figure 1. In the long term, the groundwater flow will be determined by natural boundary conditions. Modifications to the permeability field in the repository domain, however, will result in differences in the groundwater conditions post-repository, compared to the initial natural regime.

The overall objective of this part of the report is thus to provide data (pathways, fluxes, pore velocities) for use in the repository - biosphere safety analyses. No attempt has been made in this study to quantify the effects of geological changes on boundary conditions or parameters, although they have been discussed qualitatively.

2. FACTORS AFFECTING GROUNDWATER FLOW

The factors influencing the long term groundwater flow patterns may be divided into:

factors independent of the existance of repository

factors due to the residual effects of the repository

2.1 Factors Independent of Repository

In general, the effects of factors independent of the repository can only be assessed in, at best, a semi-quantitative manner. This may be accomplished by considering the effect on parameters or boundary conditions for typical models already analysed.

2.1.1 Natural Factors

Isostatic change in sea level

In general, an isostatic change in sea level will have only a nominal effect on the regional topographic gradient. Since this gradient controls the regional hydraulic gradient, the effect will be insignificant. However, in exceptional cases, the regional drainage may be modified. This could lead to draining of lakes or formation of new lakes, which will, in turn, alter the groundwater regime in the area. The magnitude of such changes cannot, however, be estimated, although it is unlikely to result in conditions markedly different from those typical of the region at the present.

Glaciation

The formation of an ice sheet over the area would result in higher lithostatic stresses at the repository level. Some reduction in permeability could therefore be expected. Under receding ice conditions, groundwater conditions are extremely volatile, as ice dammed lakes form and are breached. Under these conditions the groundwater regime could vary markedly from the present day. In particular, high gradients could develop under certain conditions.

T e c t o n i c a c t i v i t y

The risk of tectonic activity is presently being assessed by other study groups for KBS. In general tectonic events would likely be experienced preferentially along the existing major tectonic structural features, as they represent weakness planes. Since the repository will be sited between such features, the probable direct effect upon the repository will be small. The seismic loading on the repository excavation could precipitate or extend latent failure zones. This result, however, may be considered as further deterioration of the room, leading to the second permeability condition for the repository described in section 2.

E r o s i o n

The sites under investigation have been specifically chosen in geologically old peneplain areas. By virtue of the preservation of the peneplain characteristics over millions of years, the erosion processes are shown to be very slow. The conditions around the repository are thus unlikely to be affected by erosion within the time period for the decay of even the most long lived radionuclides.

2.1.2 Man-made Factors

C h a n g e s t o t h e s u r f a c e w a t e r r e g i m e

These may occur by draining existing lakes or by creating other. The results may be estimated by considering the possible regional gradient change. Thus, for example, if the elevation of Finnsjön were to be artificially raised by 5 m, the cross site gradient would increase from 2.06×10^{-3} to 4.91×10^{-3}. Pore velocities and fluxes would be increased proportionally.

C h a n g e s t o t h e g r o u n d w a t e r r e g i m e

This could arise for example from the development of wells or the construction of deep excavations or mines in the area. The effect on the cross site gradient will depend upon the extent and proximity to the repository of the development. In general, the effects will be most noticeable if the groundwater levels in the bounding tectonic features to the repository are modified.

2.2 Factors Dependent on the Repository

The residual effects of the repository on the groundwater flow are primarily due to changes in permeability in and around the repository. The permeability of the repository plane itself will depend upon the sealing measures adopted. In addition, deterioration of the adjacent rock over long time periods will result in changes in the surrounding rock. The methodology for assessing these effects is described in Section 3 of this report.

In addition to the repository itself, the effect of ancillary facilities required during investigation, construction, emplacement and decommissioning must be considered, including:

Site exploration drillholes

Site exploration drillholes will or have been sunk at prospective sites. The possibility of them becoming waste migration pathways must be investigated and minimised by the development of plugging and sealing techniques. Details of work undertaken to date in the USA is contained in references (1), (2), (3)[x].

Shafts

The effect of shaft sinking and subsequent methods of sealing, on the groundwater flow, is very important. Poor sealing may result in the introduction of ground surface potentials (head of water) at depth. This could have a considerable effect on the flow patterns and pathways in and around the repository.

Construction facilities

During construction, it may be necessary to drive tunnels specifically for grouting, drainage, water injection etc. The sealing measures to be adopted, and the effects upon the final flow patterns must be considered at a later date when more information is available.

[x]Numbers in parentheses refer to references at end of text.

Operational facilities

Site grading and construction and operation of the underground handling facilities will affect the groundwater surface, particularly in the short term. The long term modifications, if any, to the flow patterns will depend upon the gross change compared to the initial conditions.

3. METHODOLOGY AND RESULTS FOR THERMOMECHANICAL EFFECTS

The thermal conditions around the repository have been predicted using two dimensional and axi-symmetric finite element methods for transient heat conduction. A complete description of the techniques, thermal loadings material properties used and results obtained is given in Technical Report No. 2 in this study (4). The effects of thermal advection due to groundwater flow have been examined (5) and found to have negligible effect on the temperature distribution at any time.

The mechanical behaviour of the rock around the repository has been simulated using two dimensional finite element methods. The technique used has the facility to include joint elasto-plastic material parameters for defined joint set orientations. A complete description of the techniques, material properties, stress conditions and results is given in Technical Report nr. 4 (7).

The mechanical behaviour has been considered in two stages:-

I. deformation and stress changes due to construction

II. deformation and stress changes resulting from the thermal cycle.

For the gross thermal loading adopted for the Swedish repository conceptual design, the effects of from the thermal cycle are small in comparison to the stress changes and deformation associated with the construction phase. (8).

The elasto-plastic analyses indicate areas of plastic deformation (failure) in the immediate vicinity of the room. No failure zones were developed in the global model. In the long term, the failure zones predicted by the elasto-plastic methods may increase. Any failure will lead to an increase in permeability. In the long term, therefore, the repositiory plane may become effectively much more permeable than the surrounding rock. It should be noted that this effect would be lagely independent of the sealing measures adopted, since it is due to failure, and hence increase in permeability, around the room. For the purpose of this study it has been

assumed that deterioration in the long term affects a cross sectional area of the room which is two to four times the initial cross sectional area. Two extreme permeability conditions for the repository plane were considered and are described in Section 4.1.

4. GROUNDWATER FLOW ANALYSES: REPOSITORY DOMAIN

4.1 Model Assumptions

For the analysis of the groundwater flow for the long term residual effect conditions the Forsmark site area two dimensional vertical section model was modified to include the repository plane. In section, the repository was 1250 m in length, and equidistant (250 m) from the bounding discontinuities (see Figure 2).

The results of the groundwater studies of the initial conditions showed that the flow pattern was not sensitive to changes in boundary conditions due to the high permeability assumed for the bounding discontinuities. For these analyses therefore only constant potential vertical boundary condition was modelled. The potential was taken as the elevation of the ground surface.

The potentials specified on the upper boundary of the model were equal to the ground surface elevation. The lower boundary of the model was considered as impervious i.e. a streamline.

Analyses were made for the three nominal permeability distributions (Figure 3) used för the initial conditions study. In addition for comparative purposes, the effect on travel times of a permeability 5×10^{-11} m/s at 500 m depth was assessed for the anisotropic conditions (case 3). This value has recently been obtained from preliminary results of the Stripa Mine in-situ permeability tests (9).

For the repository itself, two extreme permeability distributions have been considered:

I m p e r v i o u s b a c k f i l l

For this condition it is assumed that the rooms are backfilled with impervious material of permeability characteristics similar to the surrounding rock mass. In addition the rock is assumed to maintain its pre-repository permeability characteristics. Under these assumptions, groundwater flow patterns will be identical to the undisturbed natural conditions, and thus represent a bound to the possible range of conditions.

Pervious backfill

For this condition the rooms are assumed to be left void or loosely backfilled with pervious material. Over the long term, deterioration will result in an equivalent continuum at the repository plane having a thickness of 5 m, with a permeability of 1 x 10^{-3} m/s and porosity of 20 percent. This value represents a room permeability of 6 x 10^{-3} m/s for a long term cross sectional area of twice the initial cross sectional area, or a room permeability of about 3 x 10^{-3} m/s for a long term or cross sectional area of four times the initial value. For these analyses, it has been assumed that the rooms are aligned parallel to the groundwater flow direction. The effects of other alignments will require the use of three-dimensional methods of analysis. These conditions were chosen to give an upper bound to the possible parameters for the repository plane.

4.2 Results

The equipotentials and pore velocity vectors for the three nominal permeability distributions and two backfill conditions, are shown in Figures 4 to 9.

For an isotropic constant permeability distribution, case 1, (Figures 4 and 5) the flow pattern is strongly influenced by the upper boundary condition (topography). The flow is generally downwards through the repository and laterally towards the vertical boundaries. For the impervious backfill case, the equipotentials are strongly curved in the vicinity of the repostiory, becoming near vertical adjacent to the vertical boundaries. The pervious backfill, however, results in the equipotentials becoming near horizontal immediately above and below the repository. The nature of the backfill also affects the fluxes and pore velocities. For the pervious backfill condition, the fluxes and pore velocities are increased around the margins of the repository and reduced through the central portion. The fluxes at the centroids of the elements immediately below the repository are plotted in figure 10. They show that the range of fluxes is larger for the pervious backfill, compared with the impervious backfill.

For the case of isotropic permeability decreasing with depth, case 2, (Figures 6 and 7) the flow patterns are similar to case 1, being strongly influenced by the topography. The flow is downwards throughout the repository area for both backfill conditions. The differences between the equipotential patterns for the two backfill cases are also similar to case 1. For the impervious backfill condition they are strongly curved in the repository area. For the pervious backfill condition however, they are nearly horizontal immediately above and below the repository. Compared with the impervious backfill, the fluxes and pore velocities are increased around the margins of the repository and reduced in the centre. The fluxes at the centroids of elements immediately below the repository are plotted in figure 11. They show that the range of fluxes is larger for pervious backfill compared with the impervious backfill.

The flow patterns for the anisotropic permeability distribution, case 3, (Figures 8 and 9) are markedly different to those for isotropic conditions. With both pervious and impervious backfill there is strong, topography induced, lateral flow in the upper 200 m. For the impervious backfill conditions, the flow paths below 200 m depth are nearly horizontal across the site. These conditions are modified with pervious backfill within a region two to three hundred metres above and below the repository. Flow is drawn into the repository on the upstream side, travels through the repository, and is discharged downstream. Over the upstream third, flow is into the roof and floor: over the centre third flow is into the roof and out from the floor; and over the downstream third, flow is out from the roof and the floor. The asymmetry is due to the regional crossflow having a slight downward component across the site.

The fluxes at the centroids of elements immediately below the repository are plotted in figure 12. They show that the range of fluxes is larger for the pervious backfill compared with the impervious backfill.

5. DISCUSSION AND ANALYSES OF RESULTS

5.1 Repository Domain and Regional Flow

The conceptual model for the groundwater flow comprises major geological structural features canying the regional flow with relatively intact bedrock between. Groundwater circulation within the major structural features is more rapid than in the intact blocks. This is evidenced by tne experience of exploration and well drillings (10), and by palaeo-salinty measurements (11,12). The latter show that at depths below about 100 m saline groundwater still exists in parts of Sweden originating from when those areas were below sea level. Tectonically sheared and altered zones, however, showed lower chloride contents indicating greater permeability and flow rates. For this study, the flow within the bedrock block has been modified by considering the effect of the repository. However, within the bounding structural discontinuities and beyond, the flow pattern will be unaffected by the presence of the repository. Data on the existing conditions, when available, will enable predictions to be made of the probable flow paths within and away from these features.

5.2 Pathways and Travel Times: Repository Domain

Flow paths from different parts of the repository to the bounding discontinuities are, together with travel times shown in figures 13, 14, 15 for the three nominal permeability distributions and two backfill conditions. The permeability distributions were selected primarily to determine the sensitivity of flow patterns to the hydraulic properties. The travel times should therefore be considered on a comparative rather than absolute basis

Since anisotropic conditions are considered more probable than isotropic at the sites, the pathway implications resulting from this model will be discussed further. As discussed in Technical Report No 1 of this study (13), permeability values obtained to date have been based on very limited measurements using borehole packer test methods. Preliminary results from a large in-situ permeability test presently being performed at the Stripa Mine test site indicate permeability values of about 5×10^{-11} m/s (9). Packer tests in the same area, however, indicate

ten tc twenty times more permeable values for the rock. For the purpose of comparison, the travel times for case 3 have been calculated for an equivalent permeability distribution with a value of 5×10^{-11} m/s at 500 m depth. These are given in Table 1. The pathways 1 to 5 are the estimated quickest routes from points A to E to the model boundaries. (Figure 15). The travel times within the repository zone backfill for pathways 1 and 2 are also given.

For the impervious backfill case, the exit pathways from all locations in the repository are below the repository. The shortest travel times are 12.1 and 289.5 years for the nominal and Stripa Test permeability values respectively. For the pervious backfill case, the quickest pathways will be through, above or below the repository depending upon the starting point. The shortest travel time, from point E to the boundary, is 6.1 or 145.7 years for the nominal and Stripa test permeability values respectively. From the vicinity of location D, the shortest pathway may be either below or above the repository. With the latter, there would be a higher probability of the pathway intersecting more active circulation patterns near surface. From the centre of the repository the quickest pathway is below the repository. However, from points A and B, the pathway will initially pass through the repository, since this portion of the repository is subjected to inflow. Once the flow reaches the centre of the repository, then the quickest route would follow pathway 3 below the repository.

For the condition of pervious backfill, it should be noted that the velocity of flow through the repository zone is largely independent of the host rock permeability, being controlled by the permeability and porosity characteristics of the backfill itself. Also, the through repository travel times assume that the rooms are oriented parallel to the groundwater flow direction i.e. parallel to the plane of the model. The actual orientation and effect of haulageways should be taken into account in the final analyses.

5.3 Pathways Beyond the Repository Domain

When the flow reaches the bounding major tectonic feature, the flow path will depend upon the flow within and through the feature, within which the flow will undergo dilution mixing and dispersion. Some of the flow from the repository will therefore travel within the feature, and some will pass out into the adjacent, downstream block. The partition of the flow, and hence concentration of any leached nuclides will depend upon the relative hydraulic characteristics (permeabiliyt, gradient) of the bedrock block and the structural feature.

Considering the discharge plume from the repository to the bounding feature, the total quantity of flow is given by the surface integral of the flux over the boundary between the pathway limits (Figures 14 & 15). These values are tabulated below, assuming the repository extends 1 km perpendicular to the plane of the model section.

Total discharge into bounding feature

	Impervious backfill	Pervious backfill
Case 3	1.751×10^{-6} m^3/s	9.655×10^{-6} m^3/s
Case 3 modified for the Stripa permeability value	2.379×10^{-8} m^3/s	13.118×10^{-8} m^3/s

The flux within the structural feature will be a function of the permeability and boundary conditions. The dilution of the repository plume will depend upon the width of the structural feature, the flux and extent of mixing and dispersion. The transport times will be a function of the flux and porosity within the feature. At present insufficient data is available relating to these features to permit estimates of dilution pathways and travel times to be made. In the meantime, conservative assessments for safety analysis purposes can be made by assuming no dilution and only nominal travel times within the tectonic feature to the biosphere. Thus the travel time from the repository to the bounding feature can be considered as a conservative estimate of the travel time to the surface.

6. SUMMARY AND CONCLUSIONS

The results of these analyses show that, for isotropic permeability distributions, the groundwater flow pattern is determined by the upper boundary potentials, i.e. topography. As a result, these flow patterns are site specific. For the anisotropic conditions, the topography affects only the upper 200 m: below that the flow is controlled by the regional gradient. The anisotropic flow patterns are therefore not as site specific, although the actual magnitudes of the fluxes and pore vlocities will depend upon the regional gradient in the area.

Compared to the impervious backfill case, pervious backfill results in a larger variation in fluxes and pore velocities in the repository area for all permeability distributions. The flow pattern for the isotropic case is similar for both backfill conditions. For the anisotropic case, however, the cross site flow becomes funnelled into the repository with a plume-like discharge downstream.

Pathways from the repository to the bounding discontinuity have been investigated and travel times determined. For the anisotropic conditions case 3 they range from 12 to 143 years with impervious backfill and from 6 to 1273 years for pervious backfill. If the permeability values at the repository level are adjusted to the value measured at Stripa, the travel times are 290 to 3421 years and 146 to 4610 years for the impervious and pervious backfill cases respectively.

The total flow into the bounding discontinuity from flow paths through the repository has been determined. However, the dilution of this flow in the discontinuity, and the pathways and travel times in the discontinuity cannot be estimated without further field data on the nature of this features at depth.

REFERENCES

1. Herndon, Joe, and Smith, Dwight K., 1976 Plugging Wells for Abandonment. A State-of-the-Art Study and Recommended Procedures, prepared by Halliburton Services for Union Carbide Corporation, Nuclear Division, Office of Waste Isolation, Y/OWI/SUB-76/99068.

2. Martin, R. Torrence, and Olsen, J.M., 1975 Feasibility of Sealing Boreholes with Compacted Natural Earthen Material, vols. I, II, and III, prepared by Department of Civil Engineering, Massachusetts Institute of Technology, for Union Carbide Corporation, Nuclear Division, Oak Ridge National Laboratory, ORNL/SUB-3960/2.

3. McGowan, C.; Nolan, E.; Morey, R.; and Palty, A.; 1976 Borehole Plugging by Compaction Process. Final Report, prepared by Charles Stark Draper Laboratory, Inc., for Union Carbide Corporation, Nuclear Division, Office of Waste Isolation, Y/OWI/SUB-7087/1

4. Ratigan J.L. 1977 "Groundwater Movements Around a Repository, Phase 2. Technical Report 2 Thermal Analyses Part I Conduction Heat Transfer", To be submitted to KBS-Kärnbränslesäkerhet, Stockholm, Sweden.

5. Ratigan J.L. 1977 "Groundwater Movements Around a Repository, Phase 2. Technical Report 2 Thermal Analyses Part II Heat Advection", to be submitted to KBS-Kärnbränslesäkerhet, Stockholm, Sweden.

6. Burgess, A.S. and Skiba E.L. 1977 "Groundwater Movements Around a Repository, Phase 2. Technical Report 5 Repository Domain Groundwater Flow Analyses Part II Inflow to Repository", To be submitted to KBS-Kärnbränslesäkerhet, Stockholm, Sweden.

7. Ratigan J.L. 1977 "Groundwater Movements Around a Repository, Phase 2. Technical Report 4 Rock Mechanics Analyses", To be submitted to KBS-Kärnbränslesäkerhet, Stockholm, Sweden.

8. Ratigan J.L. 1977 "Groundwater Movements Around a Repository, Phase 2.Technical Report 5 Repository Domain Groundwater Flow Analyses, Part I Permeability Perturbations", To be submitted to KBS-Kärnbränslesäkerhet, Stockholm, Sweden.

9. Stille H. and Lundström L. 1977 Permeabilitetsprovning i bergmassan vid Stripa Gruva, KBS 23:03.

10. Larsson, I., 1972 "Groundwater in granite rocks and tectonic models" Nordic Hydrology vol 3 pp 111 - 129.

11. Jacks, G. 1972, "Chemistry of groundwater in igneous rocks at Angered",Gothenburg, Nordic Hydrology, vol 3 p 140.

12. Jacks, G. 1973 "Chemistry of some groundwaters in igneous rocks" Nordic Hydrology, vol 4 p 207.

13. Stille, H., 1977. "Groundwater Movements Around a repository, Phase 2. Technical Report 1 Geological and Geotechnical Conditions". To be submitted to KBS-Kärnbränslesäkerhet, Stockholm, Sweden.

TABLE 1 TRAVEL TIME COMPARISONS

Path	Start/Finish location	TRAVEL TIMES IN YEARS Permeability Distribution in Host Rock			
		Case 3 Anisotropic		Stripa Test Anisotropic	
		Impervious Backfill	Pervious Backfill	Impervious Backfill	Pervious Backfill
1	A-J (A-C-J for pervious backfill)	143	1127 in backfill 145 in rock 1273 Total	3421	1127 in backfill 3483 in rock 4610 Total
2	B-I (B-C- I for pervious backfill)	96	459 in backfill 145 in rock 605 Total	2288	459 in backfill 3483 in rock 3942 Total
3	C-H	60	145	1443	3483
4	D-G	33	55	789	1317
5	E-F	12.1	6.1	290	146

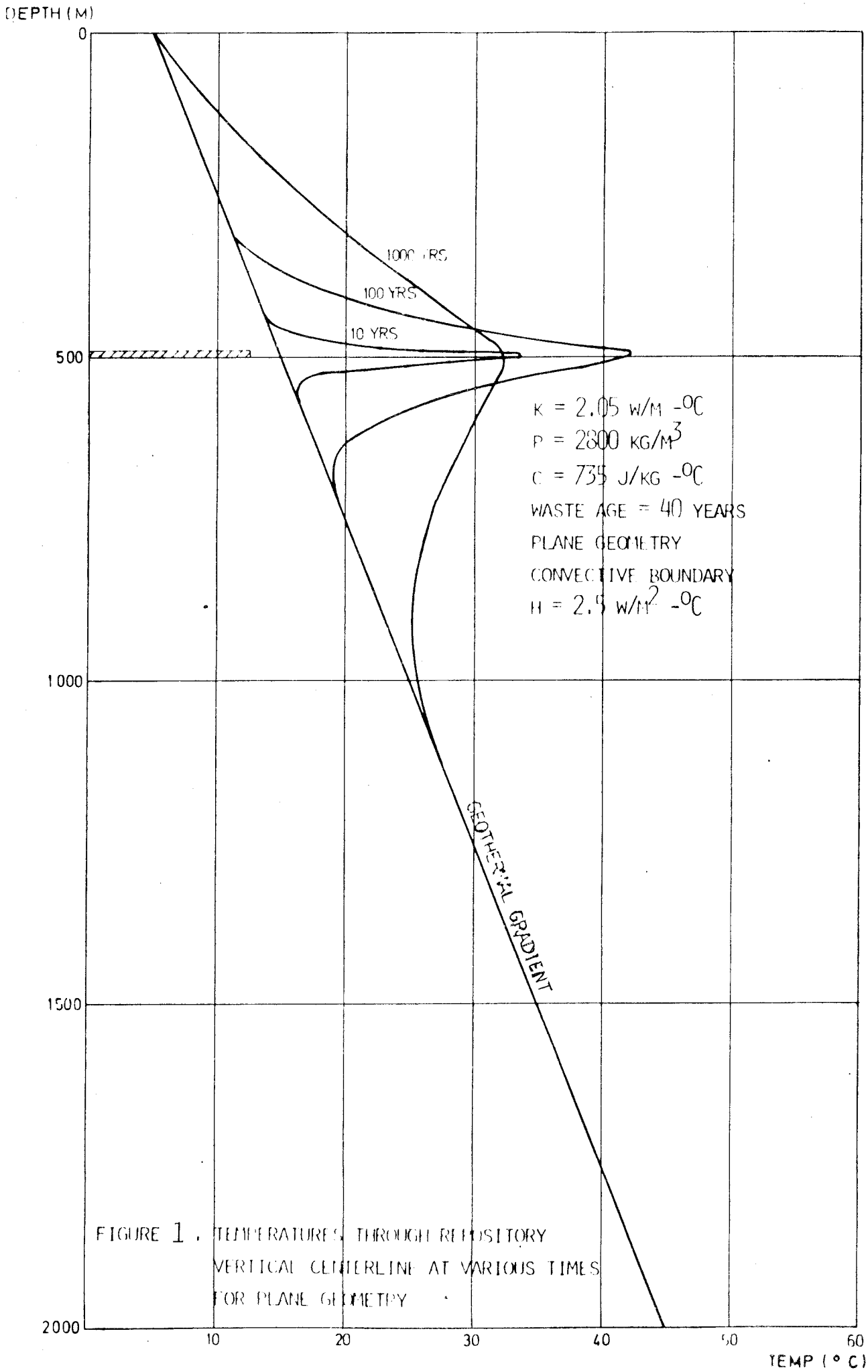

FIGURE 1. TEMPERATURES THROUGH REPOSITORY VERTICAL CENTERLINE AT VARIOUS TIMES FOR PLANE GEOMETRY

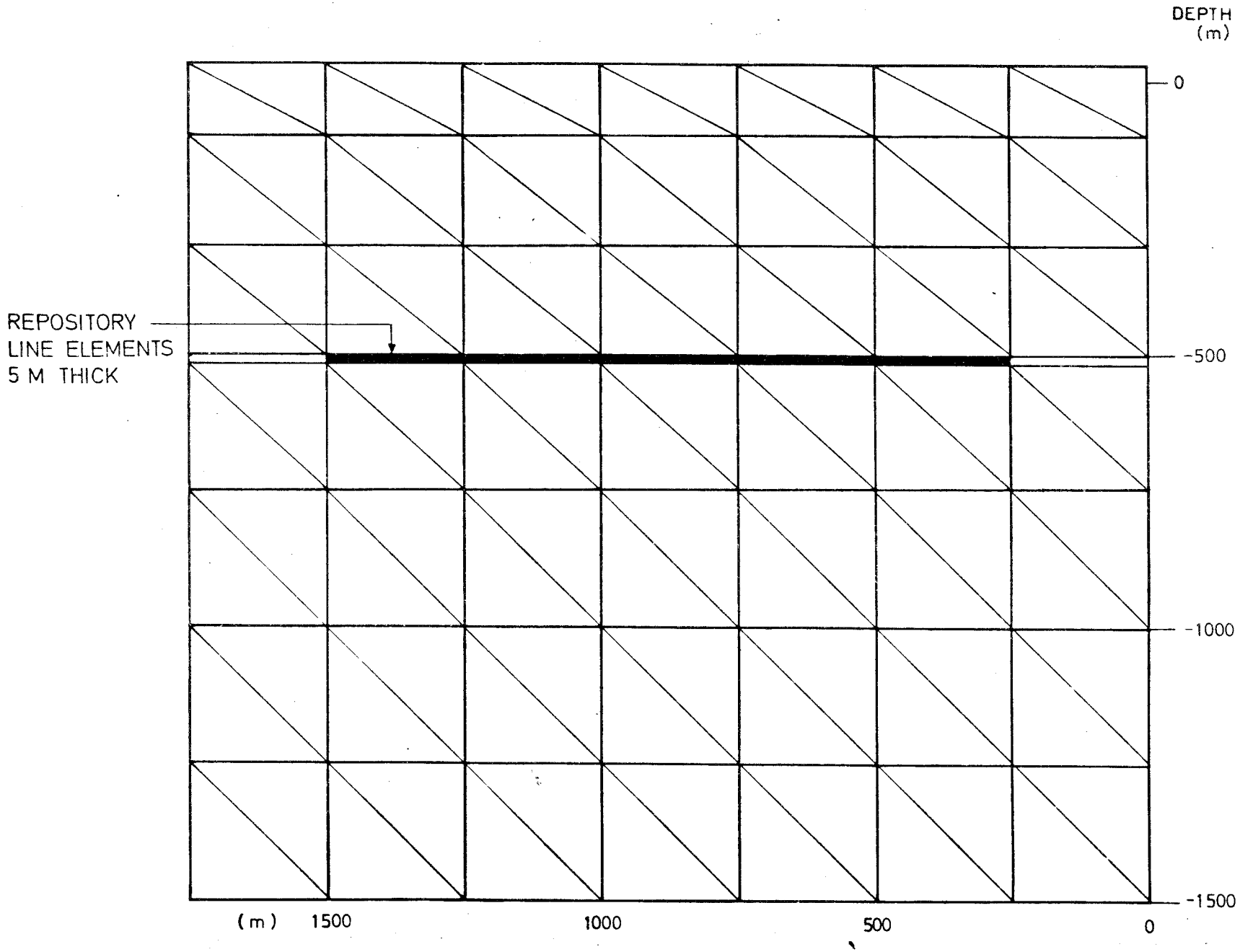

FIGURE 2. FORSMARK: SITE MODEL WITH REPOSITORY FINITE ELEMENT MESH.

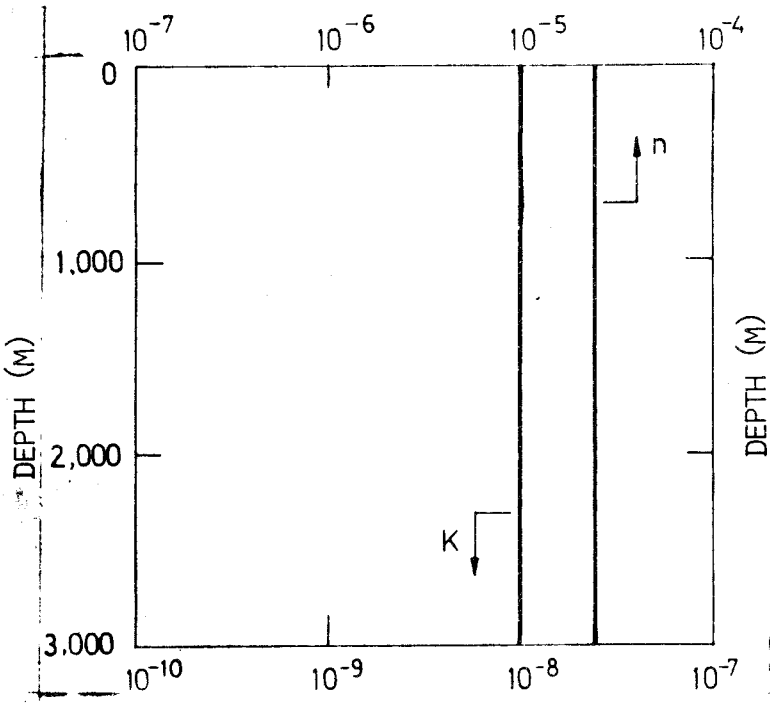

PERMEABILITY K(M/S)

CASE 1: ISOTROPIC, HOMOGENEOUS

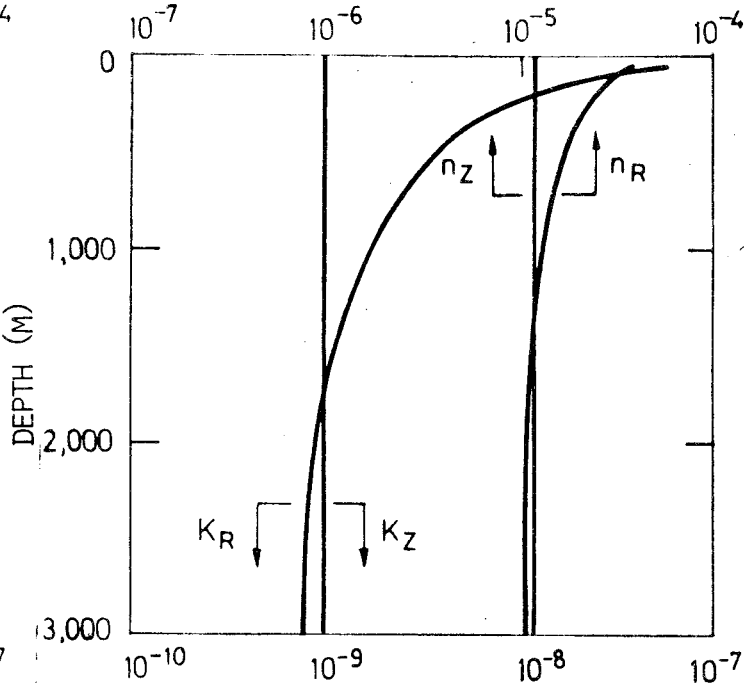

PERMEABILITY K(M/S)

CASE 2: ISOTROPIC, NON-HOMOGENEOUS

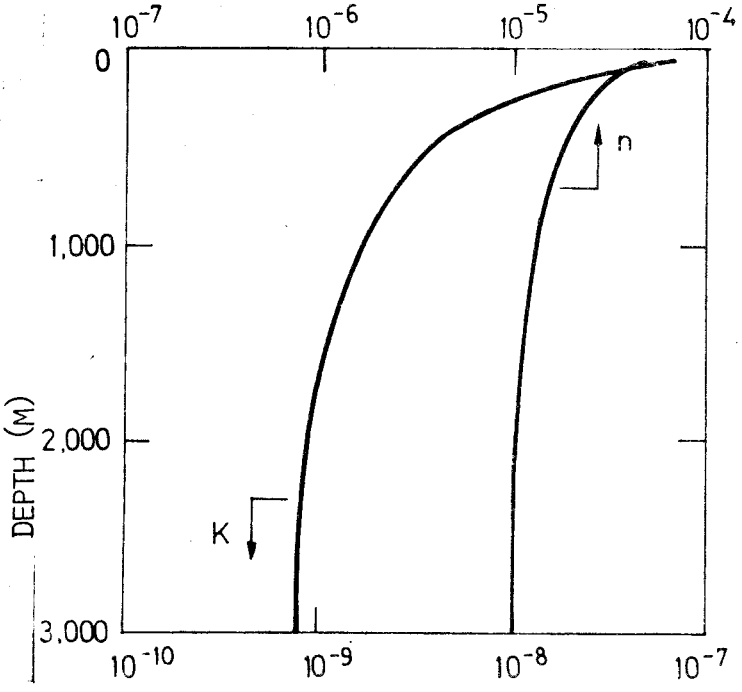

PERMEABILITY K(M/S)

CASE 3: ANISOTROPIC, NON-HOMOGENEOUS

FIGURE 3. NOMINAL PERMEABILITY, POROSITY DISTRIBUTION

KBS – Kärnbränslesäkerhet

GROUNDWATER MOVEMENTS AROUND A REPOSITORY

RESIDUAL CONDITIONS

FORSMARK SITE MODEL : CASE 1 WITH IMPERVIOUS BACKFILL

Hagconsult ab Stockholm Sept. 1977 **FIGURE: 4**

KBS – Kärnbränslesäkerhet

GROUNDWATER MOVEMENTS AROUND A REPOSITORY

RESIDUAL CONDITIONS

FORSMARK SITE MODEL : CASE 1 WITH PERVIOUS BACKFILL

Hagconsult ab Stockholm Sept. 1977 **FIGURE: 5**

KBS – Karnbranslesakerhet

GROUNDWATER MOVEMENTS AROUND A REPOSITORY

RESIDUAL CONDITIONS

FORSMARK SITE MODEL : CASE 2 WITH IMPERVIOUS BACKFILL

Hagconsult ab Stockholm Sept. 1977 **FIGURE: 6**

KBS – Kärnbränslesäkerhet

GROUNDWATER MOVEMENTS AROUND A REPOSITORY

RESIDUAL CONDITIONS

FORSMARK SITE MODEL : CASE 2 WITH PERVIOUS BACKFILL

Hagconsult ab Stockholm Sept. 1977 **FIGURE: 7**

PERMEABILITY (K) & POROSITY (n)

PORE VELOCITY VECTORS

Scale 0 10×10^{-6} m/s

EQUIPOTENTIALS

BOUNDARY CONDITIONS

——— Zero flux boundary

– – – – Fixed potential boundary

KBS – Kärnbränslesäkerhet

GROUNDWATER MOVEMENTS AROUND A REPOSITORY

RESIDUAL CONDITIONS

FORSMARK SITE MODEL : CASE 3 WITH IMPERVIOUS BACKFILL

Hagconsult ab Stockholm Sept. 1977 **FIGURE: 8**

KBS – Kärnbränslesäkerhet

GROUNDWATER MOVEMENTS AROUND A REPOSITORY

RESIDUAL CONDITIONS

FORSMARK SITE MODEL : CASE 3 WITH PERVIOUS BACKFILL

Hagconsult ab Stockholm Sept. 1977 FIGURE: 9

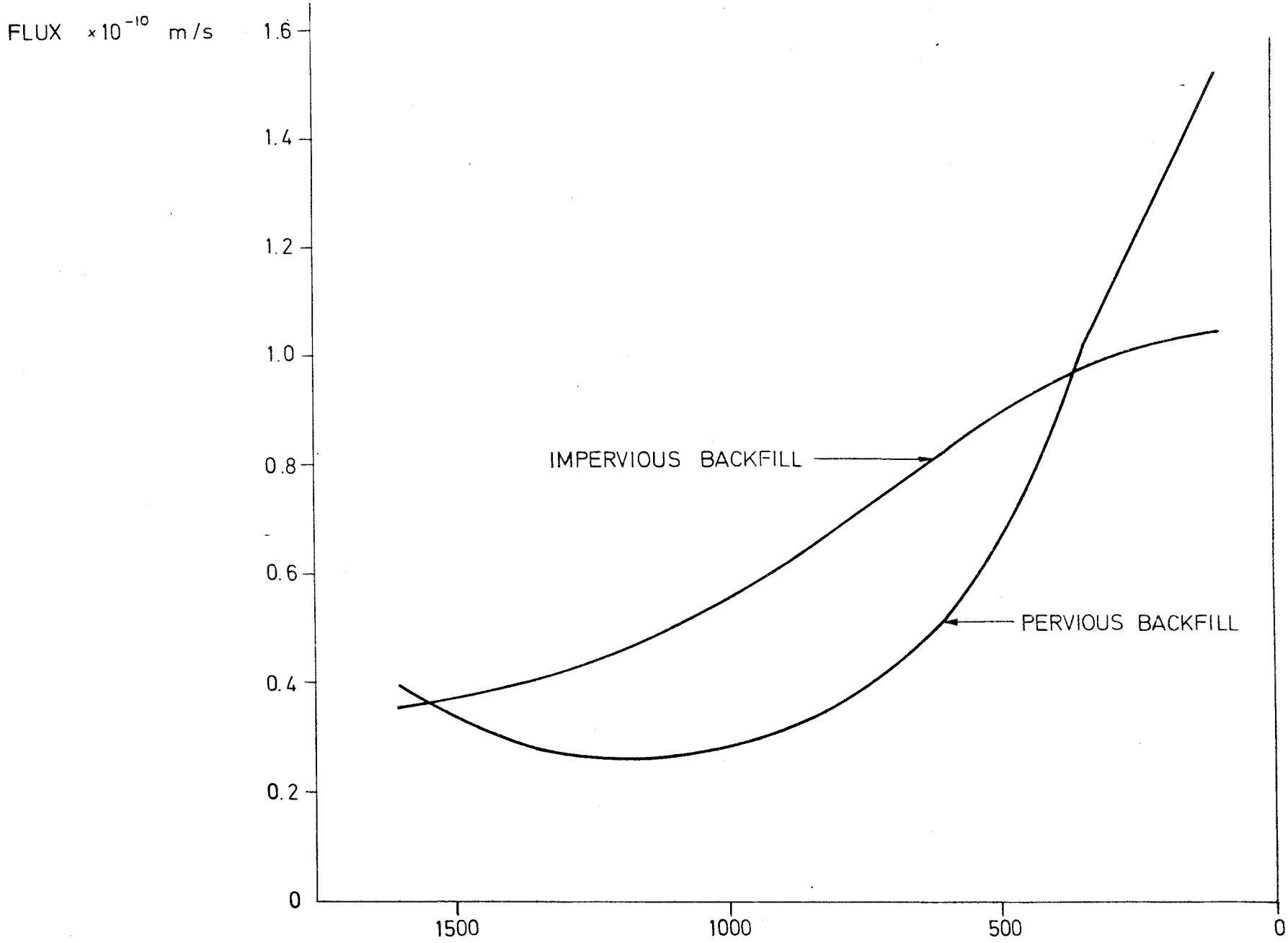

FIGURE 10. FLUXES BELOW REPOSITORY CASE 1

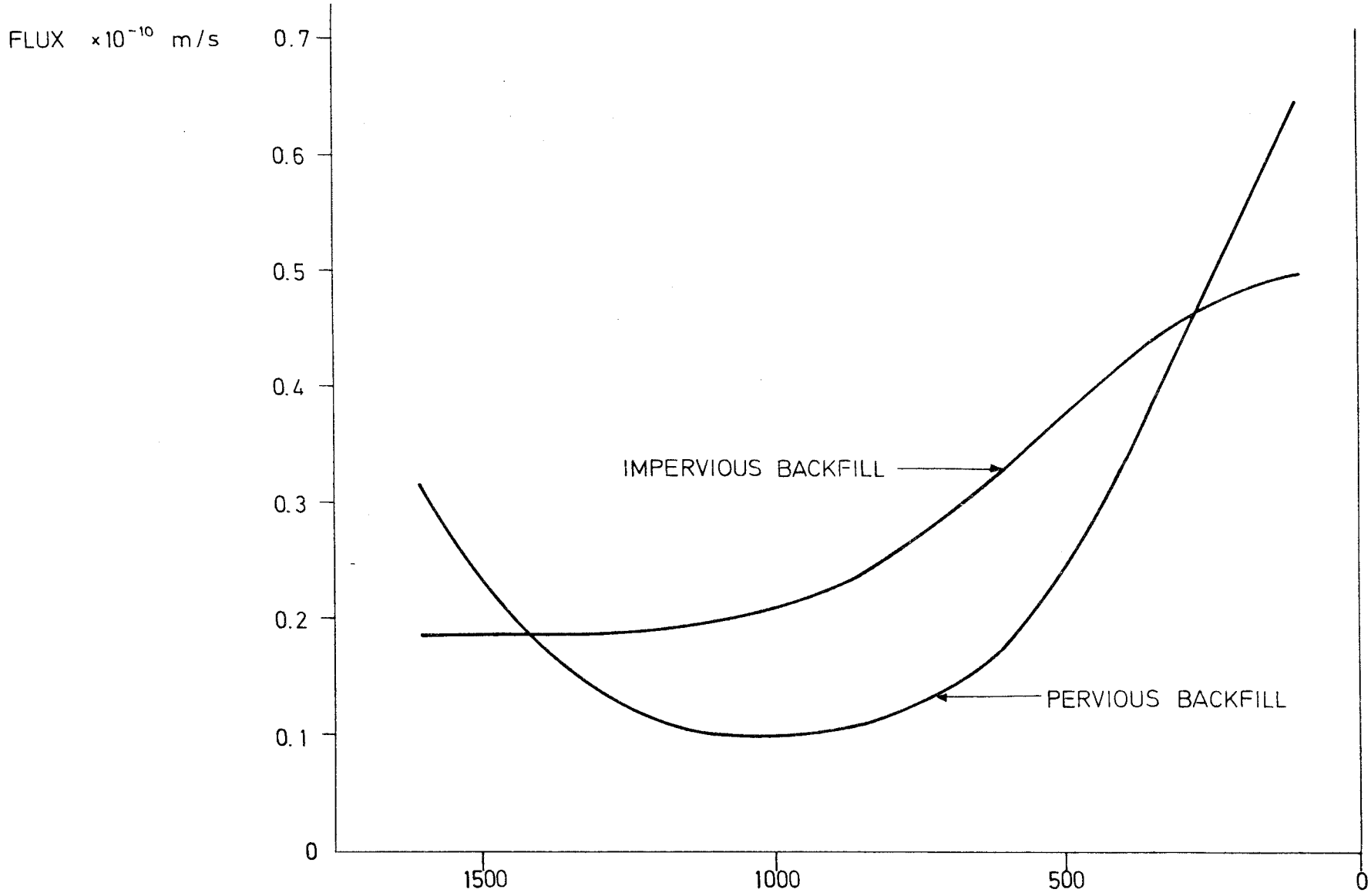

FIGURE 11. FLUXES BELOW REPOSITORY CASE 2

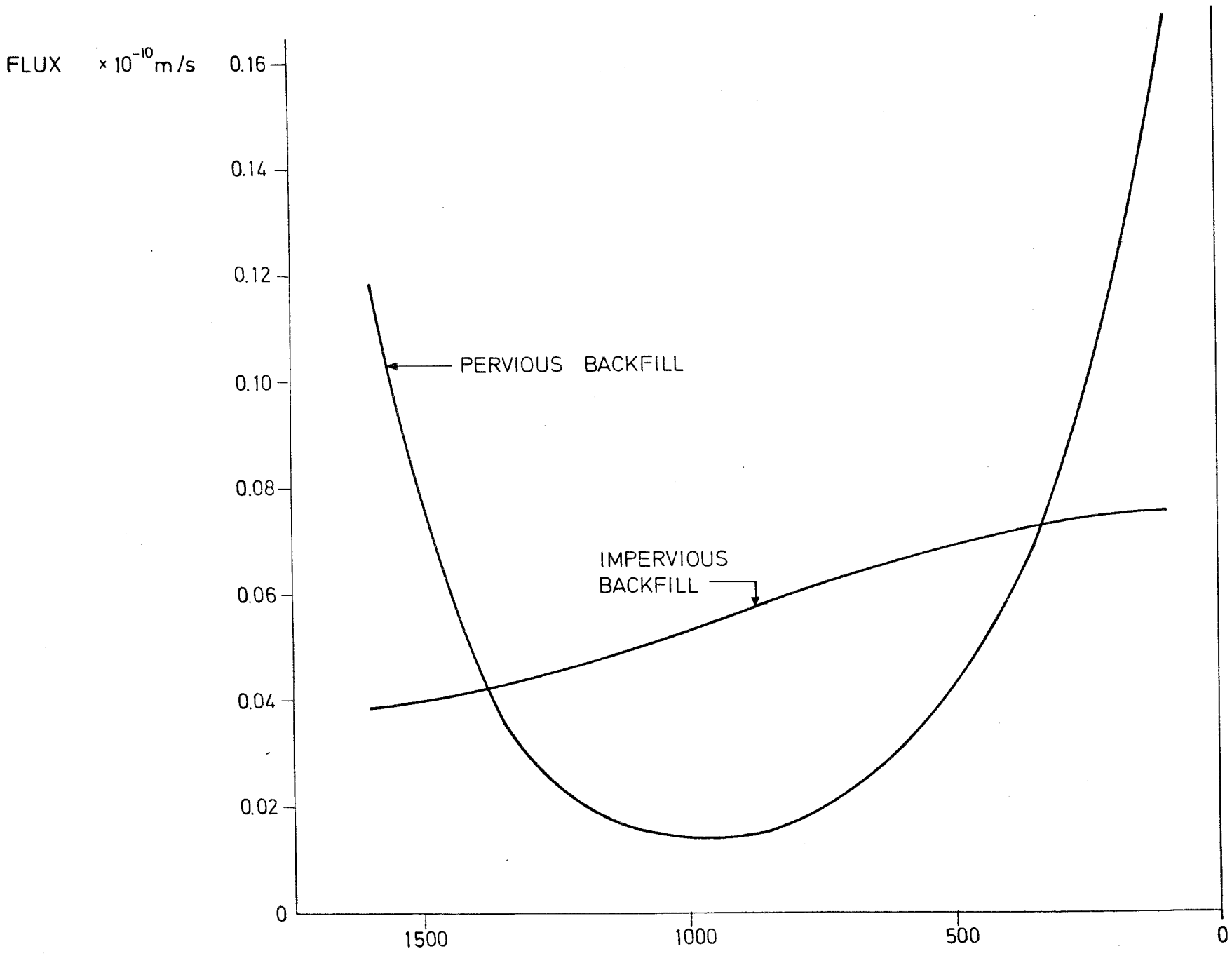

FIGURE 12. FLUXES BELOW REPOSITORY CASE 3

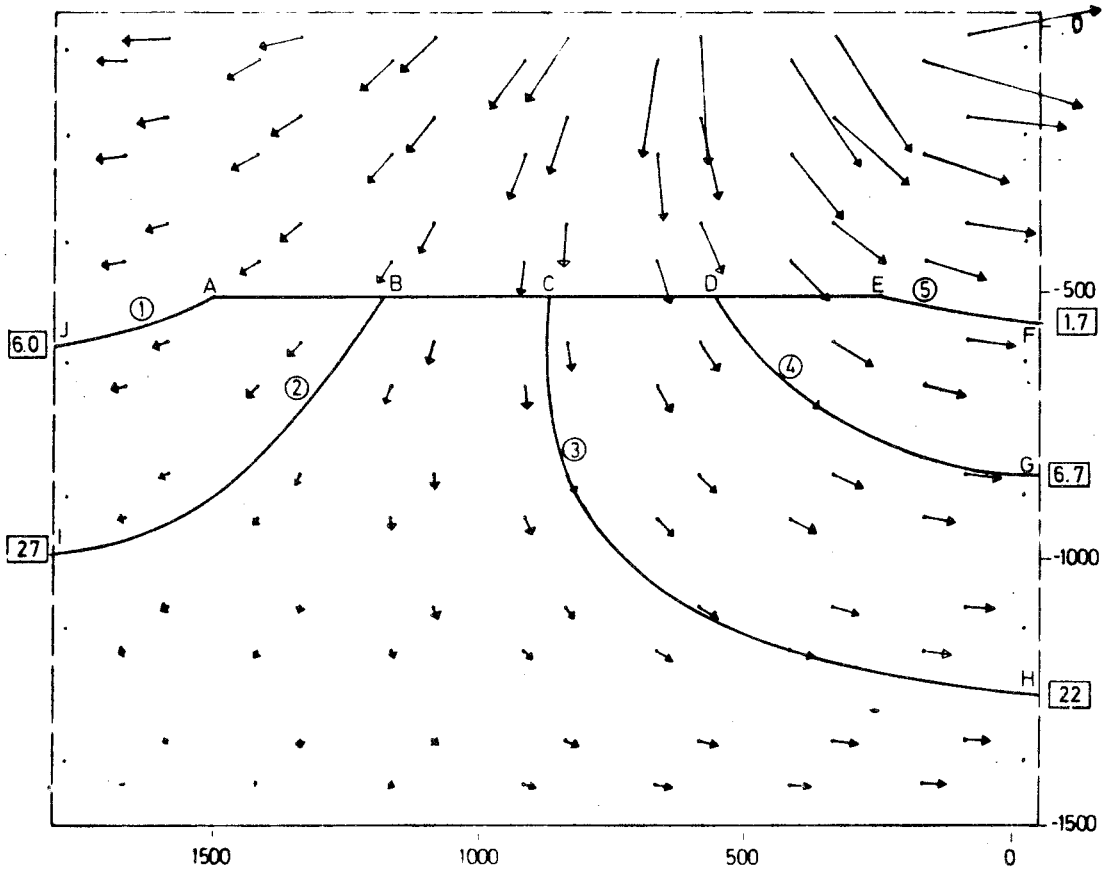

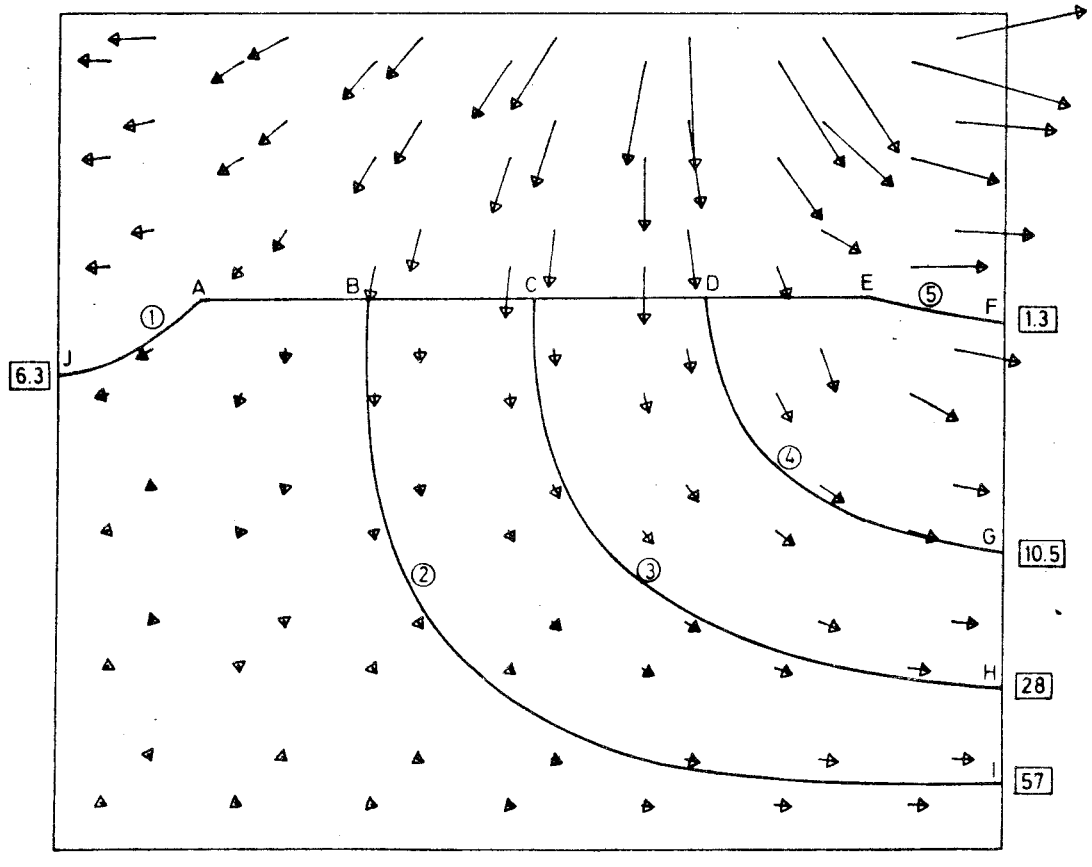

FIGURE 13. PATHWAYS AND TRAVEL TIMES IN REPOSITORY DOMAIN CASE 1

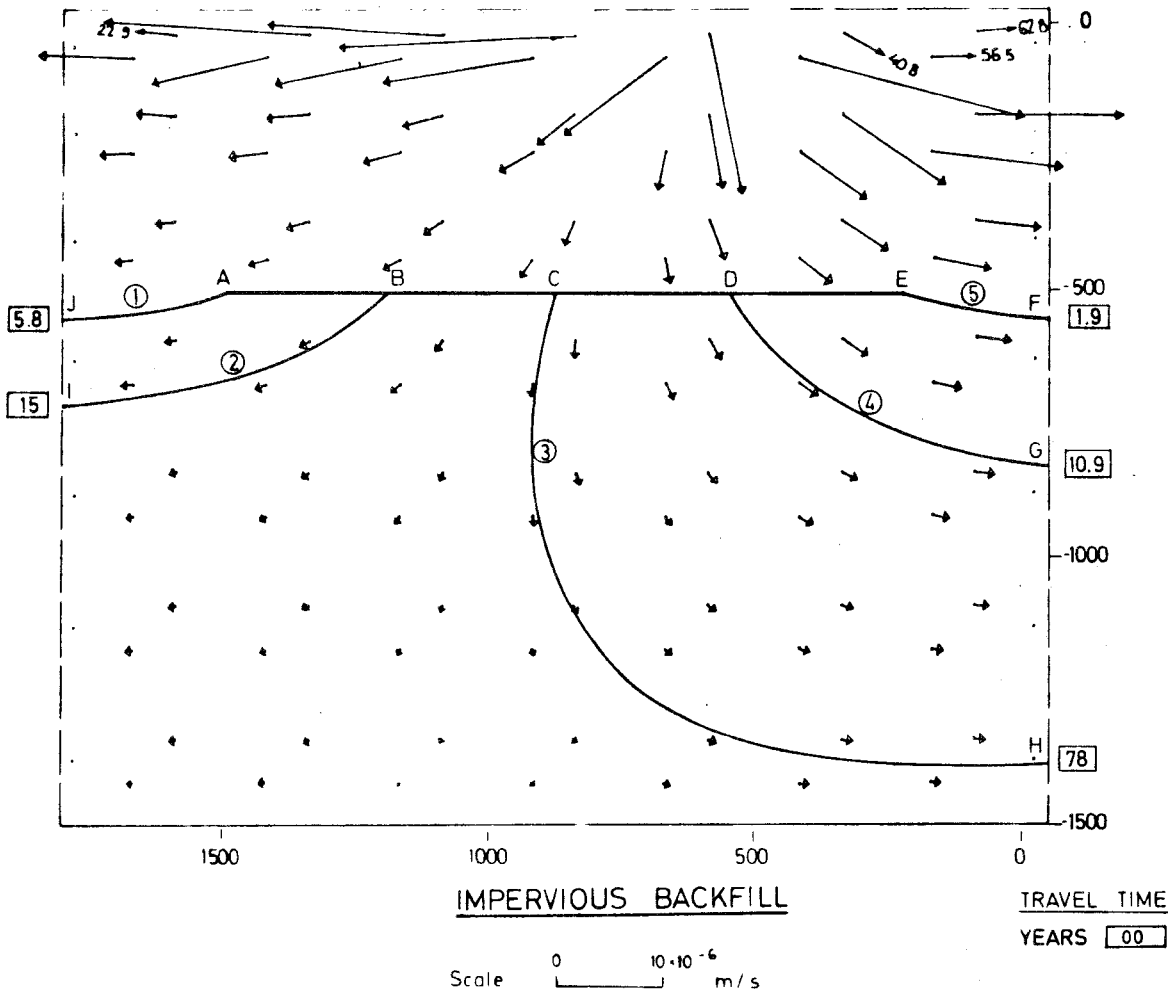

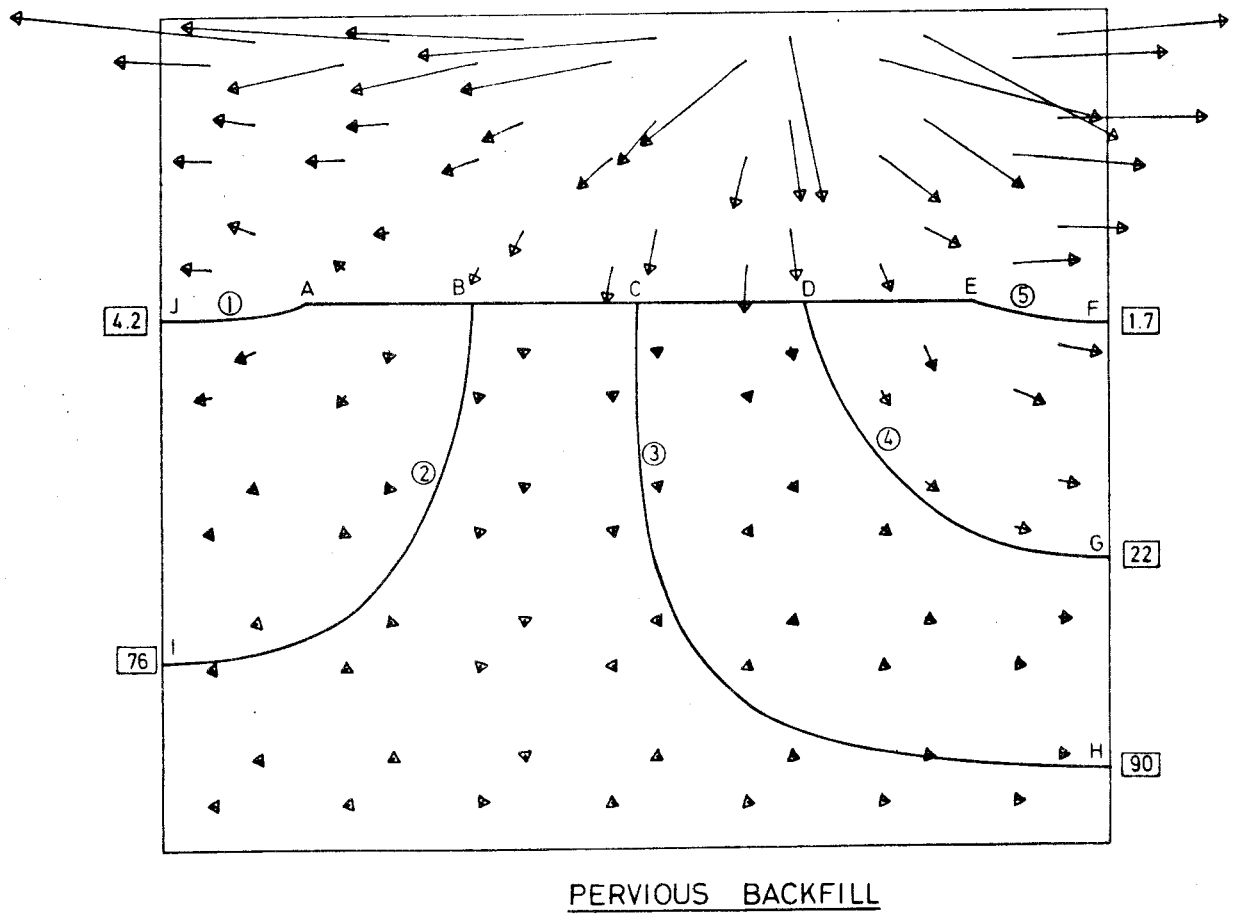

FIGURE 14. PATHWAYS AND TRAVEL TIMES REPOSITORY DOMAIN CASE 2

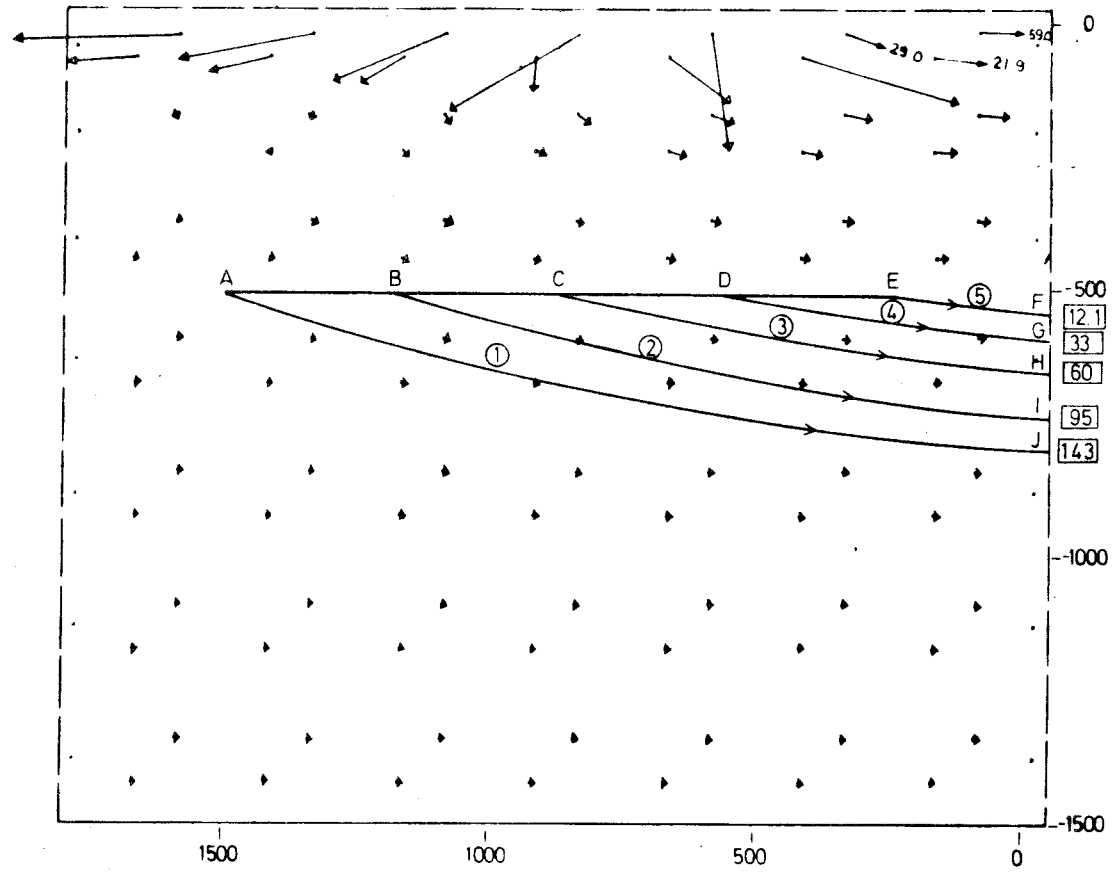

IMPERVIOUS BACKFILL

TRAVEL TIME
YEARS 000

Scale 0 10×10^{-6} m/s

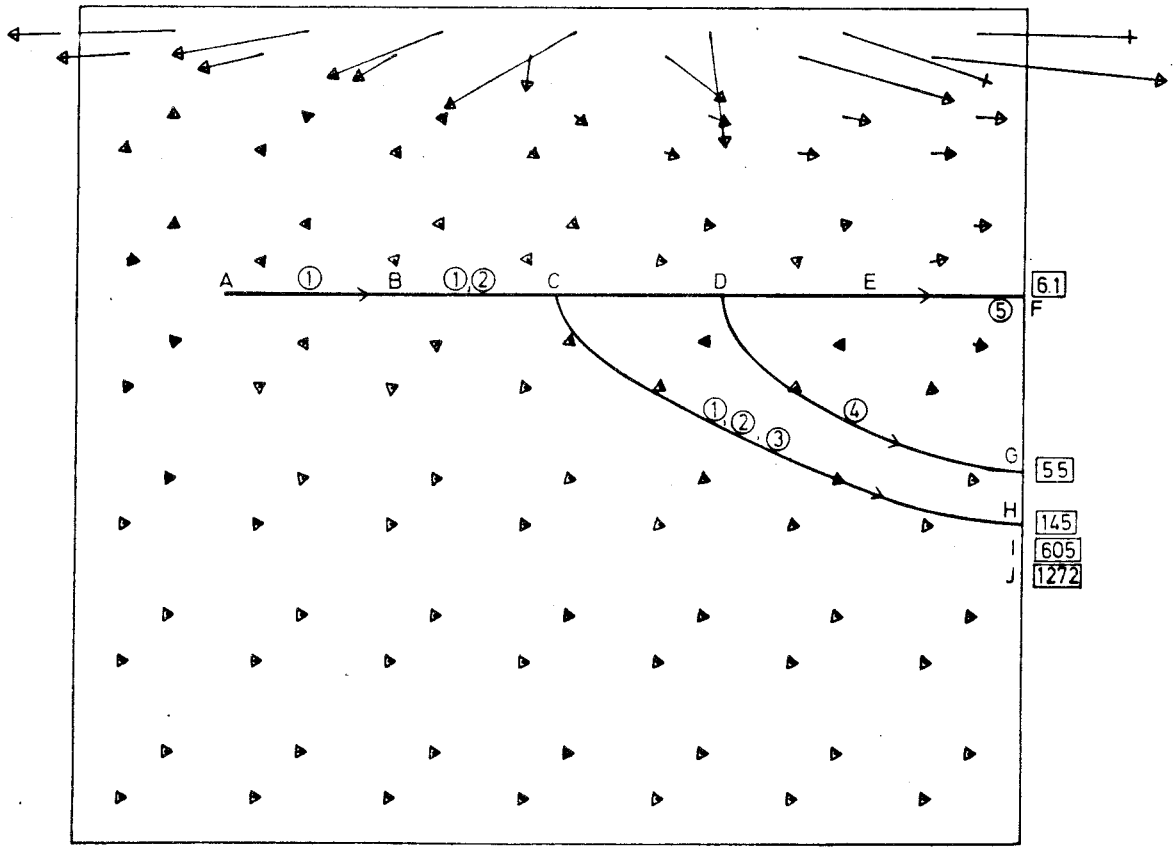

PERVIOUS BACKFILL

FIGURE 15. PATHWAYS AND TRAVEL TIMES IN REPOSITORY DOMAIN CASE 3

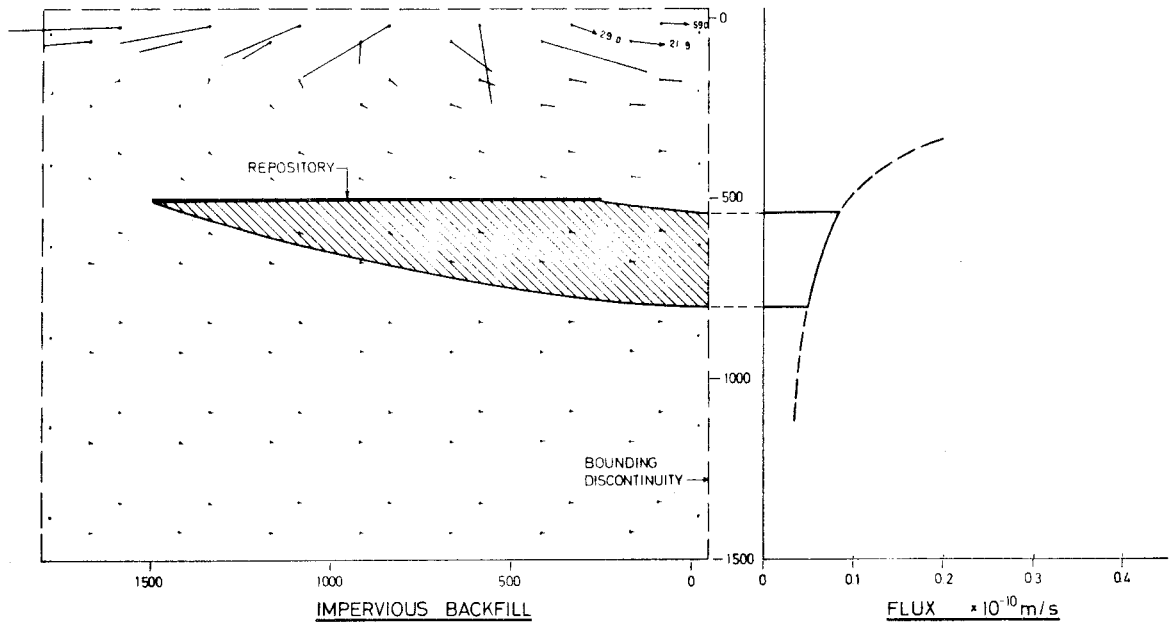

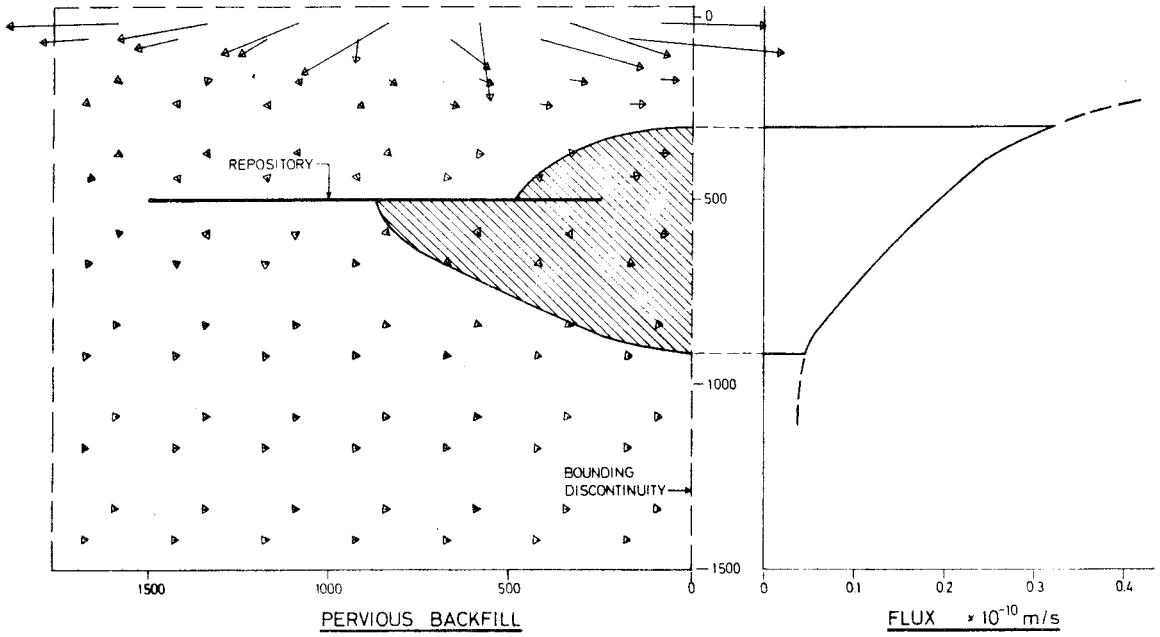

FIGURE 16. FLUXES AT BOUNDARY IN REPOSITORY PLUME

FÖRTECKNING ÖVER KBS TEKNISKA RAPPORTER

01 Källstyrkor i utbränt bränsle och högaktivt avfall från en PWR beräknade med ORIGEN
Nils Kjellbert
AB Atomenergi 77-04-05

02 PM angående värmeledningstal hos jordmaterial
Sven Knutsson
Roland Pusch
Högskolan i Luleå 77-04-15

03 Deponering av högaktivt avfall i borrhål med buffertsubstans
Arvid Jacobsson
Roland Pusch
Högskolan i Luleå 77-05-27

04 Deponering av högaktivt avfall i tunnlar med buffertsubstans
Arvid Jacobsson
Roland Pusch
Högskolan i Luleå 77-06-01

05 Orienterande temperaturberäkningar för slutförvaring i berg av radioaktivt avfall, Rapport 1
Roland Blomqvist
AB Atomenergi 77-03-17

06 Groundwater movements around a repository, Phase 1, State of the art and detailed study plan
Ulf Lindblom
Hageonsult AB 77-02-28

07 Resteffekt studier för KBS
Del 1 Litteraturgenomgång
Del 2 Beräkningar
Kim Ekberg
Nils Kjellbert
Göran Olsson
AB Atomenergi 77-04-19

08 Utlakning av franskt, engelskt och kanadensiskt glas med högaktivt avfall
Göran Blomqvist
AB Atomenergi 77-05-20

09 Diffusion of soluble materials in a fluid filling a porous medium
Hans Häggblom
AB Atomenergi 77-03-24

10 Translation and development of the BNWL-Geosphere Model
Bertil Grundfelt
Kemakta Konsult AB 77-02-05

11 Utredning rörande titans lämplighet som korrosionshärdig kapsling för kärnbränsleavfall
Sture Henriksson
AB Atomenergi 77-04-18

12 Bedömning av egenskaper och funktion hos betong i samband med slutlig förvaring av kärnbränsleavfall i berg
Sven G Bergström
Göran Fagerlund
Lars Rombén
Cement- och Betonginstitutet 77-06-22

13 Urlakning av använt kärnbränsle (bestrålad uranoxid) vid direktdeponering
Ragnar Gelin
AB Atomenergi 77-06-08

14 Influence of cementation on the deformation properties of bentonite/quartz buffer substance
Roland Pusch
Högskolan i Luleå 77-06-20

15 Orienterande temperaturberäkningar för slutförvaring i berg av radioaktivt avfall
Rapport 2
Roland Blomquist
AB Atomenergi 77-05-17

16 Översikt av utländska riskanalyser samt planer och projekt rörande slutförvaring
Åke Hultgren
AB Atomenergi augusti 1977

17 The gravity field in Fennoscandia and postglacial crustal movements
Arne Bjerhammar
Stockholm augusti 1977

18 Rörelser och instabilitet i den svenska berggrunden
Nils-Axel Mörner
Stockholms Universitet augusti 1977

19 Studier av neotektonisk aktivitet i mellersta och norra Sverige, flygbildsgenomgång och geofysisk tolkning av recenta förkastningar
Robert Lagerbäck
Herbert Henkel
Sveriges Geologiska Undersökning september 1977

20 Tektonisk analys av södra Sverige, Vättern - Norra Skåne
Kennert Röshoff
Erik Lagerlund
Lunds Universitet och Högskolan Luleå september 1977

21 Earthquakes of Sweden 1891 - 1957, 1963 - 1972
Ota Kulhánek
Rutger Wahlström
Uppsala Universitet september 1977

22 The influence of rock movement on the stress/strain situation in tunnels or bore holes with radioactive consisters embedded in a bentonite/quartz buffer mass
Roland Pusch
Högskolan i Luleå 1977-08-22

23 Water uptake in a bentonite buffer mass
A model study
Roland Pusch
Högskolan i Luleå 1977-08-22

24 Beräkning av utlakning av vissa fissionsprodukter och aktinider från en cylinder av franskt glas
Göran Blomqvist
AB Atomenergi 1977-07-27

25 Blekinge kustgnejs, Geologi och hydrogeologi
Ingemar Larsson KTH
Tom Lundgren SGI
Ulf Wiklander SGU
Stockholm, augusti 1977

26 Bedömning av risken för fördröjt brott i titan
Kjell Pettersson
AB Atomenergi 1977-08-25

27 A short review of the formation, stability and cementing properties of natural zeolites
Arvid Jacobsson
Högskolan i Luleå 1977-10-03

28 Värmeledningsförsök på buffertsubstans av bentonit/pitesilt
Sven Knutsson
Högskolan i Luleå 1977-09-20

29 Deformationer i sprickigt berg
Ove Stephansson
Högskolan i Luleå 1977-09-28

30 Retardation of escaping nuclides from a final depository
Ivars Neretnieks
Kungliga Tekniska Högskolan Stockholm 1977-09-14

31 Bedömning av korrosionsbeständigheten hos material avsedda för kapsling av kärnbränsleavfall. Lägesrapport 1977-09-27 samt kompletterande yttranden.
Korrosionsinstitutet och dess referensgrupp

32 Long term mineralogical properties of bentonite/quartz buffer substance
Preliminär rapport november 1977
Slutrapport februari 1978
Roland Pusch
Arvid Jacobsson
Högskolan i Luleå

33 Required physical and mechanical properties of buffer masses
Roland Pusch
Högskolan Luleå 1977-10-19

34 Tillverkning av bly-titan kapsel
Folke Sandelin AB
VBB
ASEA-Kabel
Institutet för metallforskning
Stockholm november 1977

35 Project for the handling and storage of vitrified high-level waste
Saint Gobain Techniques Nouvelles October, 1977

36 Sammansättning av grundvatten på större djup i granitisk berggrund
Jan Rennerfelt
Orrje & Co, Stockholm 1977-11-07

37 Hantering av buffertmaterial av bentonit och kvarts
Hans Fagerström, VBB
Björn Lundahl, Stabilator
Stockholm oktober 1977

38 Utformning av bergrumsanläggningar
Arne Finné, KBS
Alf Engelbrektson, VBB
Stockholm december 1977

39 Konstruktionsstudier, direktdeponering
ASEA-ATOM
VBB
Västerås

40 Ekologisk transport och stråldoser från grundvattenburna radioaktiva ämnen
Ronny Bergman
Ulla Bergström
Sverker Evans
AB Atomenergi

41 Säkerhet och strålskydd inom kärnkraftområdet.
Lagar, normer och bedömningsgrunder
Christina Gyllander
Siegfried F Johnson
Stig Rolandson
AB Atomenergi och ASEA-ATOM

42 Säkerhet vid hantering, lagring och transport av använt kärnbränsle och förglasat högaktivt avfall
Ann Margret Ericsson
Kemakta november 1977

43 Transport av radioaktiva ämnen med grundvatten från ett bergförvar
Bertil Grundfelt
Kemakta november 1977

44 Beständighet hos borsilikatglas
Tibor Lakatos
Glasteknisk Utveckling AB

45 Beräkning av temperaturer i ett envånings slutförvar i berg för förglasat radioaktivt avfall Rapport 3
Roland Blomquist
AB Atomenergi 1977-10-19

46 Temperaturberäkningar för använt bränsle
Taivo Tahrandi
VBB

47 Teoretiska studier av grundvattenrörelser
Preliminär rapport oktober 1977
Slutrapport februari 1978
Lars Y Nilsson
John Stokes
Roger Thunvik
Inst för kulturteknik KTH

48 The mechanical properties of Stripa granite
Graham Swan
Högskolan i Luleå 1977-09-14

49 Bergspänningsmätningar i Stripa gruva
Hans Carlsson
Högskolan i Luleå 1977-08-29

50 Lakningsförsök med högaktivt franskt glas i Studsvik
Göran Blomqvist
AB Atomenergi november 1977

51 Seismotechtonic risk modelling for nuclear waste disposal in the Swedish bedrock
F Ringdal
H Gjöystdal
E S Husebye
Royal Norwegian Council for scientific and industrial research

52 Calculations of nuclide migration in rock and porous media, penetrated by water
H Häggblom
AB Atomenergi 1977-09-14

53 Mätning av diffusionshastighet för silver i lera-sand-blandning
Bert Allard
Heino Kipatsi
Chalmers tekniska högskola 1977-10-15

54 Groundwater movements around a repository

54:01 Geological and geotechnical conditions
Håkan Stille
Anthony Burgess
Ulf E Lindblom
Hagconsult AB september 1977

54:02 Thermal analyses
Part 1 Conduction heat transfer
Part 2 Advective heat transfer
Joe L Ratigan
Hagconsult AB september 1977

54:03 Regional groundwater flow analyses
Part 1 Initial conditions
Part 2 Long term residual conditions
Anthony Burgess
Hagconsult AB oktober 1977

54:04 Rock mechanics analyses
Joe L Ratigan
Hagconsult AB september 1977

54:05 Repository domain groundwater flow analyses
Part 1 Permeability perturbations
Part 2 Inflow to repository
Part 3 Thermally induced flow
Joe L Ratigan
Anthony S Burgess
Edward L Skiba
Robin Charlwood

54:06 Final report
Ulf Lindblom et al
Hagconsult AB oktober 1977

55 Sorption av långlivade radionuklider i lera och berg
Del 1 Bestämning av fördelningskoefficienter
Del 2 Litteraturgenomgång
Bert Allard
Heino Kipatsi
Jan Rydberg
Chalmers tekniska högskola 1977-10-10

56 Radiolys av utfyllnadsmaterial
Bert Allard
Heino Kipatsi
Jan Rydberg
Chalmers tkniska högskola 1977-10-15

57 Stråldoser vid haveri under sjötransport av kärnbränsle
Anders Appelgren
Ulla Bergström
Lennart Devell
AB Atomenergi

58 Strålrisker och högsta tillåtliga stråldoser för människan
Gunnar Walinder
FOA 4 november 1977

59 Tectonic lineaments in the Baltic from Gävle to Simrishamn
Tom Flodén
Stockholms Universitet 1977-12-15